Electronic Thesis and Dissertation Repository

8-23-2018 10:00 AM

Chemical Modification of Lignin into Advanced Materials

Soheil Hajirahimkhan, *The University of Western Ontario*

Supervisor: Chunbao (Charles) Xu, *The University of Western Ontario*
Joint Supervisor: Paul J. Ragogna, *The University of Western Ontario*
A thesis submitted in partial fulfillment of the requirements for the Doctor of Philosophy degree in Chemical and Biochemical Engineering
© Soheil Hajirahimkhan 2018

Follow this and additional works at: https://ir.lib.uwo.ca/etd

Part of the Polymer and Organic Materials Commons, and the Polymer Science Commons

Abstract

Fossil fuel resources are being used today for most of humankind's energy and chemical/material needs. The inevitable demise of these resources has created significant interest in the field of biomass and particularly, lignin valorization. As the world's second most abundant polymer, more than 98% of the annually produced lignin is under-utilized either as an on-site heat source or as landfill. Thus, finding practical approaches to modifying this inexpensive, sustainable resource into materials of high value can be the next leap in lessening the dependence on fossil fuel resources and thus, developing a sustainable future.

In this thesis, kraft lignin is modified into methacrylated lignin (**ML**), lignin grafted with methacrylate functionalities at its hydroxyl sites. **ML** was incorporated at loading percentages of 10-31 wt.% into UV-cured coatings, and the developed coatings were characterized according to their different properties.

The methacrylation process was optimized via response surface methodology using a central composite design to determine the effect of different reaction variables on the process' recovered mass yield and to obtain the maximum possible recovered **ML**. The **ML** obtained from the optimized reaction conditions was then incorporated at 30 wt.% into a siloxane-based UV-cured coating as a proof of concept for the practicality of the optimization process.

ML was afterwards converted into a primary polyphosphine (lignophine) by a phosphane-ene reaction. The primary lignophine was then capped into tertiary alkylated and fluorinated lignophines, respectively using corresponding alkenes. The ability of the tertiary alkylated lignophine to coordinate to transition metals and sequester transition metal-containing catalysts was determined using silver triflate a ring closing metathesis (RCM) reaction using Grubbs I (GI) catalyst, respectively.

Finally, the tertiary alkylated lignophine was converted into a free-standing UV-cured polyphosphonium (lignophonium) network. The obtained films showed high cure percentages and water contact angles, along with a surface charge density value well over the necessary threshold for antimicrobial films and swelling degrees suitable for controlled drug release. The

films were probed for their controlled drug release ability using diclofenac as the loaded drug and examining the release in PBS and showed a promising release profile.

Keywords

Co-Authorship Statement

Chapter 3: UV-curable Coatings of Modified Lignin

Authors: Soheil Hajirahimkhan, Chunbao (Charles) Xu, Paul J. Ragogna

The experimental work, characterization and, result analyses were conducted by Soheil Hajirahimkhan under the supervision of Prof. Paul J. Ragogna and Prof. Chunbao (Charles) Xu. The manuscript was written by Soheil Hajirahimkhan and revised by Prof. Paul J. Ragogna and Prof. Chunbao (Charles) Xu and submitted to "*Sustainable Chemistry and Engineering*".

Chapter 4: Methavrylation of Kraft Lignin for UV-curable Coatings: Process Optimization Using Response Surface Methodology

Authors: Soheil Hajirahimkhan, Paul J. Ragogna, Chunbao (Charles) Xu

The experimental work, characterization, and result analyses were conducted by Soheil Hajirahimkhan under the supervision of Prof. Paul J. Ragogna and Prof. Chunbao (Charles) Xu. The manuscript was written by Soheil Hajirahimkhan and revised by Prof. Chunbao (Charles) Xu and Prof. Paul J. Ragogna and submitted to "*Biomass and Bioenergy*".

Chapter 5: "Lignophines": Lignin-based Tertiary Phosphines with Metal-Scavenging Ability

Authors: Soheil Hajirahimkhan, Devon E. Chapple, Johanna M. Blacquierre, Chunbao (Charles) Xu, Paul J. Ragogna

Reactor setup for the hydrophosphination reaction, tertiary lignophine synthesis, all product characterizations, and silver triflate coordination studies was conducted by Soheil Hajirahimkhan under the supervision of Prof. Paul J. Ragogna and Prof. Chunbao (Charles) Xu. The PH_3 line was operated by Dr. Tyler J. Cuthbert, Dr. Cameron M. E. Graham, Tristan D. Harrison, Vanessa A. Béland, and Dr. Kaijie Ni at different times during the project under the supervision of Prof. Paul J. Ragogna. Metal sequestration studies were performed, and the results were analyzed by Devon E. Chapple under the supervision of Dr. Johanna M. Blacquierre. The manuscript was written by Soheil Hajirahimkhan and Devon E. Chapple and

revised by Prof. Paul J. Ragogna, Prof. Johanna M. Blacquierre, and Prof. Chunbao (Charles) Xu and submitted to "*Angewandte Chemie International Edition*".

Chapter 6: "Lignophoniums": Stimuli-Responsive Lignin-based Polyphosphonium Networks for Controlled Drug Delivery

Authors: Soheil Hajirahimkhan, Tristan D. Harrison, Chunbao (Charles) Xu, Paul J. Ragogna

All synthesis, characterization, and result analyses were conducted by Soheil Hajirahimkhan under the supervision of Prof. Paul J. Ragogna and Prof. Chunbao (Charles) Xu. Drug release studies and result analyses were carried out with the collaboration of Tristan D. Harrison. The manuscript was written by Soheil Hajirahimkhan and Tristan D. Harrison and revised by Prof. Paul J. Ragogna and Prof. Chunbao (Charles) Xu and will be submitted to "*Chemical Communications*".

Acknowledgments

I want to thank every past and present member of the Ragogna group, Ryan, Tyler, Mahboubeh, Cameron, Erin, Chrissie, Lauren, Josh, Jen, Daniella, Olga, and Rabi. A special shout-out to the more recent members of the group, Tristan, Benjamin, Vanessa, Taylor, and Matt. Our terribly amusing conversations were definitely something to look forward to every day. I was extremely fortunate to spend the bulk of my grad life with all of you and am grateful for all the amazing memories. My gratitude is also extended to the amazing graduate student body, as well as the staff at the Chemistry department. It was a great pleasure spending the past four years with you all.

I would also like to thank Dr. Charles Xu for giving me the chance to become a member of his research group at ICFAR. I'm grateful for the opportunity and the support. I also want to thank the members of the Xu group at ICFAR.

A great deal of gratitude goes to Dr. Paul J. Ragogna. Every one-on-one and group meeting was a great learning opportunity for me. Thank you for teaching me the importance of self-criticism, out of the box thinking, innovating, and hard work. I hope that you will find it in your heart to order fries at sushi one day!

I also want to thank my parents, Shahin (Zahra) and Abbas for their continuing support and never-ending love, as well as my brothers, Saeed and Sepehr and their families, Maryam, Gandom, and Ilia.

Finally, my wife, Ava. None of this would have been possible without you. You are the sum of all the good and beautiful things in my life. You have been there, always, through all the ups and downs. We have the rest of our lives to look forward to and I cannot wait.

Table of Contents

List of Tables

List of Figures

List of Schemes

List of Abbreviations and Symbols

°	Degrees
1MIM	1-methylimidazole
AA	Acetic anhydride
AAL	Acetic Acid Lignin
ABDA	4-acryloyloxybutyl dehydroabieticcarboxylate
ABP	Acryloyl benzophenone
AEDA	2-acryloyloxyethyl dehydroabieticcarboxylate
AIBN	azobisisobutyronitrile
AIKL	Acetone Insoluble Kraft Lignin
ANOVA	Analysis of variance
ASKL	Acetone Soluble Softwood Kraft Lignin
ASTM	American Society for Testing and Materials
ATRP	Atom Transfer Radical Polymerization
BA	n-butyric anhydride
BiBB	2-bromoisobutyryl bromide
BT	Billion Tons
cm	Centimeter
°C	Degrees Celsius
δ_H	Hydrogen Chemical Shift (ppm)
δ_P	Phosphorus Chemical Shift (ppm)
CCD	Central Composite Design
CER	Cation Exchange Resin
CL	Cardanol-Lignin

CLPU	Cardanol-lignin-based polyurethane
CTAC	Cetyltrimethylammonium chloride
DA	Dimerized acid
DA-*g*-EHL	Dimerized acid-grafted enzymatically hydrolyzed lignin
DETA	Diethylenetriamine
DHA	dehydroabietic acid
DKL	Demethylated Kraft Lignin
DMBA	Dimethylbenzylamine
DMPA	2,2-Dimethoxy-2-phenylacetophenone
DMS	Dimethyl sulfide
DMSO	Dimethylsulfoxide
DSA	Drop Shape Analysis
EB-1360	EBERCYL® 1360
EG	Ethylene glycol
EGDGE	ethylene glycol diglycidyl ether
EGDMA	Ethyleneglycol dimethacrylate
EHL	Enzymatically Hydrolyzed Lignin
EOM	Extent of Methacrylation
FPInnovations	Forestry Products Innovations
FT-IR	Fourier Transform Infrared
G	Guaiacyl
GI	Grubbs I
GLY	Glycerol
GLYDGE	Glycerol diglycidyl ether
H	*p*-hydroxyphenyl

HDMAP	2-hydroxy-2-methylpropiophenone
in vacuo	In a vacuum
KL	Kraft Lignin
KWF	Aminosilane-Treated Wood Flour
LGA	Lignin-based Hydrogel
LGBA	ABDA polymer grafted lignin
LGEA	AEDA polymer grafted lignin
LGEMA	MAEDA polymer grafted lignin
Lignin-*g*-DHA	DHA-grafted lignin
Lignin-*g*-PS	lignin-graft-polystyre
LPF	Lignin-Phenol-Formaldehyde
LS	Sodium lignosulfonate
LWF	Lignin Amine-Treated Wood Flour
MA	Maleic anhydride
MAEDA	2-methacryloyloxyethyl dehydroabieticcarboxylate
MC	Methacryloyl chloride
Me$_6$-TREN	tris[2-(dimethylamino)ethyl] amine
MeCN	Acetonitrile
MEHQ	Monomethyl ether hydroquinone
MethA	Methacrylic anhydride
MethAcid	Methacrylic acid
ML	Methacrylated Lignin
MR$_{500}$	Mass residue at 500 °C
MT	Million Tons
Mw	Molecular Weight

NEt$_3$	Triethylamine
NL	Nitrolignin
NMR	Nuclear Magnetic Resoance
OIT$_{temp}$	Oxidation Induction Temperature
PA	Propionic anhydride
PAA	Phenolic Aldehyde Amine
PBD-(COOH)$_2$	Dicarboxy-terminated polybutadiene
PBS	Phosphate buffered saline
PEG	Polyethylene glycol
PEI	Polyethyleneimine
PF	Phenol Formaldehyde
PhD	Doctor of Philosophy
phr	Parts per Hundred parts of Rubber
PS	Polystyrene
PU	Polyurethane
PUNL	Nitrolignin-incorporated Polyurethane
PVC	Polyvinyl chloride
RCM	Ring Closing Metathesis
RSM	Response surface methodology
S	Syringyl
SAH	Succinic acid anhydride
SC	Sebacoyl chloride
SL	Soda Lignin
SPF	Sun Protection Factor
SPS	Solvent Purification System

TC	Terphthaloyl chloride
TCI	Tokyo Chemical Industry
T_d	thermal decomposition temperature
TDI	2,4-toluene diisocyanate
T_d onset	Onset decomposition temperature
T_g	Glass transition temperature
TEGDA	Tetraethyleneglycoldiacrylate
TGA	Thermogravimetric Analysis
THF	Tetrahydrofuran
TRS	Totally Reduced Sulfur
UATR	Universal Attenuated Total Reflection
UV	Ultraviolet
UWF	Untreated Wood Flour
WCA	Water Contact Angle
wt%	Weight percent

Dedication

To Ava

Chapter 1

1 General Introduction

1.1 Objective

The overall objective of this PhD project was to synthesize and develop novel advanced functional materials from lignin, a byproduct of the pulp and paper milling industries and an industrial waste material. In this thesis, lignin was chemically modified using a methacrylation process to convert it into a more suitable material for post-modification processes. The methacrylation process was optimized using a response surface method, and the modified lignin was post-modified as part of three different classes of materials: UV-cured coatings, tertiary polyphosphines, and free-standing polyphosphonium films. The synthesized lignin-based tertiary polyphosphines reported in this thesis were probed for their metal-scavenging abilities, and the polyphosphonium films were probed as suitable materials for utilization as potential antimicrobial and controlled drug delivery vehicles.

1.2 Background

Almost all carbon-based products such as synthetic polymers currently used are derivatives of petroleum.[1] This high demand for fossil fuel resources, as well as their high prices and their consequently inevitable depletion, along with their detrimental effects on climate change and the environment, have been the main driving points behind the pursuit of renewable, abundant, and comparably clean alternatives.[2–4] Another critical issue these resources is that their products (e.g. synthetic polymers) are generally resistant to biodegradation, which has resulted in excessive increase of fossil fuel-based waste in the environment.[5] Renewable resources on the other hand have various unique functions and are vastly available, which turn them into viable potential candidates for reducing the cost and improving the properties of existing products derived from non-renewable resources.[6]

Biomass is organic matter available on a renewable basis[7] and can be used to produce fuels, as well as chemicals that are currently being produced from fossil fuel sources.[8] Biomass

also carries significant environmental advantages, such as being carbon neutral and abundant.[9] More than 220 BT of biomass is produced worldwide each year[10,11] from different sources such as grains, sugar and oilseed crops, agricultural residues, food processing wastes (liquid and solid), wood and wood chips, bark, mill residues, forestry residues and by-products (such as lignin), animal fats, manures, algae, and exotic crops (i.e. guayule, jojoba, and euphorbia).[12,13] Each biomass resource, depending on its origin, has varying compositions of three main components: cellulose, hemicellulose, and lignin,[14] while lignocellulosic biomass (woody biomass and crop residues) containing a significant amount of lignin is of particular interest in this thesis work.

Lignocellulosic biomass is the most readily available renewable source of carbon (next to CO_2) and can be used to produce various chemicals.[10,15,16] The term "lignocellulosic biomass", otherwise known as lignocellulose, refers to biomass that comes from plant dry matter (i.e. woody biomass and crop residues)[17] and like any other form of biomass, consists of three major components: cellulose (30 – 50%), hemicellulose (20 – 35%), and lignin (15 – 30%).[18,19]

Cellulose (Figure 1-1A) is perhaps the most well-known constituent of lignocellulose. It is the world's most abundant biopolymer. It has two main structural parts including a crystalline (organized) component and an amorphous (unorganized) section. Strains of cellulose are linked to each other to form cellulose fibrils (bundles), which are usually independent and bound weakly via hydrogen bonding.[20,21]

Hemicellulose (Figure 1-1B) is a complex carbohydrate made of different polymers (i.e. pentoses, hexoses, and sugar acids). While cellulose is made of long unbranched fibrils of glucose, the dominant component of each hemicellulose sample can vary depending on its source. For example, the hemicellulose from hardwoods and agricultural plants (e.g. grass and straw) consists mostly of xylan, whereas hemicellulose from softwood is mainly made of glucomannan.[18,22] One function of hemicellulose is to act as a connection between the cellulose fibres and lignin that increase the rigidity of the cellulose-hemicellulose-lignin network in the plant cell walls.[20]

(A)

(B)

D-Mannose ; **D-Galactose**
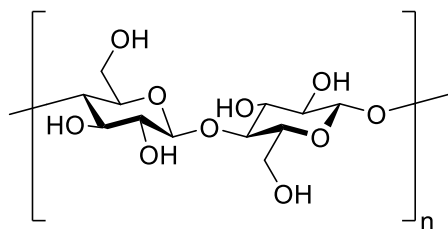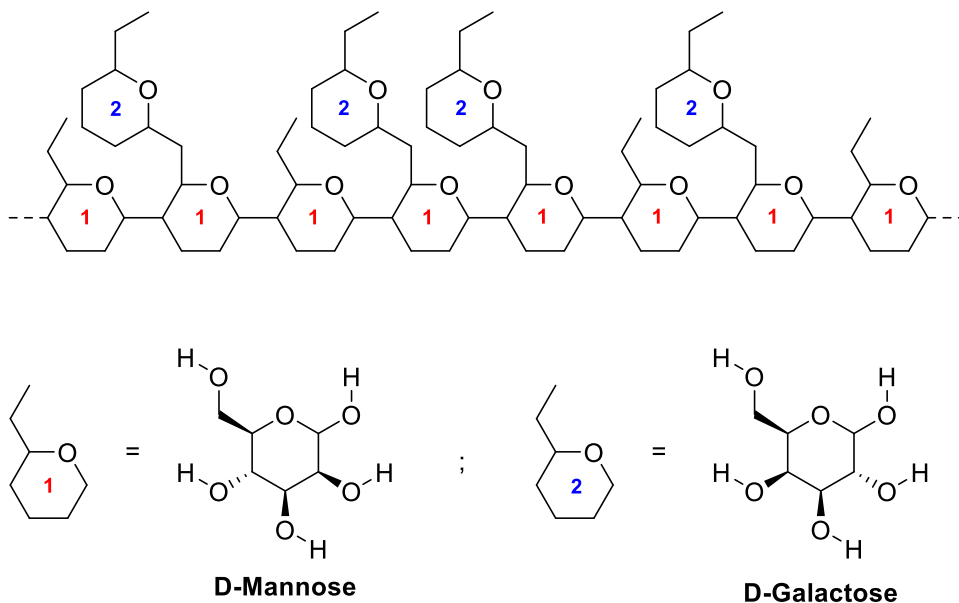
Figure 1-1 Representative chemical structures of cellulose and Galactomannan hemicellulose (typical of Fabaceae seeds).[23] Copyright 2010, reproduced with permission from Annual Reviews.

Last but not least, lignin is the world's second most abundant biopolymer. It is a three-dimensional heteropolymer that occurs naturally through an *in vivo* enzyme-mediated dehydrogenation polymerization process, otherwise known as "lignification".[24] Following the lignification process and during the cell differentiation of plants, lignin is deposited in the cell wall. Lignin is considered responsible for giving structural integrity to plant cells, as well as contributing to the total stiffness of the plants.[25,26] Due to its hydrophobicity, lignin plays a crucial role in transporting water and other nutrients inside the plant while protecting it from insect- or pathogen-invasion.[27,28]

As a byproduct of the pulp and paper milling industry, lignin is today considered an industrial waste, meaning that of the sheer volume of lignin being produced each year, only a small portion (less than 2%) has defined industrial usage and the rest, is either burned as a source of heat or buried in landfill.[29] Facile approaches to utilizing this natural polymer are of utmost importance and can play an important role in the future of sustainable development.

Many reports are available on utilizing lignin as a filler or an additive (without chemical modification) in various systems such as rubber latexes, starch films, and sunscreens.[30–32] However, the main challenge in such incorporations is that valorization processes that don't chemically modify lignin before utilizing it in a system, generally can incorporate limited amounts of the material in their respective systems and the reports on this class of incorporation generally utilize a low percentage of lignin in the final material. On the other hand, various studies have focused on adding value to lignin by chemically modifying the macromolecule to make it a better candidate for incorporation in different systems. Several reactions have been used in this research area such as phenolation,[33,34] esterification,[35–37] and oxopropylation,[38–40] all of which aim at replacing an existing component in a specific system with modified lignin and examining the effect of the replacement. Moreover, lignin has also been utilized in advanced functional materials, where many studies have focused on converting the macromolecule into an advanced system with unique and specific properties such as carbon fibres and nanofibers,[41–44] nanocarriers,[45] and hydrogels.[46–48]

Despite the headway made in upconverting this natural polymer, the material is still woefully underutilized, which highlight the great need for more research in the area of lignin valorization and the development of facile processes capable of converting lignin into new and highly valuable advanced functional systems such as UV-curable coatings, bio-based metal-scavengers, and antimicrobial and controlled drug delivery vehicles, which are targeted in this PhD project.

1.3 Research Objectives

The overall objective of this PhD project was to develop novel, facile processes for the conversion of lignin into high-value materials. This overall objective was achieved by accomplishing the following tasks:

Task 1: Developing a facile methacrylation process for lignin.

Methacrylation was chosen as the desired chemical modification process for the purpose of introducing vinyl groups onto the chemical structure of lignin. Such modification has the ability to convert lignin into a material suitable for post-modification into various useful systems.

Task 2: Optimizing the developed methacrylation process.

Response surface methodology and central composite design were used to accomplish this task, which gave the ability to obtain the maximum possible yield of the desired product (methacrylated lignin) under the optimal process parameters, particularly the reaction time, temperature, and the catalyst/lignin molar ratio.

Task 3: Incorporating the methacrylated lignin into UV-curable coatings.

Introduction of the vinyl groups onto the chemical structure of lignin gave the ability to incorporate the macromolecule as a crosslinked moiety in UV-curable coatings at high percentages (31 wt%).

Task 4: Synthesizing lignin-based polyphosphines.

This task was achieved by performing a hydrophosphination reaction on lignin using phosphine gas, reported for the first time. Utilizing -C-P linkages within the chemical structure of lignin became the first step in synthesizing a new class of advanced functional materials with metal-scavenging abilities from lignin.

Task 5: Synthesizing lignin-based polyphosphonium salts.

This task was achieved by further modifying the synthesized lignin-based polyphosphines. The synthesized polyphosphonium salts were crosslinked to obtain UV-cured free-standing films, which showed promise in being used as antimicrobial surfaces and controlled drug delivery vehicles.

1.4   Scope of Thesis

This thesis focuses on developing strategies for converting lignin, a pulp and paper industry waste, into value-added materials.

Chapter 1 provides a general introduction to bioresources, particularly lignin and the research motivation and objectives, as well as the scope of the thesis.

Chapter 2 presents a detailed introduction of lignin, establishing the significant need for more research in lignin valorization, as well as a comprehensive literature review of the most common lignin valorization procedures and research themes in general, identifying knowledge gaps in this research field.

Chapter 3 describes the synthesis of methacrylated lignin as an approach to introducing UV-curability into the structure of lignin, followed by the comprehensive characterization of the final products. This chapter then reports a modified method developed for the quantification of the hydroxyl functionalities within lignin using a halo-phosphine. The methacrylated lignin preparation procedure, characterization, and analysis data for lignin-incorporated UV-cured coatings containing 10-31 wt.% methacrylated lignin are reported.

Chapter 4 Reports a process optimization study for the synthesis of methacrylated lignin as reported in chapter 3, using response surface methodology, employing a central composite design. Three variables were examined and optimized via the CCD: reaction time, reaction temperature, and catalyst/lignin molar ratio, and their corresponding effects on the recovered mass yield were investigated. The mathematical model derived from the employed CCD was proved accurate in predicting the optimal reaction conditions and consequently, optimizing the recovered mass yield of the lignin methacrylation reaction. The methacrylated lignin synthesized under the optimal reaction conditions was

characterized and proved to be of great promise in a UV-curable coating system at 30 wt.% loading.

Chapter 5 describes the synthesis of primary and tertiary "lignophines", lignin-based polyphosphines. Methacrylated lignin was reacted with phosphine gas to prepare a phosphorus-rich bio-based polymer containing PH/PH_2 functional groups, which were converted to tertiary phosphine units via the phosphane-ene reaction. The synthesized tertiary alkylated lignophine was then probed for its ability to coordinate to transition metals using silver triflate and subsequently, analyzed for its effectiveness in metal sequestration, where it was shown to effectively sequester the Grubbs I catalyst from a ring closing metathesis reaction system under normal laboratory conditions.

Chapter 6 reports the synthesis and characterization of "lignophoniums", lignin-based polyphosphonium networks, from lignophines as synthesized in chapter 5. The lignophonium was then incorporated into siloxane-crosslinked UV-cured free-standing films at 15 wt.% and analyzed with regards to its surface-accessible charge density, water contact angle, cure percentage, and swelling degree and showed great potential as antimicrobial and controlled drug delivery vehicles.

Chapter 7 presents the main conclusions obtained from the research presented in this thesis and suggests future research avenues.

1.5 References

(1)   Sun, N.; Rodríguez, H.; Rahman, M.; Rogers, R. D. Where Are Ionic Liquid Strategies Most Suited in the Pursuit of Chemicals and Energy from Lignocellulosic Biomass. *Chem. Commun.* **2011**, *47* (5), 1405–1421.

(2)   Tester, J. W.; Drake, E. M.; Driscoll, M. W.; Peters, W. A. *Sustainable Energy*; MIT Press, 2012.

(3)   Pandey, M. P.; Kim, C. S. Lignin Depolymerization and Conversion: A Review of Thermochemical Methods. *Chem. Eng. Technol.* **2011**, *34* (1), 29–41.

(4)   Huber, G. W.; Iborra, S.; Corma, A. Synthesis of Transportation Fuels from Biomass: Chemistry, Catalysts, and Engineering. *Chem. Rev.* **2006**, *106* (9), 4044–4098.

(5)   Pan, H. Synthesis of Polymers from Organic Solvent Liquefied Biomass: A Review. *Renew. Sustain. Energy Rev.* **2011**, *15* (7), 3454–3463.

(6)   *Chemical Modification, Properties, and Usage of Lignin*; Hu, T. Q., Ed.; Springer US, 2002.

(7)   Lucia, L. A.; Argyropoulos, D. S.; Adamopoulos, L.; Gaspar, A. R. Chemicals and Energy from Biomass. *Can. J. Chem.* **2006**, *84* (7), 960–970.

(8)   Amen-Chen, C.; Pakdel, H.; Roy, C. Production of Monomeric Phenols by Thermochemical Conversion of Biomass: A Review. *Bioresour. Technol.* **2001**, *79* (3), 277–299.

(9)   Mohan, D.; Pittman, Charles U.; Steele, P. H. Pyrolysis of Wood/Biomass for Bio-Oil: A Critical Review. *Energy Fuels* **2006**, *20* (3), 848–889.

(10)   Zhang, M.-L.; Fan, Y.-T.; Xing, Y.; Pan, C.-M.; Zhang, G.-S.; Lay, J.-J. Enhanced Biohydrogen Production from Cornstalk Wastes with Acidification Pretreatment by Mixed Anaerobic Cultures. *Biomass Bioenergy* **2007**, *31* (4), 250–254.

(11)   Tye, Y. Y.; Lee, K. T.; Wan Abdullah, W. N.; Leh, C. P. The World Availability of Non-Wood Lignocellulosic Biomass for the Production of Cellulosic Ethanol and Potential Pretreatments for the Enhancement of Enzymatic Saccharification. *Renew. Sustain. Energy Rev.* **2016**, *60*, 155–172.

(12)   Rasmussen, H. Carbohydrate Degradation Mechanisms and Compounds from Pretreated Biomass, Technical University of Denmark, Department of Chemical and Biochemical Engineering, **2016**.

(13)   Rossi, A. Fuel Characteristics of Wood and Nonwood Biomass Fuels. In *Progress in Biomass Conversion*; Tillman, D. A., Jahn, E. C., Eds.; Elsevier, **1984**; Vol. 5, pp 69–99.

(14)   Tokay, B. A. Biomass Chemicals. In *Ullmann's Encyclopedia of Industrial Chemistry*; Wiley-VCH Verlag GmbH & Co. KGaA, **2000**.

(15)   Luterbacher, J. S.; Alonso, D. M.; Dumesic, J. A. Targeted Chemical Upgrading of Lignocellulosic Biomass to Platform Molecules. *Green Chem.* **2014**, *16* (12), 4816–4838.

(16)   Lanzafame, P.; Centi, G.; Perathoner, S. Catalysis for Biomass and CO2 Use through Solar Energy: Opening New Scenarios for a Sustainable and Low-Carbon Chemical Production. *Chem. Soc. Rev.* **2014**, *43* (22), 7562–7580.

(17)   Carroll, A.; Somerville, C. Cellulosic Biofuels. *Annu. Rev. Plant Biol.* **2009**, *60* (1), 165–182.

(18)   Feldman, D. Wood—chemistry, Ultrastructure, Reactions, by D. Fengel and G. Wegener, Walter de Gruyter, Berlin and New York, 1984, 613 Pp. Price: 245 DM. *J. Polym. Sci. Polym. Lett. Ed.* **1985**, *23* (11), 601–602.

(19)   Hendriks, A. T. W. M.; Zeeman, G. Pretreatments to Enhance the Digestibility of Lignocellulosic Biomass. *Bioresour. Technol.* **2009**, *100* (1), 10–18.

(20)   Laureano-Perez, L.; Teymouri, F.; Alizadeh, H.; Dale, B. E. Understanding Factors That Limit Enzymatic Hydrolysis of Biomass. *Appl. Biochem. Biotechnol.* **2005**, *124* (1–3), 1081–1099.

(21)   Nishiyama, Y.; Langan, P.; Chanzy, H. Crystal Structure and Hydrogen-Bonding System in Cellulose Iβ from Synchrotron X-Ray and Neutron Fiber Diffraction. *J. Am. Chem. Soc.* **2002**, *124* (31), 9074–9082.

(22)   Saha, B. C. Hemicellulose Bioconversion. *J. Ind. Microbiol. Biotechnol.* **2003**, *30* (5), 279–291.

(23)   Scheller, H. V.; Ulvskov, P. Hemicelluloses. *Annu. Rev. Plant Biol.* **2010**, *61* (1), 263–289.

(24)   Sakakibara, A. A Structural Model of Softwood Lignin. *Wood SciTechnol* **1980**, *14* (2), 89–100.

(25)   Jones, L.; Ennos, A. R.; Turner, S. R. Cloning and Characterization of Irregular xylem4 (irx4): A Severely Lignin-Deficient Mutant of Arabidopsis. *Plant J.* **2001**, *26* (2), 205–216.

(26)   Chabannes, M.; Ruel, K.; Yoshinaga, A.; Chabbert, B.; Jauneau, A.; Joseleau, J.-P.; Boudet, A.-M. In Situ Analysis of Lignins in Transgenic Tobacco Reveals a Differential Impact of Individual Transformations on the Spatial Patterns of Lignin Deposition at the Cellular and Subcellular Levels. *Plant J.* **2001**, *28* (3), 271–282.

(27)   Vermerris, W.; Sherman, D. M.; McIntyre, L. M. Phenotypic Plasticity in Cell Walls of Maize Brown Midrib Mutants Is Limited by Lignin Composition. *J. Exp. Bot.* **2010**, *61* (9), 2479–2490.

(28)   Marton, J. *Lignins Occurence, Formation, Structure and Reactions*; Sarkanen, K. V., Ludwig, C. H., Eds.; Wiley Interscience: New York, **1971**.

(29)   Upton, B. M.; Kasko, A. M. Strategies for the Conversion of Lignin to High-Value Polymeric Materials: Review and Perspective. *Chem Rev* **2016**, *116* (4), 2275–2306.

(30)   Keilen, J. J.; Pollak, A. Lignin for Reinforcing Rubber. *Ind. Eng. Chem.* **1947**, *39* (4), 480–483.

(31)   Baumberger, S.; Lapierre, C.; Monties, B.; Valle, G. D. Use of Kraft Lignin as Filler for Starch Films. *Polym. Degrad. Stab.* **1998**, *59* (1), 273–277.

(32)   Qian, Y.; Qiu, X.; Zhu, S. Lignin: A Nature-Inspired Sun Blocker for Broad-Spectrum Sunscreens. *Green Chem.* **2015**, *17* (1), 320–324.

(33)   Jiang, X.; Liu, J.; Du, X.; Hu, Z.; Chang, H.; Jameel, H. Phenolation to Improve Lignin Reactivity toward Thermosets Application. *ACS Sustain. Chem. Eng.* **2018**, *6* (4), 5504–5512.

(34)   Podschun, J.; Saake, B.; Lehnen, R. Reactivity Enhancement of Organosolv Lignin by Phenolation for Improved Bio-Based Thermosets. *Eur. Polym. J.* **2015**, *67*, 1–11.

(35)   Cachet, N.; Camy, S.; Benjelloun-Mlayah, B.; Condoret, J.-S.; Delmas, M. Esterification of Organosolv Lignin under Supercritical Conditions. *Ind. Crops Prod.* **2014**, *58*, 287–297.

(36)   Thielemans, W.; Wool, R. P. Lignin Esters for Use in Unsaturated Thermosets: Lignin Modification and Solubility Modeling. *Biomacromolecules* **2005**, *6* (4), 1895–1905.

(37)   Gordobil, O.; Herrera, R.; Llano-Ponte, R.; Labidi, J. Esterified Organosolv Lignin as Hydrophobic Agent for Use on Wood Products. *Prog. Org. Coat.* **2017**, *103*, 143–151.

(38)   Bernardini, J.; Cinelli, P.; Anguillesi, I.; Coltelli, M.-B.; Lazzeri, A. Flexible Polyurethane Foams Green Production Employing Lignin or Oxypropylated Lignin. *Eur. Polym. J.* **2015**, *64*, 147–156.

(39)   Nadji, H.; Bruzzèse, C.; Belgacem, M. N.; Benaboura, A.; Gandini, A. Oxypropylation of Lignins and Preparation of Rigid Polyurethane Foams from the Ensuing Polyols. *Macromol. Mater. Eng.* **2005**, *290* (10), 1009–1016.

(40)   Sadeghifar, H.; Cui, C.; Argyropoulos, D. S. Toward Thermoplastic Lignin Polymers. Part 1. Selective Masking of Phenolic Hydroxyl Groups in Kraft Lignins via Methylation and Oxypropylation Chemistries. *Ind Eng Chem Res* **2012**, *51* (51), 16713–16720.

(41)   Park, C.-W.; Youe, W.-J.; Han, S.-Y.; Kim, Y. S.; Lee, S.-H. Characteristics of Carbon Nanofibers Produced from Lignin/Polyacrylonitrile (PAN)/Kraft Lignin-G-PAN Copolymer Blends Electrospun Nanofibers. *Holzforschung* **2017**, *71* (9), 743–750.

(42)   Sadeghifar, H.; Sen, S.; Patil, S. V.; Argyropoulos, D. S. Toward Carbon Fibers from Single Component Kraft Lignin Systems: Optimization of Chain Extension Chemistry. *ACS Sustain. Chem. Eng.* **2016**, *4* (10), 5230–5237.

(43)   Steudle, L. M.; Frank, E.; Ota, A.; Hageroth, U.; Henzler, S.; Schuler, W.; Neupert, R.; Buchmeiser, M. R. Carbon Fibers Prepared from Melt Spun Peracylated Softwood Lignin: An Integrated Approach. *Macromol. Mater. Eng.* **2017**, *302* (4), 629–635.

(44)   Zhang, M.; Ogale, A. A. Carbon Fibers from Dry-Spinning of Acetylated Softwood Kraft Lignin. *Carbon* **2014**, *69*, 626–629.

(45)   Yiamsawas, D.; Beckers, S. J.; Lu, H.; Landfester, K.; Wurm, F. R. Morphology-Controlled Synthesis of Lignin Nanocarriers for Drug Delivery and Carbon Materials. *ACS Biomater. Sci. Eng.* **2017**, *3* (10), 2375–2383.

(46)   Farhat, W.; Venditti, R.; Mignard, N.; Taha, M.; Becquart, F.; Ayoub, A. Polysaccharides and Lignin Based Hydrogels with Potential Pharmaceutical Use as a Drug Delivery System Produced by a Reactive Extrusion Process. *Int. J. Biol. Macromol.* **2017**, *104*, 564–575.

(47)   Feng, Q.; Li, J.; Cheng, H.; Chen, F.; Xie, Y. Synthesis and Characterization of Porous Hydrogel Based on Lignin and Polyacrylamide. *BioResources* **2014**, *9* (3), 4369–4381.

(48)   Larrañeta, E.; Imízcoz, M.; Toh, J. X.; Irwin, N. J.; Ripolin, A.; Perminova, A.; Domínguez-Robles, J.; Rodríguez, A.; Donnelly, R. F. Synthesis and Characterization of

Lignin Hydrogels for Potential Applications as Drug Eluting Antimicrobial Coatings for Medical Materials. *ACS Sustain. Chem. Eng.* **2018**, *6* (7), 9037–9046.

Chapter 2

2 Literature Review

In this chapter, lignin is introduced regarding its origin, biosynthesis, chemical structure, isolation, and annual production and demand, highlighting the need for its valorization. Subsequently, current lignin valorization techniques are fundamentally categorized into techniques without and with chemical modification of lignin and are each discussed in depth. In accordance to the interest of this thesis, valorization techniques employing a chemical modification of lignin are categorized into fragmentation/depolymerization, addition of new chemical active sites, and hydroxyl group modification, and several notable reports for each category are introduced and discussed in detail. Finally, lignin-based materials as the most promising lignin valorization avenue are introduced and knowledge gaps in the field of lignin valorization are discussed.

2.1 Lignin

Lignin is a complex, water-insoluble, amorphous, racemic,[1] and aromatic heteropolymer that has higher carbon and a lower oxygen content compared to the holocellulose (cellulose and hemicellulose) fraction of lignocellulosic biomass and thus, can be an attractive candidate as the feedstock for the production of fuels and chemicals.[2] Lignin is primarily derived from three hydroxycinnamyl alcohol monomers (monolignols): *p*-coumaryl (**2-1**), sinapyl (**2-2**), and coniferyl (**2-3**) alcohol, which only differ in their degree of methoxylation (Figure 2-1).[3]
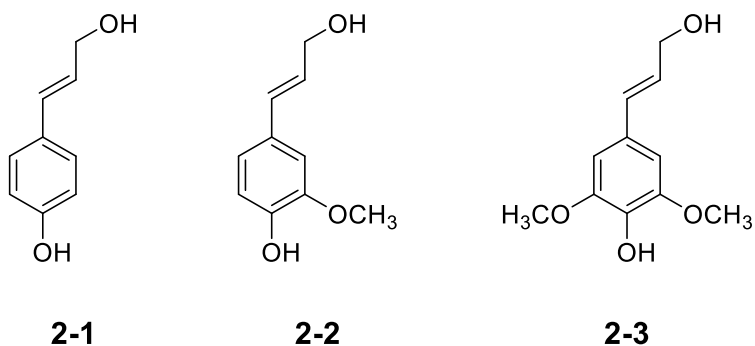
Figure 2-1 Three standard monolignols of p-coumaryl alcohol (**2-1**), coniferyl (**2-2**), and sinapyl alcohol (**2-3**) as the building blocks of lignin.

2.1.1 Biosynthesis of Lignin

As the monolignols are incorporated into lignin, they are turned into corresponding phenylpropanoid units (Figure 2-2) of *p*-hydroxyphenyl (**H**, from *p*-coumaryl alcohol), guaiacyl (**G**, from coniferyl alcohol), and syringyl (**S**, from sinapyl alcohol).
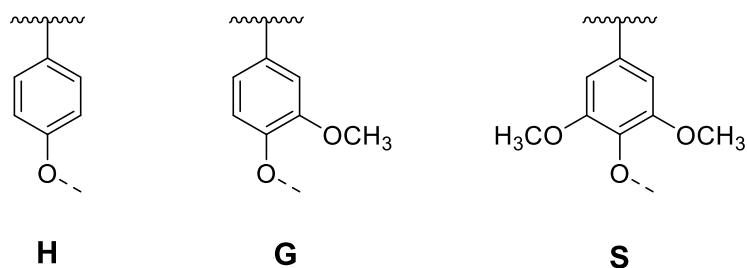
Figure 2-2 Representative general chemical structures for *p*-hydroxyphenyl (**H**), guaiacyl (**G**), and syringyl (**S**) groups.

Lignin is deposited in plants cell walls during the cell differentiation process. As a filler material in the cell walls, lignin is vital to plant life as it is responsible for the structural stiffness of the cells and subsequently, the stiffness of the plants.[4,5]

Depending on the taxon, the cell type, and the individual cell wall layers, the volume, and composition of lignins in different plants can differ, as it can be profoundly affected by environmental and developmental cues.[6] For example, dicotyledonous angiosperm (hardwood) lignins are composed mainly of **G** and **S** units and trace amounts of **H** units,

while gymnosperm (softwood) lignins mostly consist **G** units and low amounts of **H** units. On the other hand, monocot lignins (lignins from grasses) are composed of comparable amounts of **G** and **S** units and have generally higher levels of **H** units than the dicots. These differences in monomer contents lead to subsequent differences in the bonds that are formed during the formation of lignin,[7] which make the task of determining the exact chemical structure of lignin an extremely difficult and maybe even impossible one.

2.1.2 Chemical Structure of Lignin

The *in vivo* enzyme-mediated dehydrogenation polymerization of monolignols to produce the cross-linked amorphous chemical structure of lignin is known as the lignification process.[8] The final chemical structure of lignin as produced through lignification can be best described as a highly branched macromolecular one. This structure consists of phenyl propyl (C9) units that have different functional groups (aliphatic and phenolic hydroxyls, carboxylic, carbonyl, and methoxy) at different sites. The C9 units are connected to each other through various (primarily ether and carbon-carbon) linkages (Figure 2-3).[9] The relative amounts of any linkage in any lignin sample are heavily dependent on each particular monomer's contribution to the lignification process. For example, conifer lignins (mainly composed of **G** units) consist of more β-5, 5-5, and 4-O-5 linkages as compared to lignins that are composed primarily of **S** units, mainly because the C_5 position is available for coupling in **G** units, whereas it is occupied by a methoxyl group in **S** building blocks. In general, the β-O-4 (ether) linkage is considered the most common within lignin and about 50% of the bonds formed during lignification are of this type.[10,11]

Over the years, various characterization methods and spectroscopic techniques have been employed with the purpose of determining the chemical structures of different lignins. However, it is unlikely that the complete chemical structure of any lignin sample will ever be interpreted entirely, primarily due to the unrestrained nature of the lignification process.[12,13] Nevertheless, it is widely accepted that the majority of linkages within the structure are formed through either the coupling of a monolignol to a growing oligomer, or the coupling of one oligomer to another.[14] On the other hand, it is believed that monomer-monomer coupling is a much rarer event than the other previously described couplings

during the lignification process due to the more challenging mechanism of monolignol dimerization.[15,16]
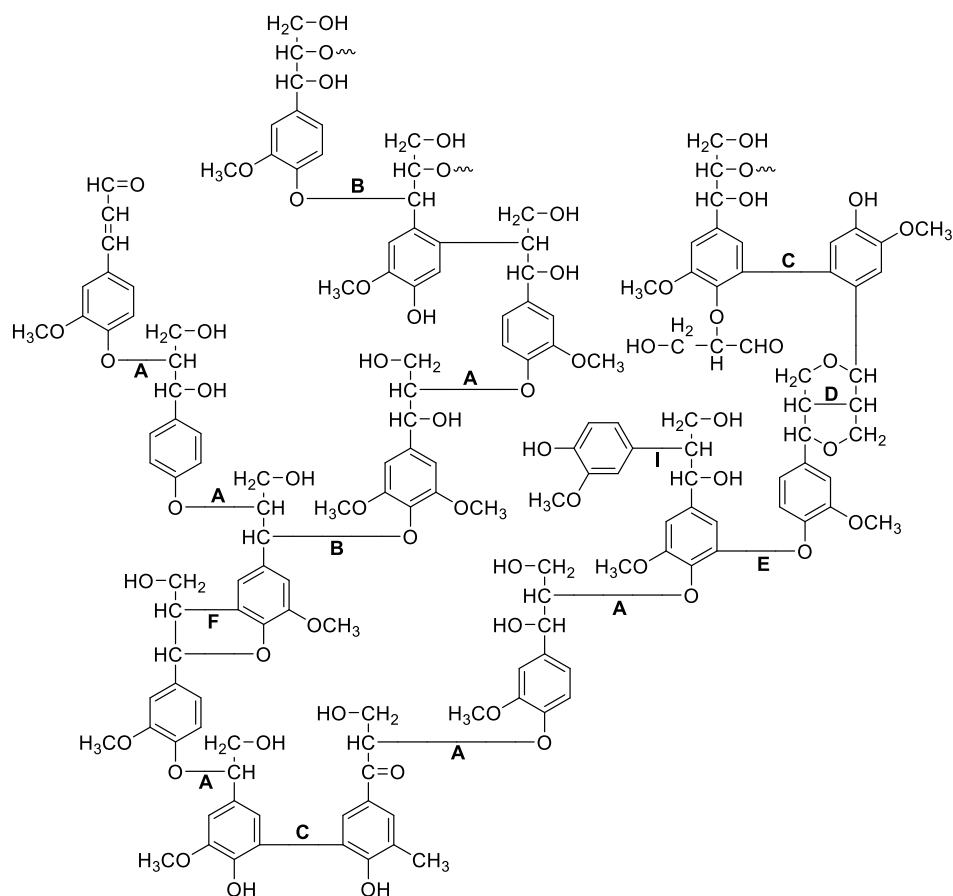
Figure 2-3 Representative general chemical structure of lignin with the most common linkages of β-O-4 (A), α-O-4 (B), 5-5 (C), β-β (D), 4-O-5 (E), β-5 (F), and β-1 (I). Copyright 2014. Reproduced with permission from Elsevier Ltd.

Different conformations can be used to include various structural characteristics of the material according to the purpose of each report. Figure 2-4 shows some of the most common representative structures of lignin proposed in the literature.
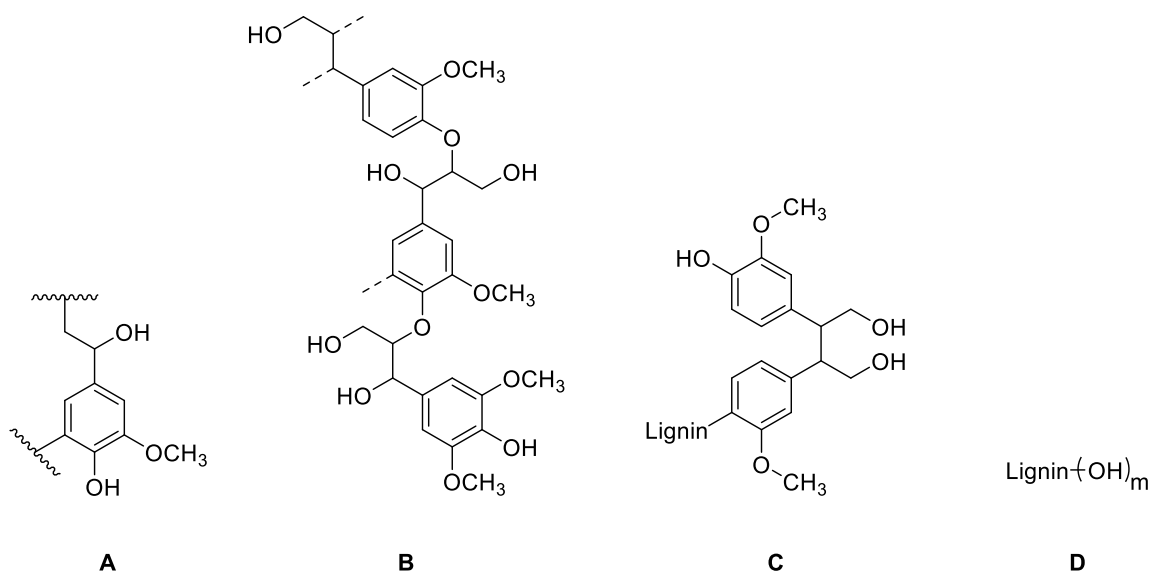
Figure 2-4 Most common representative chemical structures of lignin.

2.1.3 Isolation of Lignin

Lignin is a by-product of the pulp and paper milling industries and its isolation methods, although different in technical aspects, all aim to degrade the chemical structure into smaller fragments that can be dissolved in the pulping media. The chemical and physical properties of the obtained lignin depend on the method of isolation used, as changing the isolation method will lead to a change in properties. Some key factors in measuring the effectiveness of a particular isolation method include the pH of the pulping system, the extent of participation of the solvent and solute in the fragmentation of lignin, and the solubility of the lignin fragments in the solvent employed.[17] Sulfur plays a vital role when it comes to categorizing isolated lignins, whereof the four most common isolation processes in use today, sulfite and kraft processes yield sulfur-containing lignins, while organosolv and soda processes lead to non-sulfur-containing lignins.[18] The lignins obtained from any of the mentioned processes are commonly referred to as technical lignins (technicalignins) and differ in properties such as purity levels, chemical structure, and molecular weight.

The sulfite process uses an aqueous solution of sulfite or bisulfite salts with ammonium, magnesium, calcium, or sodium countercations under heat. Approximately 1000 T of

sulfite lignin is currently being produced every year, worldwide.[19] The obtained lignosulfonates (lignins obtained from the sulfite process) are water-soluble, a property that cannot be found in the other types of technical lignin. The soda process is mainly employed for the pulping of sugarcane bagasse, flax, and all types of non-woody biomass in general. During the soda process, the lignin in the lignocellulosic biomass is dissolved in sodium hydroxide and then recovered through precipitation in acid, maturation of the mixture, and filtration of the precipitate to obtain sulfur-free lignin.[20] The third most common isolation process, the organosolv (Alcell) process, uses an aqueous-organic solvent mixture (e.g. ethanol, acetone, methanol, acetic acid, or formic acid) to simultaneously isolate hemicellulose, cellulose, and lignin in high purities (<1 wt.% carbohydrate content).[21] However, Alcell has not been successfully incorporated as a large-scale industrial process to this date, mainly due to the non-optimized recovery methods for the used materials (e.g. solvents), leading to relatively higher process costs when compared to the other isolation processes.[22]

Finally, the kraft process (kraft pulping) uses an aqueous solution of sodium sulfide and sodium hydroxide (white liquor) to fragment the lignin. The fragmentation is conventionally followed by a three-phase delignification process (separation of the lignin fragments from the cellulose and hemicellulose) occurring in the initial (150 °C, diffusion-controlled), bulk (150-170 °C, chemical reaction-controlled), and final/residual phases, with the most lignin removed during the bulk phase.[23,24] Over the past decade, several improved separation processes have been reported for the kraft pulping which have significantly enhanced and optimized the global production of kraft lignin. Systems such as Westvaco, LignoBoost, and LignoForce are the major processes developed to improve the production of kraft lignin, among which the LignoBoost system is currently the one employed the most. The LignoBoost system can produce a high purity product through displacement washing. More precisely, in this system lignin is first precipitated in acidic media (CO_2) and then filtered. Afterwards, the filtered cake is re-dispersed at pH = 2-4 to form a suspension, which is then filtered again and washed through displacement washing to obtain kraft lignin.[25] On the other hand, The LignoForce system includes an oxidation stage, where the black liquor is oxidized under controlled conditions before acidification. As a result, the precipitated lignin in the acidic media has better filterability. The

LignoForce system has better potential in reducing the TRS (totally reduced sulfur) compounds in the obtained kraft lignin and can also reduce SO_2 emissions as compared to the other systems, which has led to increased interest from the pulping industries towards this system in the past few years.[26]

2.1.4 Annual Production and Demand

It is estimated that approximately 56.8 BT of biomass is annually produced worldwide and while the primary target application for the produced biomass is the energy sector (biofuels), this production volume is deemed not enough to cover the entire energy needs for sustainable energy production. However, the produced biomass can perfectly cover the world's chemical needs in terms of feedstocks and thus, developing methods for converting biomass and its resulting feedstocks into materials that are today produced from non-renewable sources is believed to be a viable approach towards sustainability, potentially capable of completely relieving the materials production industries of their dependence on fossil-based resources.[27–29] As one of the major constituents of biomass and simultaneously the least utilized, it is estimated that approximately 50-55 MT of technical lignin is produced worldwide, annually which highlights the role of lignin valorization (adding value) in sustainable development.[30,31]

The major source of technical lignin in North America is kraft lignin. As the main internal source of energy, kraft pulp mills fire the black liquor into the recovery boiler to generate energy and recover the pulping chemicals, which has over the years helped them become completely independent and sustainable in terms of operational energy needs. However, over the past 30 years, the production at these mills have outgrown the increase in their need for energy, which has led to the recovery boiler becoming the production bottleneck and in constant need of offloading. Thus, these pulp mills have been removing tons of kraft lignin from the black liquor in their recovery boilers as means of offloading them. It has been determined that a typical kraft pulp mill can produce an additional ton of pulp for every ton of lignin that is removed from the recovery boiler[26] and given that the kraft pulp mills around the globe are producing more than 130 MT kraft pulp annually[32], kraft lignin has now become part of the product stream at many kraft pulp mills, especially in North America. This highlights the importance of discovering viable methods to convert kraft

lignin into materials of higher value (value-added materials). Valorizing lignin as a sustainable bio-based material will not only have significant environmental benefits; it will also add a new and valuable stream of income to the kraft pulp mills and can eventually be the potential next leap into a sustainable future.

2.2   Valorization of Lignin

The current strategies for valorizing lignin can be best categorized based on whether or not chemical modification (by using in a chemical reaction) is implemented. Scheme 2-1 describes the general global algorithm for the valorization of lignin.
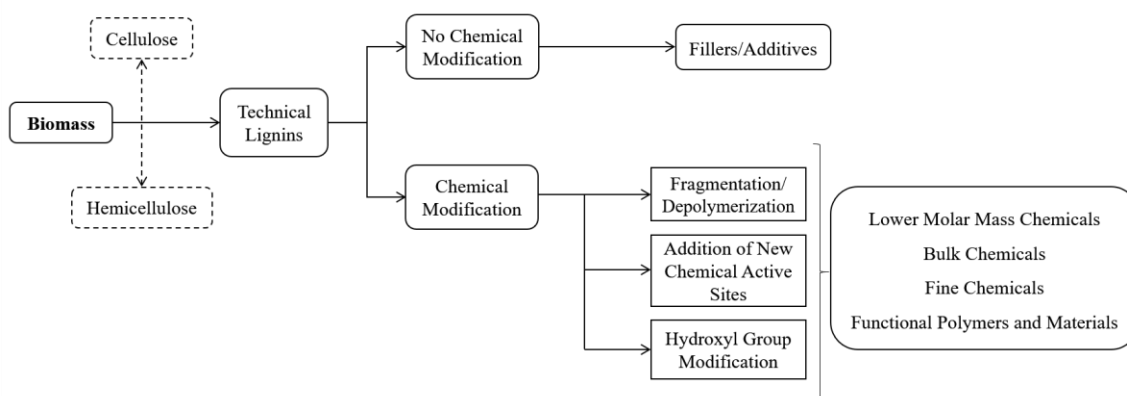
Scheme 2-2-1 General scheme of current valorization processes employed for lignin.[33] Copyright 2014. Reproduced with permission from Elsevier Ltd.

2.2.1 Valorization of Lignin Without Chemical Modification

Historically, valorization strategies in which lignin did not undergo chemical modification have been around for much longer than their counterparts (strategies that included chemical modification). Because of the unique physical and chemical properties of lignin, the first attempts at adding value to it focused on physical-blending as a bulk material. Properties such as hydrophobicity, thermal stability, thermo-oxidation resistance, UV-absorption, and having a highly crosslinked structure were the major ones that made lignin a suitable component as a filler in such blends.

Reports on utilizing lignin as a filler/additive material date back to mid-1900s, where in 1948 Keilen and Pollak[34] incorporated up to 38.5% lignin into natural and synthetic rubber

latexes via coprecipitation and reported that the resulting rubbers showed superior abrasion resistance, tensile strength, and tear resistance in comparison rubber made with conventional inorganic fillers. Years later, in 1998, Baumberger *et al.*[35] used lignin as a filler in starch films to overcome the high swelling degrees and the partial dissolution of starch films in a moist environment, caused by the hydrophilicity of starch. As a naturally hydrophobic filler, up to 30 wt.% lignin was incorporated into the starch films through mixing with wheat starch by extrusion and subsequent thermal molding or casting of the films. They reported that incorporation of up to 20% lignin into starch films at 58% relative humidity had a negligible effect on film elongation and stress at break, whereas it reduced the water affinity of the prepared films noticeably. However, they also determined that at 71% relative humidity and up to 30% incorporated lignin, the resistance to elongation decreased significantly in the prepared films, likely due to the incompatibility between the hydrophilic starch and the hydrophobic lignin components.

Lignin has also been probed as an excellent antioxidant filler/additive. Kosikova *et al.*[36] reported that using up to 30 phr (parts per hundred parts of rubber) of lignin as a filler in natural rubber-based composites significantly improved their resistance to thermo-oxidative degradation. Moreover, they reported that other physiochemical properties such as elongation, 100% modulus, and the tensile strength at break were improved in the prepared composites by the addition of lignin. Moreover, Sadeghifar and Argyropoulos[37] determined that the antioxidant properties of lignin are highly correlated with the number of phenolic hydroxyl groups on its chemical structure, due to the free radical-scavenging nature of these groups. They utilized lignin samples containing different amounts of phenolic hydroxyl functionalities as fillers in polyethylene blends to determine the effect of such combinations on the oxidation induction temperature (OIT_{temp}) of the prepared blends. Consequently, they discovered that using acetone soluble softwood kraft lignin (ASKL) as the filler in the polyethylene blends increased their OIT_{temp} by 50 °C in comparison to when acetone insoluble kraft lignin (AIKL) was used and concluded that lignin samples with higher phenolic hydroxyl contents showed significantly improved antioxidant properties, as the ASKL contained 54% more phenolic units than the AIKL sample.

Lignin has also been utilized as an additive in sun blocker materials. With chromophores such as phenolic and ketone functionalities present in its chemical structure, lignin can act as a natural broad-spectrum sun blocker. Qian *et al.*[38] reported that lignin could be utilized as an additive (2-10 wt%) suitable for commercial sunscreens. They blended dry, finely powdered lignin with pure creams (NIVEA Cream-N moisturizing cream and LIFE glycerin hand cream) at 1000 rpm for 24 h and measured the UV-transmittance and the sun protection factor (SPF) of the obtained lotions in comparison to commercial sunscreen (BIOTHERM and LIFE SPF 15, 30, and 50) lotions. They reported that while the blend of pure cream and 10 wt% lignin had higher UV-transmittance than that of LIFE SPF 15 sunscreen, it showed lower transmittance in the UVA area (especially at 385-400 nm) which, along with the fact that the lignin sunscreen at 10 wt% lignin contained less active ingredient than the SPF 15 sunscreen, were taken as evidence towards the suitability of lignin as a natural candidate for broad-spectrum sunscreens. Furthermore, they reported that adding 2 wt% of lignin to SPF 15 commercial sunscreen lotions resulted in their sunscreen effect to increase to that of SPF 30 sunscreen lotions of the same brands. Finally, adding 10 wt% lignin to the SPF 15 lotions resulted in them out-performing the sunscreen effects of SPF 50 sunscreen lotions of the same brands. Thus, they concluded that lignin can be probed both as the sole active ingredient or in parallel with other active ingredients in commercial sunscreen lotions. However, lignin has a dark-brown color, which can potentially have an adverse effect on developing a commercial lignin-mixed sunscreen lotion, which might very well be the main reason why lignin has not yet been utilized in sunscreen lotions on a commercial level.

Lignin has also been utilized as an additive to improve the flame retardance of target polymer networks. With an aromatic ring-rich chemical structure, lignin shows relatively high char formation and thus, has been utilized as an additive to promote char formation in different blends. De Chirico *et al.*[39] examined the effect of using lignin as an additive in polypropylene blends on the final material's flame retardancy. They used thermogravimetric analysis (TGA) to compare the char formation in polypropylene networks containing known flame retardants (melamine phosphate, ammonium polyphosphate, aluminum hydroxide, and poly(vinyl alcohol)) to the same values in polypropylene networks containing known mixtures of the mentioned flame retardants and

lignin. Thus, they discovered that adding up to 15 wt% lignin to polypropylene networks that already contain one of the mentioned flame retardants, improved the char formation in the resulting networks by up to 6 wt%. Furthermore, they reported that the networks that were only incorporated with lignin had higher char formations compared to when melamine phosphate, aluminum hydroxide, or poly(vinyl alcohol) was used, although they showed a lower char formation than when ammonium polyphosphate was used in the blends.

Although promising, the utilization of lignin into existing systems as an additive, without any chemical modification, has been proved to be somewhat limited in terms of target applications and/or only applicable to blends with relatively low sensitivity (e.g. rubbers) and not capable of adding refined properties to the final products. These limitations amplify the need to modify lignin into a compound that can be incorporated into the backbone of various systems in large percentages and thus, take full advantage of the unique properties and the rich chemical structure of this natural polymer.

2.2.2 Valorization of Lignin with Chemical Modification

Given the interesting chemical structure of lignin and the abundance of different functional groups on its structure, many researchers have examined modifying such groups by chemical reactions. Overall, the examined approaches toward chemically modifying lignin can be divided into 3 main categories of fragmentation/depolymerization, synthesis of new chemically active sites, and hydroxyl group modification which are herewith discussed in detail.

Fragmentation/Depolymerization

Lignin has been the subject of several fragmentation/depolymerization processes, e.g., hydrolytic/reductive/oxidative de-polymerization and pyrolysis, mainly to produce lower molar mass chemicals and/or fuels.

Among all the reported fragmentation processes for lignin, pyrolysis is the most studied. Generally, pyrolysis refers to the thermal treatment (thermolysis) of an organic compound in the absence of air, with or without a catalyst, to break down its molecular structure into

smaller substructures while disallowing further combustion to carbon dioxide. Depending on the pyrolysis conditions, the dominant product from pyrolyzing lignin can be a liquid (pyrolysis oil) or a gas and increasing the time and temperature of pyrolysis will typically cause lignin to fragment into components with lower molecular weights.[40,41] Several factors such as feedstock's origin[42], reaction temperature[43], heating rate, and the use of additives[44] can affect the pyrolysis of lignin. Nonetheless, lignin pyrolysis produces gaseous hydrocarbons, carbon monoxide, carbon dioxide, volatile liquids (e.g. acetone, acetaldehyde, and methanol), monophenolic compounds (guaiacol, syringol, cathecol, and phenol) and several other polysubstituted phenols as its products.[45] The liquid product of pyrolysis, i.e., pyrolysis oil, typically consists of about 20% aqueous compounds (acetone, acetic acid, methanol, and water) along with about 15% tar (condensed volatiles yielding phenolics, primarily).[46] Figure 2-6 depicts the primary aromatic compounds that can be obtained from the pyrolysis of lignin.
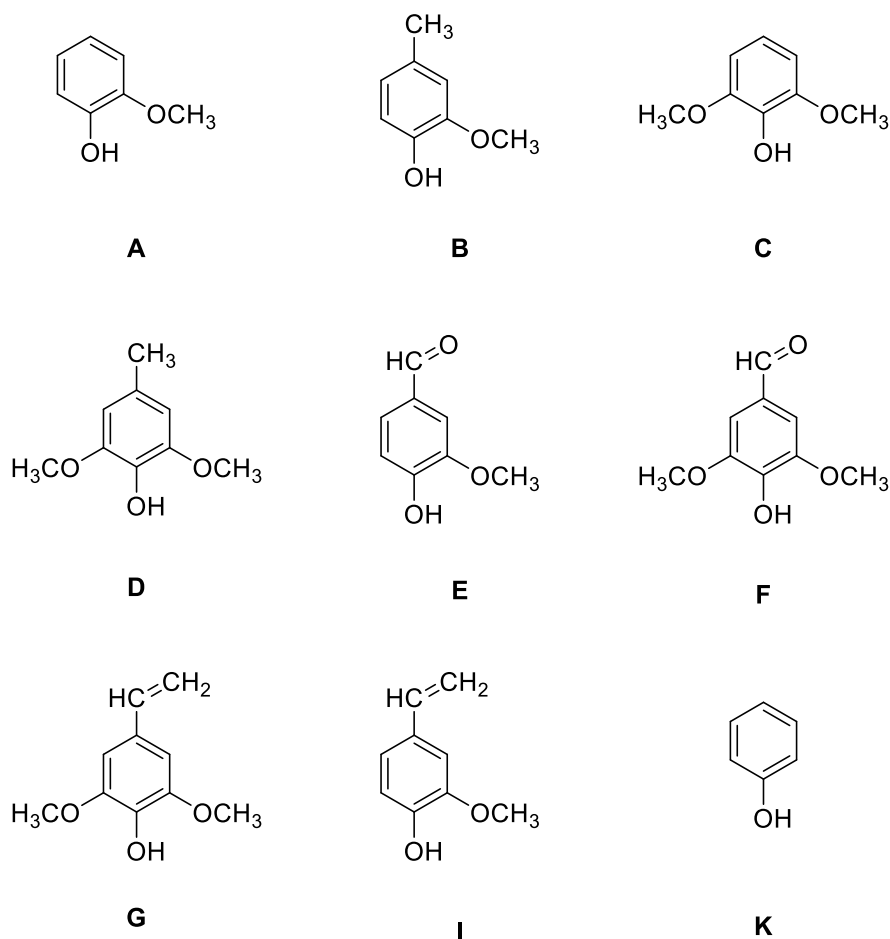
Figure 2-5 Major products obtained from the pyrolysis of lignin: guaiacol (**A**), methyl guaiacol (**B**), syringol (**C**), methyl syringol (**D**), vanillin (**E**), syringaldehyde (**F**), vinyl syringol (**G**), vinyl guaiacol (**I**), and phenol (**K**).[47]

In addition to the mentioned products, a group of thermally stable fractions, commonly known as char, can also be obtained from the pyrolysis of lignin, the yield of which has a reverse correlation with the pyrolysis temperature.[48]

The pyrolysis of lignin happens over a wide range of temperatures (100-900 °C)[49] with different products being yielded at different temperature ranges. For instance, formic acid, formaldehyde, carbon dioxide, carbon monoxide, and water can be obtained at a relatively lower temperature range (120-300 °C) as compared to the other pyrolysis products. The type of obtained products can be attributed to the type and subsequently the strength of the bonds being cleaved during the pyrolysis. For example, aryl ether linkages (e.g. β-O-4) are

relatively easier to break during thermal treatment than ether linkages at γ carbons, which are themselves more easily broken than methoxyl groups. While every lignin sample follows the same general trend in terms of the obtained pyrolysis products, the yield of each product and the specific temperature range for obtaining it differs depending on the type of lignin used.[43,49–51] An excellent example for temperature-specific pyrolysis products was reported by Liu *et al.*[52] where they used coupled TGA-FTIR to determine the temperature ranges of different pyrolysis products of birch and fir strong acid detergent fiber lignins. They reported that at around 100 °C, carbon dioxide and water were obtained as the first products of the pyrolysis process for both samples, followed by the production of carbon monoxide, formic acid, aldehydes, and phenols, along with more water and carbon dioxide at around 225 °C. The vast amounts of monomeric phenols obtained at 225 °C were attributed to the breakage of ether linkages and although the same products were obtained for both samples at this temperature, they observed a more obvious peak for carbon monoxide in birch lignin compared to fir lignin, which they took as evidence toward the lateral chains being more easily broken in the birch lignin samples. Furthermore, they reported that hydrocarbons (primarily methane), methanol, carbon monoxide, and carbon dioxide were the major products at temperatures around 375 °C for fir lignin and 425 °C for birch lignin.

Principally, pyrolysis can be categorized into conventional (slow) and flash pyrolysis in terms of the heating rate. In slow pyrolysis, such as the one reported by Liu *et al.*[52] earlier, the heating process of lignin happens at a much lower rate than in flash pyrolysis, with a vapor residence time varying anywhere from 5 to 30 minutes and thus, the components in the vapor phase of slow pyrolysis will have more time to react with each other and subsequently, form more char and gaseous components. On the other hand, the higher heating rates of flash pyrolysis lead to vapor residence times of 2 seconds, which make it possible to produce a predominantly liquid product (bio-oil) with a yield of up to 75 wt%. The generated bio-oil and char can both be employed as fuels, and the produced gas can be recycled back into the process. However, despite the high interest in pyrolysis and especially flash pyrolysis over the past 20 years, it has yet to become a viable process for valorizing lignin, as the produced bio-oil contains significant amounts of oxygen-

containing compounds that are corrosive, less stable, and contain a lower heating value. Thus, pyrolysis has yet to become a valorization process capable of taking full advantage of the complex chemical structure of lignin in its entirety.[43,53–55]

Oxidation is another well-studied fragmentation method of lignin, primarily for obtaining phenolic compounds of lower molar masses, such as phenolic aldehydes (vanillin and syringic) and their acids (vanillic and syringic).[56] Several oxidants have been reported to effectively oxidize lignin into such compounds, including oxygen, air, nitrobenzene, and metal oxides. Vanillin (4-hydroxy-3-methoxybenzaldehyde) is the most valuable product that has been obtained from the oxidation of lignin, and successful high-yield vanillin isolation has over the years been the primary goal of most lignin oxidation studies.[57–61]

Villar *et al.*[62] reported that the oxidation of lignin at 170, 180, and 190 °C under oxygen pressures of 10, 12, and 15 atm yielded syringaldehyde, vanillin, syringic acid, and vanillic acid with the total yields ranging between 4-11%. They reported the maximum conversion of 11% at 190 °C under 12 atm of oxygen. Furthermore, they examined the same oxidation processes in the presence of Co(II) salen (N,N'-bis(salicynidene)ethylenediamine monohydrate), $CuSO_4.5H_2O$, $CoCl_2$, and two commercial platinum-alumina (referred to as A and B due to their proprietary compositions) catalysts and determined that the addition of catalysts did not have a positive effect on fragmentation into the mentioned products, particularly the aldehydes. Thus, they concluded that at the optimal oxidation conditions under oxygen, the maximum yield of aldehydes was approximately 4%. In a separate study, Villar *et al.*[63] examined the oxidation behavior of kraft lignin using nitrobenzene and copper(II) oxide at 170, 180, and 190 °C for 10-120 minutes. For nitrobenzene, oxidant/lignin ratios (v/w) of 6.3, 9.4, and 12.6 were examined, and CuO/lignin molar ratios of 1.33, 2.66, and 3.99 were chosen for oxidations using copper(II) oxide. They reported that at the optimal oxidation conditions, lignin conversion was 23% with nitrobenzene (14% aldehyde yield) and 13% with copper(II) oxide (8% aldehyde yield). Optimal oxidation conditions as reported in this study were 40 min, 190 °C, and 6 (mL nitrobenzene/g lignin) for nitrobenzene and 70 min, 190 °C, and 4 (mol CuO/mol lignin) with copper(II) oxide.

While the oxidation of lignin has proven to be especially viable for producing aldehydes, specifically vanillin and syringaldehyde, both the total conversion of lignin to fragmented molecules and the aldehyde yields remain at relatively low percentages to date, which means that most of the lignin incorporated in such oxidation processes will still be depleted as process waste. Thus, much like pyrolysis, oxidation is yet to become a viable process capable of converting lignin to positive-value products at high conversion percentages.

More recently the Xu group developed highly efficient processes for depolymerization of kraft lignin based on hydrolytic reactions[64] or reductive reactions.[65] Kraft lignin was effectively depolymerized into polyols of moderately high hydroxyl number and yield with moderately low weight-average molecular weight (Mw) via direct hydrolysis using NaOH as a catalyst.[64] The best operating condition was found to be at 250 °C, 1 h, and NaOH/lignin ratio $\approx$ 0.28 with 20 wt% substrate concentration, leading to <0.5% solid residues and ~ 92% yield of depolymerized lignin (aliphatic-hydroxyl number $\approx$ 352 mgKOH/mg and Mw $\approx$ 3310 g/mole), suitable for replacing polyols in polyurethane foam synthesis. In the latter work, formic acid was employed as an in-situ hydrogen donor for the reductive de-polymerization of kraft lignin. Under the optimum operating conditions, i.e., 300 °C, 1 h, 18.6 wt.% substrate concentration, 50/50 (v/v) water-ethanol medium with formic acid at a formic acid-to-lignin mass ratio of 0.7, kraft lignin (Mw ~10,000 g/mol) was effectively de-polymerized, producing de-polymerized lignin (Mw 1270 g/mol) at a yield of ~90 wt.% and <1 wt.% yield of solid residue.[65]

Addition of New Chemical Active Sites

The generally high waste production and relatively low yield of the fragmentation processes, plus their inability to benefit from all that the chemical structure of lignin can offer, has led to much interest being placed on modifying the functional groups present on lignin, namely hydroxyl, methoxy, carbonyl, and carboxyl groups, with the purpose of increasing its reactivity. Adding/synthesizing new chemical active sites through modifying lignin can enhance its incorporation behavior in various systems. This section will address the studies on reactions employed for modifying the functional groups on the structure of lignin, namely alkylation/dealkylation, hydroxyalkylation, amination, and nitration.

Chemical modification of the hydroxyl groups of lignin will be discussed in a separate section, due to the relatively higher importance of this type of modification and its closer relevance to this thesis.

Alkylation of lignin is an essential class of chemical modification employed for this material. Most alkylation processes include pre-treatment of the lignin samples to fractionate their structure and decrease their molecular weight to increase their solubility in common organic solvents.[66,67] On the other hand, a lignin dealkylation process was developed by Gaylord Chemical (US)[68], in which the demethylation of lignin is employed for producing dimethylsulfoxide (DMSO). During this process, lignin is reacted with molten sulfur in basic media, and dimethyl sulfide (DMS) is synthesized via the transfer of two methyl groups from lignin to sulfur, which is then oxidized using nitrogen dioxide to produce DMSO (Scheme 2-2).[68]

Scheme 2-2 Synthesis of dimethylsulfide (DMS) from lignin and molten sulfur and subsequent oxidation to dimethylsulfoxide (DMSO).[69] Copyright 2010, reproduced with permission from John Wiley and Sons.

However, as shown in Scheme 2-2, the only remaining components of lignin in the final product of this process are the two methyl groups that were used in the synthesis of dimethylsulfide and DMSO, most of the lignin used in this process is still being disposed of as process waste. Other processes are today available that aim to utilize demethylated lignin in a less wasteful manner. For example, Liu *et al.*[70] prepared a formaldehyde-free water-resistant wood adhesive, using alkaline demethylated kraft lignin (DKL) and polyethyleneimine (PEI), where the demethylated lignin was prepared by suspending DKL

in water, dissolving the suspension in sodium hydroxide, and freeze-drying the obtained solution. DKL-PEI wood adhesive samples were then prepared through mixing the DKL (14-25 wt%) and PEI in water for 2-120 minutes. It was reported that at DKL percentages higher than 25 wt%, the resulting adhesives became too viscous to be uniformly applied to the wood's surface. Afterwards, the adhesive was applied to two layers of maple veneer boards, lapped together, and cured using a hot-press. It was reported that at the DKL percentage of 20 wt% and PEI samples with $M_w = 750,000$, with the hot-press duration of 5 minutes at 120 °C, the shear strength of the bonded lap-shear specimens (calculated using the maximum force at breakage for each bonded lap-shear sample) was the highest (7 MPa). This report, despite the multi-step pre-treatment procedure for preparing the DKL and the relatively low weight percentages of the demethylated lignin in the adhesives, can be counted among the more viable approaches to valorizing lignin and can also highlight the potential benefit of chemically modifying lignin as the first step in incorporating it in different systems.

Apart from the several reports available on incorporating dealkylated lignin in wood adhesives, such as the one discussed earlier by Liu and Li,[70] the abundance of phenolic groups on lignin has made it a desirable substitute for the non-renewable phenol in phenol formaldehyde (PF) resins and other adhesives.[71–73] Notably, the structural similarities between lignin and phenol, along with their comparable reactivities with formaldehyde, marks an interesting potential application for lignin in the production of lignin-phenol-formaldehyde (LPF) resins.

Alonso *et al*.[74] hydroxymethylated (methylolated) softwood ammonium lignosulfonate by dissolution in an 8% NaOH solution at 80 °C, followed by reaction with formaldehyde at room temperature (Scheme 2-3). They later probed the ability of this metholylated lignosulfonate to partially substitute the phenol in PF resins through a comparative study with a commercial resol phenolic resin. They determined that the maximum possible percentage of incorporated methylolated lignosulfonate in the PF resins that would keep different properties of the prepared LPFs (pH, free phenol, viscosity, and gelation time) comparable to the commercial PF resin, and in compliance with the requirements for utilization in plywood manufacture, was 35%.[75]
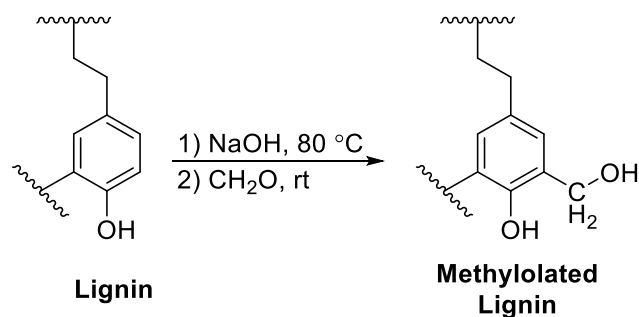
Scheme 2-3 Hydroxymethylation of lignin as reported by Alonso *et al.*

Amination is another class of reactions performed on lignin to introduce new chemical active sites on its structure. Principally, the amination of lignin is carried out using the Mannich reaction.[76] Matsushita and Yasuda[77] used 1-guaiacyl-1-*p*-hydroxyphenylethane as a model compound in a reaction with dimethylamine and formaldehyde in acetic acid and dioxane and reported that as resulted by the Mannich reaction, the aminoethyl group was introduced onto the model compound at the ortho position to the phenolic hydroxyl groups, giving 4 different products (Scheme 2-4), proposing that the same procedure can be utilized for the amination of lignin itself.

1-guaiacyl-1-*p*-hydroxyphenylethane
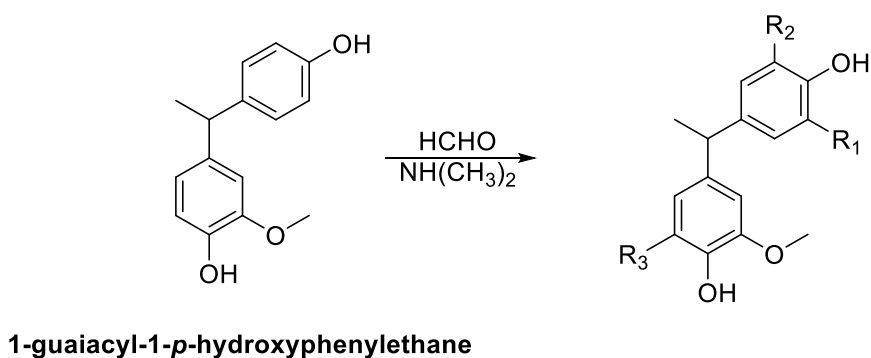
Scheme 2-4 Representation of the amination of the lignin model compound 1-guaiacyl-1-*p*-hydroxyphenylethane with formaldehyde and dimethylamine as reported by Matsushita and Yasuda. 4 products were isolated from this reaction: R_1 = -CH$_2$N(CH$_3$)$_2$, $R_{2,3}$ = H; $R_{1,2}$ = H, R_3 = -CH$_2$N(CH$_3$)$_2$; $R_{1,3}$ = -CH$_2$N(CH$_3$)$_2$, R_2 = H; $R_{1,2,3}$ = -CH$_2$N(CH$_3$)$_2$.[77]

Yue *et al.*[78] reacted fractionated softwood soda lignin (SL) with diethylenetriamine (DETA) and formaldehyde at a controlled pH of 11.5 to obtain lignin amine. Afterwards,

they examined the effects of using the lignin amine in the surface treatment of wood flour by preparing similar PVC composites from untreated wood flour (PVC-UWF), lignin amine-treated wood flour (PVC-LWF), and aminosilane-treated wood flour (PVC-KWF). They reported that the optimal lignin amine loading percentage for the PVC-LWF composites was at 2%, where the tensile strength in the PVC-LWF composites increased from 35 MPa to 42.5 MPa and their impact strength increased from 27.5 kJ/m^2 to 37.5 kJ/m^2. However, they determined that using aminosilane, the same increases can be achieved in the PVC-KWF composites at 1% loading. Furthermore, they evaluated the water absorption behaviors of the composites after 10 days immersion and determined that again, while both lignin amine and aminosilane decreased the weight gain of the composites by ca. 3%, similar decrease in weight gain was observed at 1% aminosilane loading and 2% lignin amine loading. Thus, based on the data reported by Yu *et al.* aminosilane outperforms lignin amine as the surface treatment agent. In addition to the low loading percentages generally reported for utilization of aminated lignin, to the best of our knowledge, no report is to date available on amination and utilization of non-fractionated lignin.

The last major class of chemical active site synthesis reactions of lignin is nitration. However, fewer reports are available on this method compared to the previously discussed ones.[79,80] Zhang and Huang[81] synthesized nitrolignin (NL) in the form of a "reddish-brown powder" through reacting alkali lignin with nitric acid and acetic anhydride and determined the nitrogen content of the synthesized NL sample to be at 6.32% using elemental analysis. They subsequently incorporated the synthesized NL samples at weight percentages from 1.4-6 wt% into polyurethane networks (PUNL) and determined that at 2.8% NL loading, both the tensile strength and the breaking elongation of the PUNL networks were 2 times higher than that of standard polyurethane (PU) networks. Loadings higher than 2.8% however, resulted in a decrease in the mentioned values. Much like amination, the product of the nitration of lignin is yet to be probed as a viable nitrogen-containing replacement with high loadings in materials.

The route of synthesizing new chemical active sites on lignin poses the potential for producing chemically modified lignin with the ability to be utilized in some common

industrial materials, mainly through dealkylation and hydroxymethylation of lignin,[70,75] as these two reactions have shown promising results with acceptable loading percentages, while the other reported chemical modifications either use lignin as a source for functional groups and treat the rest of the macromolecule as waste,[68] or fractionate the structure and employ only a fraction of it,[78] or are not yet able to utilize the chemically modified lignin in the target systems at appreciable loading percentages.[79–81] However, when it comes to chemical modification, there is another functionality within the chemical structure of lignin with considerably higher reactivity than the other functional groups discussed, the hydroxyl groups.

Hydroxyl Group Modification

As the most reactive sites within the structure of lignin, the various types of hydroxyl groups have been the subject of numerous studies.[82–86] With the densely crosslinked structure of lignin and its subsequent relatively limited solubility in common organic solvents, such modifications can positively affect the solubility and thus, the reactivity of lignin in these solvents and provide potential routes for incorporating this sustainable natural polymer, in its entirety, in different supramolecular systems.[12,87,88] Processes such as esterification, phenolation, and etherification, and the corresponding incorporations of the modified lignins in materials (where applicable) are discussed in this section as the most promising approaches toward this goal.

Esterification reactions are perhaps the most straightforward chemical modifications that can be employed for lignin, as these reactions often require relatively mild conditions to produce esterified lignin. Commonly, acyl anhydrides, acyl chlorides, and acidic compounds are used as the modifying reagents in these types of reaction, using a base (e.g. triethylamine, 1-methylimidazole, and potassium hydroxide) in catalytic amounts. As a result, numerous reports are available regarding the esterification of the hydroxyl functionalities within lignin.[89–97]

Guo and Gandini[98] esterified kraft lignin using two different diacyl chlorides, sebacoyl chloride (SC) and terphthaloyl chloride (TC), and triethylamine as the base, followed by copolymerization with polyethylene glycol (PEG) to obtain TC-based and SC-based lignin

copolyesters. They conducted the first step of the process (esterification) at 0 °C for SC and 60 °C for TC, followed by the second step (copolymerization) at 120-130 °C for SC and 180-190 °C for TC (9 h) to obtain the corresponding copolyesters with 15, 25, and 35 % lignin loadings. They reported that a portion of the obtained products was pyridine-soluble (used for extraction) and thus, that portion proved to be extremely difficult to remove and could not be included in the reported characterizations, as well as the reported yields. For the extracted portion, however, they reported that both the TC- and the SC-based copolyesters containing 25 % lignin were stable at up to 300°C, which was higher than the same values for the initial lignin and the lignin copolyesters without PEG (reported in a separate study by Guo *et al.*[99]). Furthermore, they reported that increasing the loading percentage of lignin in the initial reaction, increased the yield of the obtained copolyesters, whereas the yields for the TC-based copolyesters were 25, 45, and 60% using 15, 25, and 35% lignin loadings, respectively. The same values were 45, 60, and 65% yield for SC-based copolyester using 15, 25, and 35% lignin loadings, respectively. They also reported that increasing the lignin loadings increased the observed T_gs for both the TC- and the SC-based copolyesters.

In a report by Fang *et al.,*[100] dimerized acid (**DA**, Scheme 2-5) was synthesized by dimerizing unsaturated fatty acids (derived from tall oil, cottonseed oil, and soybean oil). **DA** was then reacted at 50 °C with enzymatically hydrolyzed lignin (**EHL**) using a cation exchange resin (**CER**) as the catalyst for 5 h to synthesize a graft copolymer, **DA-g-EHL**, through an esterification reaction between **DA** and **EHL**.

Scheme 2-5 Esterification of **EHL** with **DA** as reported by Fang *et al.*

Afterward, they employed the **DA-g-EHL** graft copolymer in the preparation of modified phenolic aldehyde amine (**PAA**) as a partial replacement for phenol. Specifically, they

replaced 25 wt% of the phenol in the **PAA** samples with either the **DA-g-EHL** or the **EHL** to obtain two samples and used a commercial **PAA** sample as the control. Subsequently, they used the three samples in 20% loadings as curing agents for epoxy resins. The epoxy resins were thereafter cured at 86 °C for 3 h. They determined that the bending strength and the elongation at break were significantly higher in the epoxy resins cured by **DA-g-EHL** modified **PAA** than in the ones cured with **EHL** modified **PAA**, which they attributed to the long aliphatic chain, and subsequently several possible conformations of the **DA**, which when grafted onto the **EHL** can improve the flexibility of the cured epoxy resins. The bending strength at break observed for the epoxy resins cured with **DA-g-EHL** modified **PAA** (89.18 MPa) was almost equal to that of the ones cured with the commercial **PAA** (90.46 MPa) and higher than that of the ones cured with **EHL** modified **PAA** (73.87 MPa). The elongation at break, however, was higher in the case of **DA-g-EHL** modified **PAA** (7.75 %) than it was for the **EHL** modified **PAA** (5.77 %) and the commercial **PAA** (6.62 %). Moreover, they determined that, because of the long chains of **DA** reducing the rigidity of **EA** and the chain stiffness of the modified **PAA**, epoxy resins cured with **DA-g-EHL** modified **PAA** had a higher tensile strength (36.22 MPa) than the ones cured with **EHL** modified **PAA** (34.41 MPa), yet still lower than that of the ones cured with the commercial **PAA** (39.55 MPa).

Gordobil *et al.*[101] esterified lignin with methacryloyl chloride (**MC**) using triethylamine as the catalyst at 14 °C (Scheme 2-6). Acyl chlorides are highly susceptible to homopolymerization, and thus, they used hydroquinone as an inhibitor to prevent such a phenomenon. They used 4 different lignin samples of organosolv eucalyptus lignin, kraft eucalyptus lignin, organosolv spruce lignin, and kraft spruce lignin in the mentioned esterification process and reported recovered mass yields of 118, 131, and 165% for organosolv eucalyptus lignin, organosolv spruce lignin, and kraft spruce lignin, respectively. They reported that yield for kraft eucalyptus lignin was lower than the amount of starting material, which they attributed to the high ash content (22.4%) of this sample. However, the high amounts of obtained final products can also be attributed to incomplete removal of unreacted reaction elements, as they reported solely using distilled water for isolating the final products.
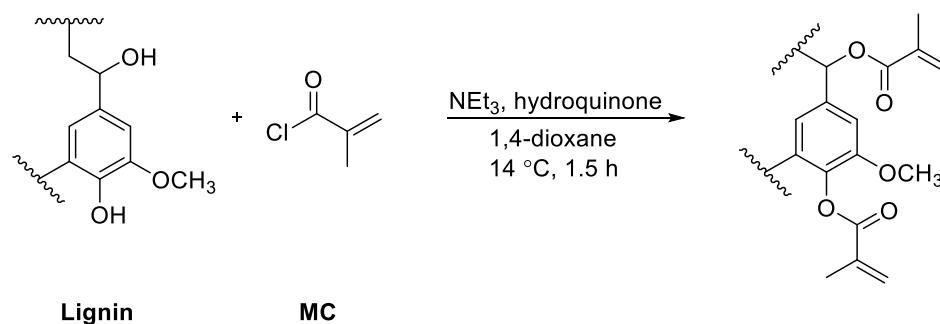
Scheme 2-6 Esterification of lignin with methacryloyl chloride.[101]

Saito *et al.*[102] reported an esterification reaction with dicarboxy-terminated polybutadiene (**PBD-(COOH)₂**) with potassium hydroxide as the catalyst on three different lignin samples of hardwood kraft lignin (**A-lignin**), methanol extracted hardwood kraft lignin (**W-lignin**), and formaldehyde-crosslinked methanol extracted hardwood kraft lignin (**F-lignin**). The reaction was carried for 24 h at 100 °C to yield corresponding lignin-polybutadiene copolymers, isolated through precipitation in methanol (Scheme 2-7). They determined that a mixture of three products were possibly obtained from this reaction as lignin bridged with telechelic butadiene via covalent bonding (Scheme 2-7A), lignin bridged with telechelic butadiene via ionic bonding (Scheme 2-7B), and formation of an interpenetrating network (Scheme 2-7C) due to the presence of K^+ cations.
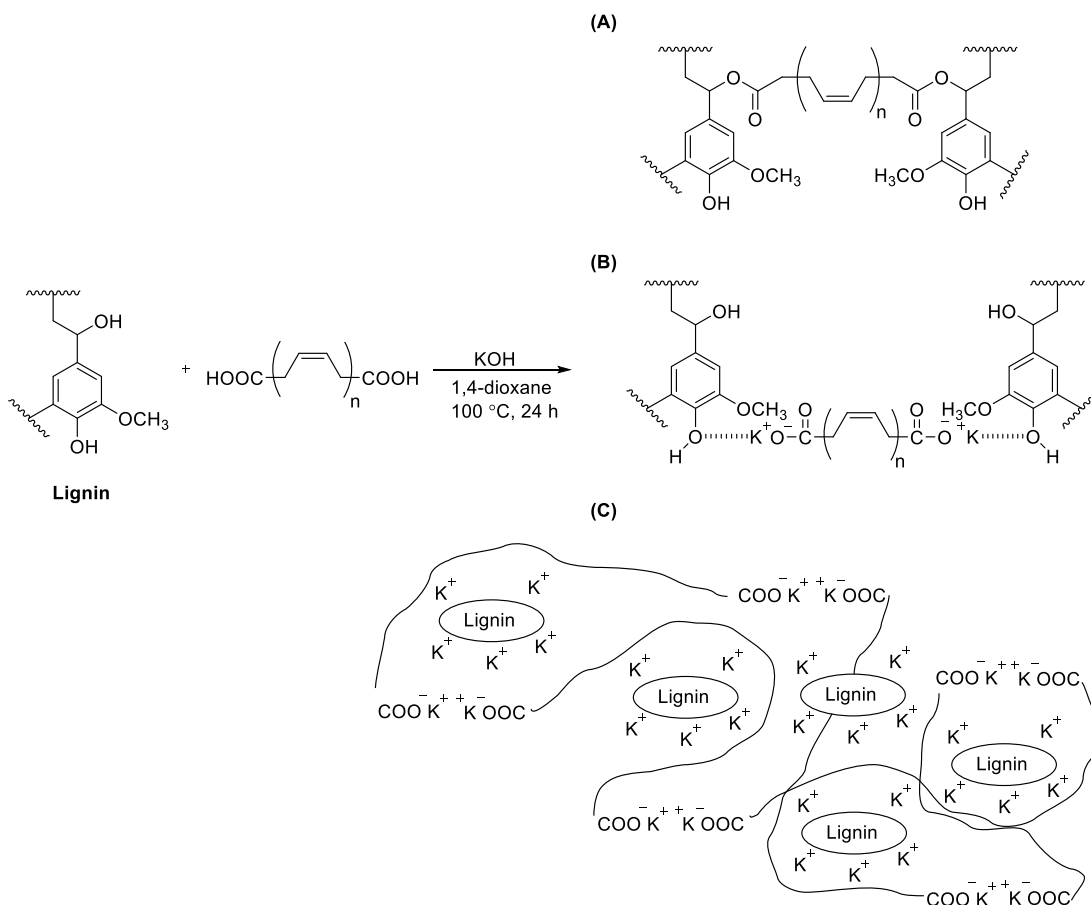
Scheme 2-7 Esterification of lignin with dicarboxy-terminated polybutadiene yielding products with ester linkages (A), ionic linkages (B), and interpenetrating network (C).[102]

They reported that the products of the esterification reactions gave copolymers in the forms of a free-standing solid for **F-lignin-PBD(COOH)₂**, a highly viscous liquid for **W-lignin-PBD(COOH)₂**, and a viscous liquid for **A-lignin-PBD(COOH)₂**. Thus, the **F-lignin-PBD** copolymer was taken as the only product capable of being utilized as a coating. They attributed this property to the fact that due to the methanol washing and the reaction with formaldehyde, the **F-lignin** samples contained a higher portion of a high molecular weight lignin fraction (as methanol extraction removes the lower molecular weight fractions and the reaction with formaldehyde crosslinks the phenolic groups) and thus, the **F-lignin** sample facilitated the formation of a more continuous network with the **PBD** bridges, while the broad distribution of molecular weight in **A-lignin** resulted in the formation of a less continuous network structure.

Among the various esterification reactions reported for lignin, one reaction, reported by Thielemans and Wool,[103] is of particular interest to this thesis. They esterified kraft lignin using 5 different anhydrides: acetic anhydride (**AA**), propionic anhydride (**PA**), *n*-butyric anhydride (**BA**), maleic anhydride (**MA**), and methacrylic anhydride (**MethA**) to obtain corresponding esterified lignins. More specifically, they performed the reactions between lignin and **AA**, **PA**, and **BA** without solvents and using lignin:anhydride molar ratio of 1:2 with 1-methylimidazole (**1MIM**, 0.5 mL/g lignin). For **MA** and **MethA** however, they used 1,4-dioxane as the solvent. For **MA**, they used 1 mL of a 0.5 g of **1MIM** in 10 mL solvent (per every gram of lignin), and for **MethA**, 6.1 mL of a 60-to-1 (**MethA**-**1MIM** by weight) mixture was used as a catalyst. lignin:solvent w/w ratios were 1:2 for **MA** and 1:4 for **MethA** (Scheme 2-8). They reported that, except for **MA**, all the anhydrides were able to successfully cap both the aliphatic and the aromatic hydroxyl groups on lignin. In the case of esterification with **MA**, they determined, through ^{1}H NMR, that only the aliphatic hydroxyls were selectively capped, and the aromatic hydroxyls remained unreacted. The broad range of anhydrides employed in this report, along with the relatively straightforward reaction conditions, make it one of the most interesting studies on lignin modification. However, no discussion was made on quantifying the extents of the esterifications, determining the optimal reaction conditions, or peak assignments (on cases such as the one with **MA** as mentioned before) in this report.
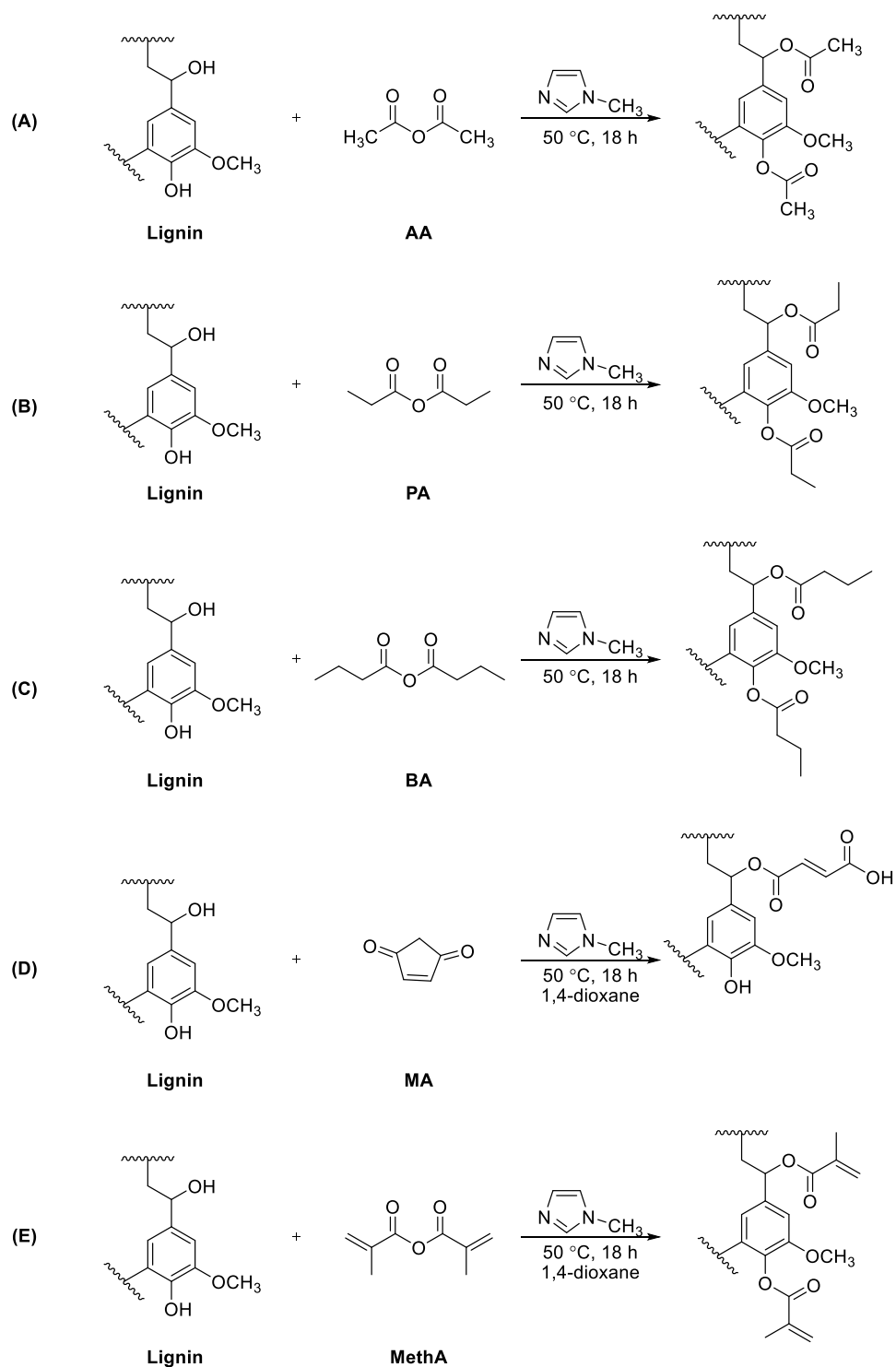
Scheme 2-8 Synthesis of acetylated (A), propionated (B), butyrated (C), maleated (D), and methacrylated (E) kraft lignin through esterification with corresponding anhydrides.

Esterification, as discussed earlier, is perhaps the most clear-cut chemical modification process available for the hydroxyl groups on lignin. However, other hydroxyl-functionalization reactions are employed that aim to lead to new applications for lignin.

Phenolation (phenolysis) is another hydroxyl functionalization reaction for lignin. Phenolation can be carried out in acidic media, where lignin is reacted with phenol to condensate the aromatic rings and the side chains on its structure. This process is particularly essential for lignosulfonates, as it can serve to increase the number of phenolic hydroxyl groups and thus, increase their susceptibility to chemical modification.[104]

Tan[105] used cardanol, a natural alkyl phenol derived from cashew nut shell liquid, as the phenol source in the phenolation of softwood kraft lignin to produce cardanol-lignin (**CL**) (Scheme 2-9). They then reacted the **CL** sample with 2,4-toluene diisocyanate (**TDI**) using stannous octoate as the catalyst to obtain cardanol-lignin-based polyurethane (**CLPU**) films. Furthermore, they determined that increasing the **CL** amount in the **CLPU** films (up to 30 wt%) increased the crosslinking density of the films, while loadings higher than 30 wt.% had an adverse effect on the crosslink density. They attributed this observation to the increase in the functionality level of the film formulations with increasing the **CL** amount. The decrease in the crosslink density after 30 wt% **CL** incorporations, however, was attributed to the increased solvent compatibility, caused by the long alkyl chains (R) on the **CL** samples at loading percentages higher than 30 wt%.
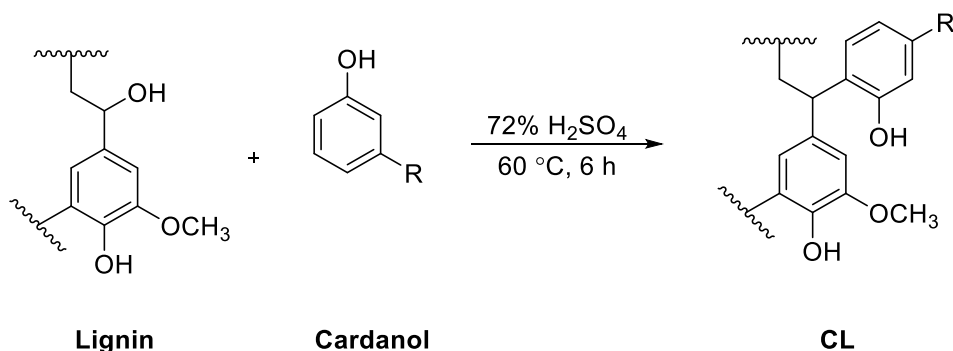
Scheme 2-9 Phenolation of kraft lignin using cardanol as reported by Tan.[105]

Etherification of the hydroxyl functionalities on lignin with alkylene oxides is another well-studied modification process available. In the case the alkylene oxide in use is propylene oxide, the etherification of lignin is referred to as "oxypropylation," which is the most well-known lignin etherification reaction and one of the most extensively-studied chemical modification reactions for lignin overall.[106] The importance of oxypropylation is highlighted in the case of incorporating lignin into polyurethane, as this reaction has the ability to convert lignin into a polyol that is soluble in most organic solvents and thus can be used in preparing polyurethane.[107–110] Sadeghifar et al.[111] oxypropylated kraft lignin through a reaction with propylene oxide (Scheme 2-10). They reported that using propylene oxide at milder conditions gave way to selectively masking the phenolic hydroxyls, while more extreme conditions would lead to simultaneous ring opening homopolymerization of the propylene oxide while masking both the aromatic and aliphatic hydroxyls. They further determined that 99% of the phenolic hydroxyl groups on kraft lignin were successfully oxypropylated when excess amounts of propylene oxide (2.5 eq.) were used under the mild conditions.
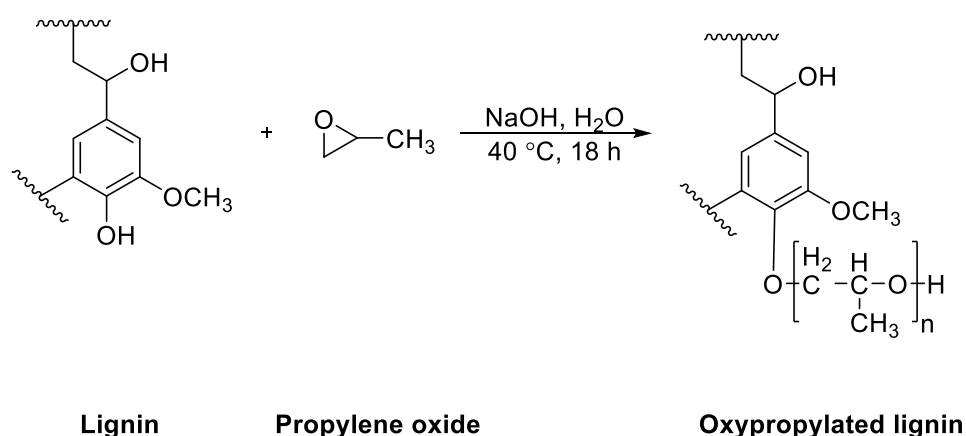
Scheme 2-10 Oxypropylation of the phenolic hydroxyls on lignin with propylene oxide.[111]

As discussed, modification of the hydroxyls on lignin poses excellent potential for valorizing lignin into materials used in various industries and substituting the fossil-based materials used in such industries with this abundant, renewable, bio-based resource.

2.2.3 Lignin-based Materials

Several reports are available today with the potential of converting lignin into a compound with the ability to be incorporated into materials in substantial percentages and/or offering unique properties. With the variety of functional groups present on lignin, comes the possibility of using those groups with the aim of adding certain properties to lignin. Depending on the end goal, such modifications can be tailored to give desired behavior to the natural polymer in target systems.
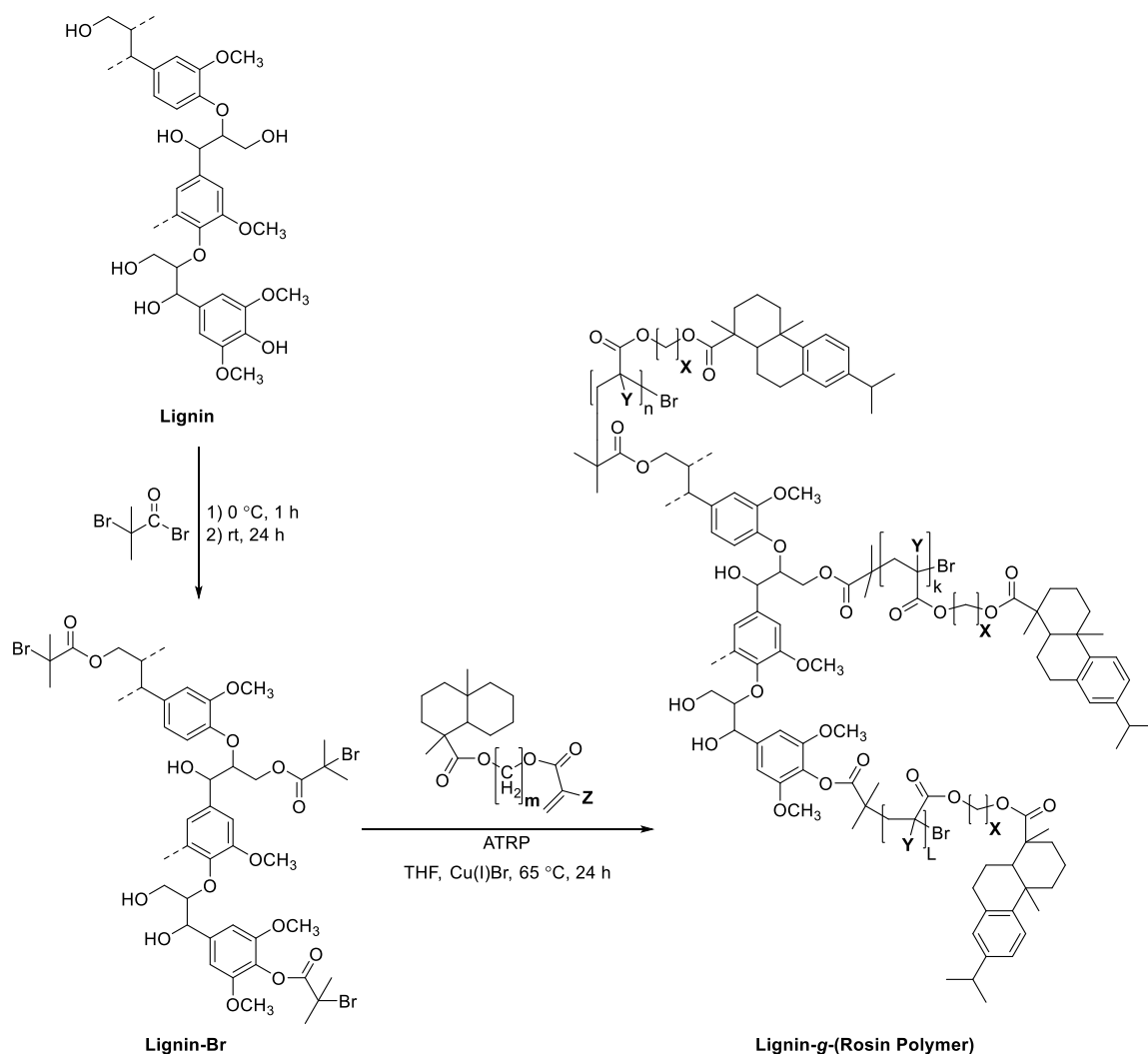
Scheme 2-11 Synthesis of lignin-Br ATRP macroinitiator and rosin polymer-grafted composites (lignin-*g*-(Rosin Polymer)): LGEMA (X = 2, Y = CH$_3$) using MAEDA (m = 2, Z = CH$_3$), LGEA (X = 2, Y = H) using AEDA (m = 2, Z = H) , and LGBA (X = 4, Y =

H) using ABDA (m = 4, Z = H) as reported by Wang *et al.*[112] Copyright 2011, reproduced with permission from John Wiley and Sons.

Wang *et al.*[112] examined the possibility of preparing highly hydrophobic composites using lignin and gum rosin as two renewable materials via ATRP polymerization. They esterified lignin with 2-bromoisobutyryl bromide (**BiBB**) using triethylamine as the catalyst to obtain lignin-Br. Afterward, they mixed tris[2-(dimethylamino)ethyl]amine (**Me$_6$-TREN**), 2-methacryloyloxyethyl dehydroabieticcarboxylate (**MAEDA**), and lignin-Br (as the ATRP macroinitiator) with Cu(I)Br at 65 °C for 24 h to obtain the **MAEDA** polymer grafted lignin (**LGEMA**). They also prepared 2-acryloyloxyethyl dehydroabieticcarboxylate (**AEDA**) polymer grafted lignin (**LGEA**) and 4-acryloyloxybutyl dehydroabieticcarboxylate (**ABDA**) polymer grafted lignin (**LGBA**) samples using the same process, substituting the **MAEDA** with **AEDA** and **ABDA**, respectively (Scheme 2-11).

Separately,[112] they synthesized dehydroabietic acid (**DHA**)-grafted lignin (**Lignin-*g*-DHA**), also referred to as rosin acid-grafted lignin, by reacting oxalyl chloride with **DHA** to obtain **OA-Cl**, which was then added to lignin using catalytic amounts of triethylamine (Scheme 2-12).
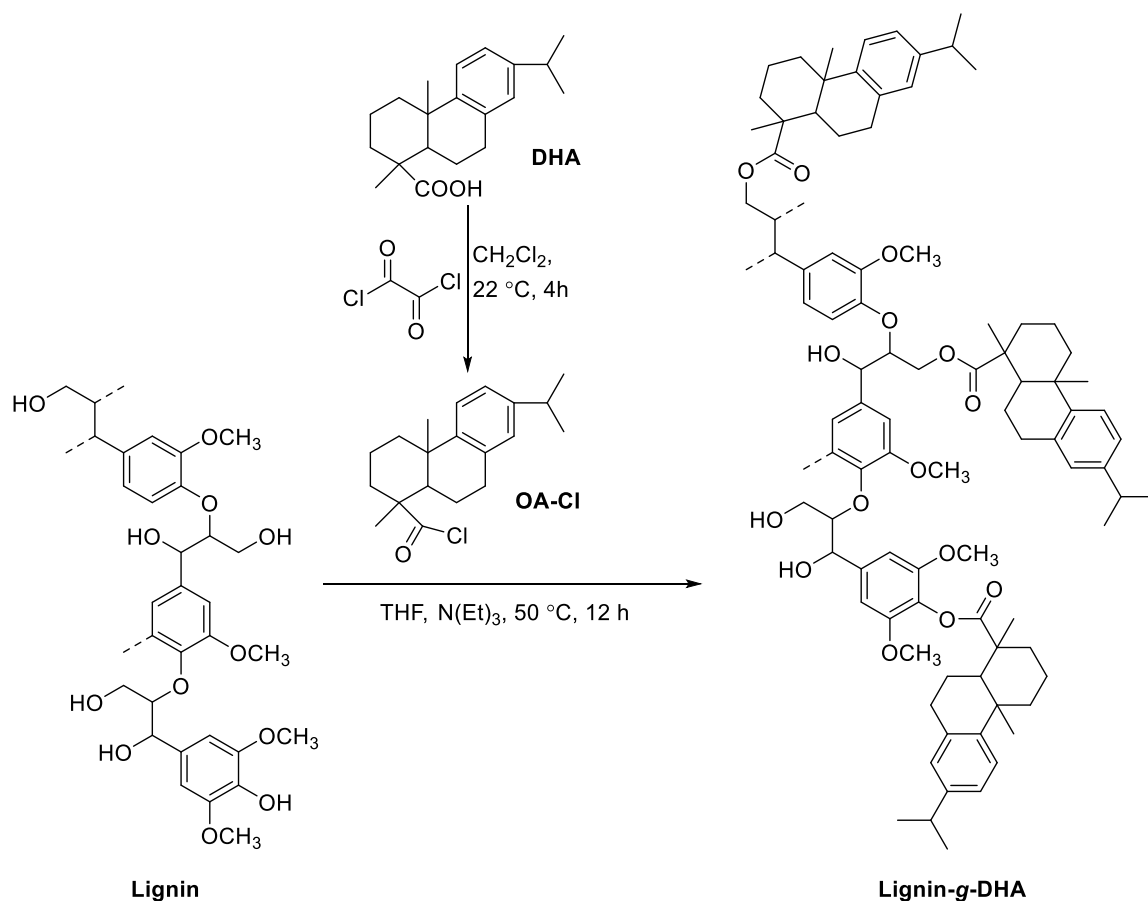
Scheme 2-12 Synthesis of rosin acid-grafted lignin (**lignin-*g*-DHA**) as reported by Wang *et al.*[112]

They reported that the length of the alkyl side groups in the acrylic rosin polymer-grafted lignin composites had a significant effect on the T_g values of the composites, as they reported T_g values of 20, 70, and 95 °C for the **LGBA**, **LGEA**, and **LGMA** composites, due to the presence of butyl, ethyl, and methacrylic side chains, respectively. Furthermore, they examined the hydrophobicity of the unmodified lignin, **lignin-Br**, **lignin-*g*-DHA**, **LGEMA**, **LGEA**, and **LGBA** samples by spin-casting thin films of them on a glass substrate and measuring the water contact angles of the prepared films. Subsequently, they determined that while the water contact angles for lignin and lignin-Br spin-cast films were close (75° and 78°, respectively), the same values increased significantly in the spin-cast films of **lignin-*g*-DHA** (92°), **LGEMA** (91°), **LGEA** (89°), and **LGBA** (91°) because of incorporating hydrophobic rosin moieties into composites of the naturally hydrophobic

lignin. The reported values were close to that of hydrocarbon-based polystyrene (90°), which was taken as evidence towards the suitability of the prepared composites to act as bio-based substitutes for packaging materials made from hydrocarbon-based polystyrene.

Ismail *et al.*[113] modified and incorporated sodium lignosulfonate (**LS**) in two series of bio-based epoxy resins (Scheme 2-13). The first resin (**Ser1LSGLYPA**) was prepared through esterification of equal amounts of **LS** and ethylene glycol (**EG**), and **LS** and glycerol (**GLY**) with excess succinic acid anhydride (**SAH**) using dimethylbenzylamine (**DMBA**) as the catalyst to synthesize corresponding ester carboxylic acid derivatives of **LSEGPA** and **LSGLYPA**, respectively, which were then used to crosslink glycerol diglycidyl ether (**GLYDGE**). The **LSGLYPA** percentages reported were at 0, 20, 40, 60, and 80%. The second resin (**Ser2GLYDGE**) was prepared by esterifying equal amounts of **LS** and **GLY** with excess **SAH** using **DMBA** as the catalyst to synthesize **LSGYPA** and subsequent crosslinking with a mixture of **GLYDGE** and ethylene glycol diglycidyl ether (**EGDGE**), where the **GLYDGE/EGDGE** mixture was varied at 0, 20, 40, 60, 80, and 100% (Scheme 2-13). They reported that the T_g values for both epoxy resins were dependent on the **GLY** content in them, as the values increased with increasing the **GLY** content in the epoxy resins. They also determined that increasing the amount of **LSGLYPA** in **Ser1LSGLYPA** and the amount of **GLYDGE** in **Ser2GLYDGE** did not affect the thermal decomposition temperature (T_d) and the mass residue at 500 °C (MR_{500}) of the prepared epoxy resins, as they both showed T_d values around 275 °C and MR_{500} values of around 22%. Such epoxy resins, prepared using chemically modified lignin, can have applications as crosslinking agents for PF resins.
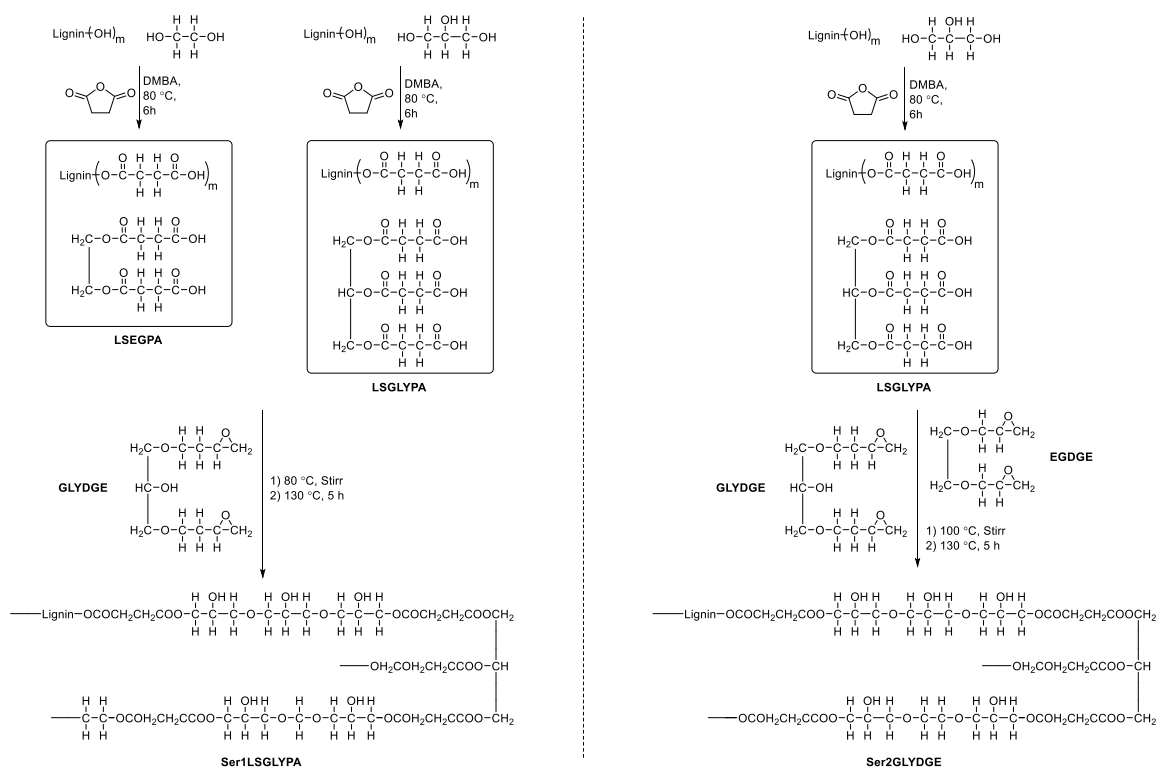
Scheme 2-13 Preparation scheme for **Ser1LSGLYPA** and **Ser2GLYDGE** epoxy resins as reported by Ismail *et al.*[113] Copyright 2009, reproduced with permission from John Wiley and Sons.

Feng *et al.*[114] prepared acetic acid functionalized lignin-based hydrogels (**LGA1**, **LGA2**, and **LGA3**) by reacting acetic acid lignin (**AAL**) with acrylamide (**AAm**) and ethyleneglycol dimethacrylate (**EGDMA**) as the crosslinker, using hydrogen peroxide as the initiator (Scheme 2-14), alongside control hydrogels of **AAm** and **EDGMA** with 2,2-azobisisobutyronitrile (**AIBN**) as the initiator (**PAAm**). The **AAL**:**AAM** weight ratios used in the preparation of the **AAL**-incorporated hydrogels were 0.5:2.5, 0.5:3.5, and 0.5:4.5 for the **LGA1**, **LGA2**, and **LGA3** hydrogels, respectively.
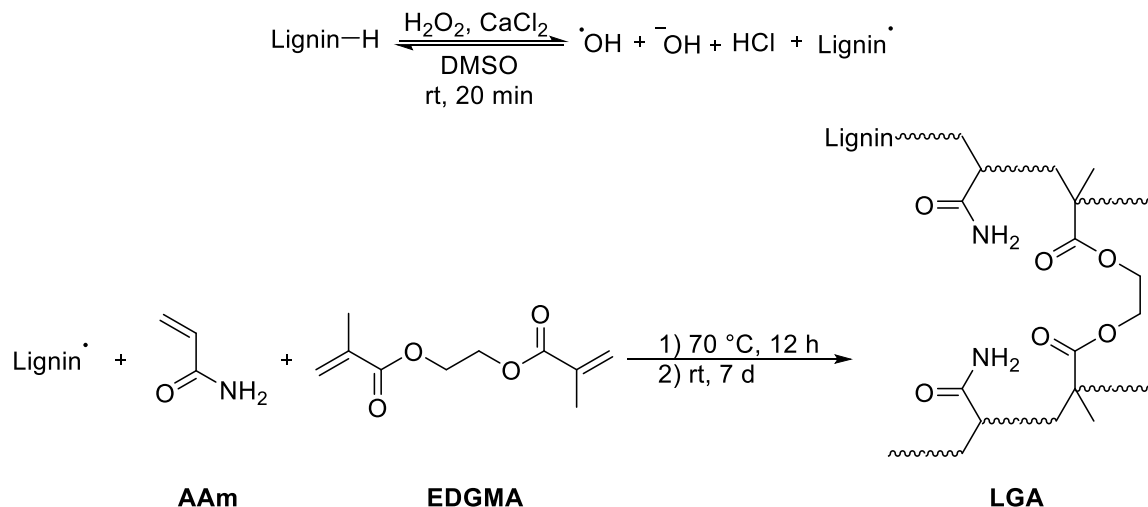
Scheme 2-14 Preparation of AAL-incorporated hydrogels (LGA) as reported by Feng *et al.*[114]

They reported that the incorporation of **AAL** into the hydrogels had minimal effect on their decomposition temperatures, as the 5% weight loss temperature remained at around 250 °C for the **AAL**, **LGA2**, and **PAAm** samples. However, the **LGA2** hydrogels showed higher char formation at 700 °C (24 wt%) than the **PAAm** hydrogels (21 wt%) as a result of the incorporation of lignin as a char formation-promoting material. Moreover, they determined that decreasing the amount of incorporated **AAL** in the hydrogels increased their swelling degrees noticeably while increasing the amount of the hydrophobic **AAL** would cause slower diffusion of water in the hydrogels. Consequently, they reported that the **LGA3** hydrogel reached the swelling ratio of 930% within 420 min, while the same value was approximately 700% and 820% for the **LGA1** and **LGA2** hydrogels, respectively within the same time frame. Finally, they determined that increasing the lignin content in the **LGA** hydrogels improved the dye-adsorption in them, as the **LGA1** hydrogel was able to adsorb 29.65 mg of methylene blue per every gram of hydrogel. Such hydrogels have the potential to be utilized as a flocculent in waste-water treatment, an unconventional potential application of lignin considering its inherent hydrophobicity.[114]

Jawerth *et al.*[115] reported the first thiol-ene click reaction on fractionated kraft lignin, by allylating the ethanol-soluble fraction of the kraft lignin with allyl chloride in the presence of sodium hydroxide to selectively allylate the phenolic hydroxyl groups. They

subsequently synthesized lignin-thiol resins by adding the allylated fractionated kraft lignin to trimethylpropane tris(3-mercaptopropionate) at different thiol/allyl ether molar ratios in silicone molds, followed by heating at 120 °C for 24 h (Scheme 2-15). They reported unsuccessful attempts at UV-curing the lignin-thiol resins due to the strong UV absorbance of the allylated lignin sample and utilizing non-depolymerized karft lignin in the same reaction was not discussed in the report.
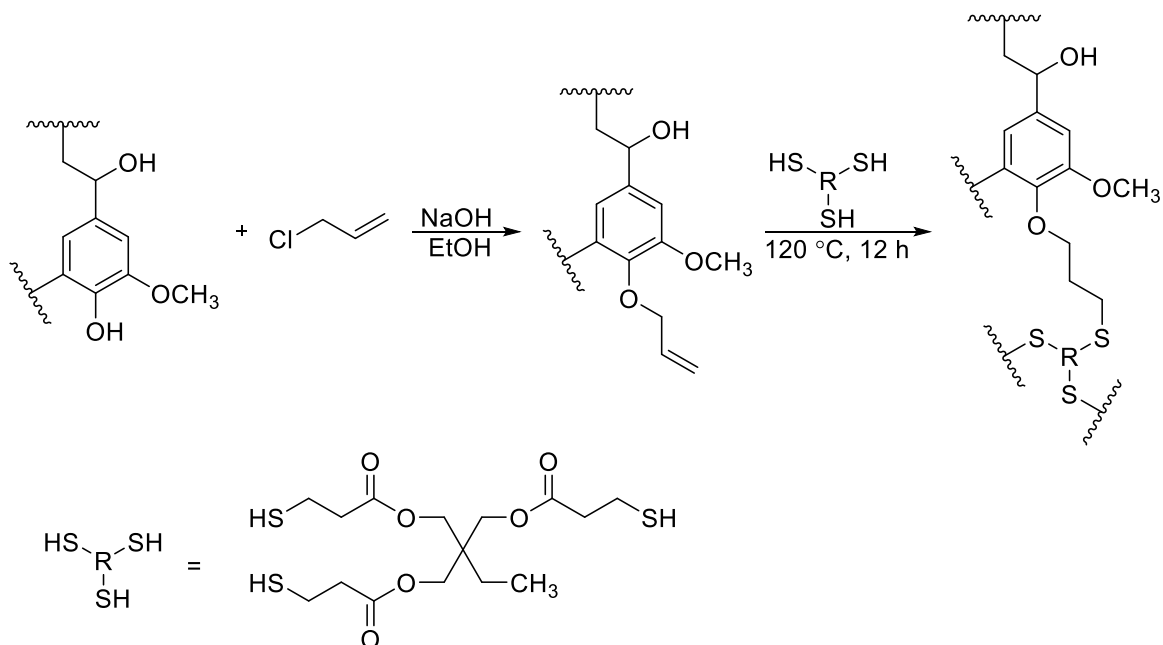
Scheme 2-15 Synthesis of lignin-thiol resins from ethanol-soluble fractionated kraft lignin as reported by Jawerth et al.[115]

2.3 Summary and Knowledge Gaps

Despite the aforementioned valorization techniques available for lignin today, it is evident by the large number of studies in this field and the sheer volume of yet underutilized lignin that is being disposed of as waste every day, that the knowledge gap in the area of lignin valorization still exists, which amplifies the need for novel, optimized, and target-specific approaches to the task of utilizing lignin or modified lignin, a relatively untapped, renewable, sustainable, and abundant natural polymer for high-value bio-based materials. As the most promising studies in this research area either employ multi-step reactions with harsh reaction conditions, seek to depolymerize or fractionate lignin prior to utilization

dispose of a portion of the material, or have only been successful at utilizing low percentages of lignin (chemically modified or not) in the reported systems, finding simple, straightforward approaches with more gentle reaction conditions, capable of incorporating appreciable percentages of lignin in its entirety in the target systems can have a detrimental effect on enhancing the scientific discoveries in this field and play a crucial role in developing a sustainable future for many classes of materials that are currently developed from non-renewable fossil fuel-based sources.

2.4 References

(1)   Ralph, J.; Peng, J.; Lu, F.; Hatfield, R. D.; Helm, R. F. Are Lignins Optically Active? *J Agric Food Chem* **1999**, *47* (8), 2991–2996.

(2)   Rinaldi, R.; Jastrzebski, R.; Clough, M. T.; Ralph, J.; Kennema, M.; Bruijnincx, P. C. A.; Weckhuysen, B. M. Paving the Way for Lignin Valorisation: Recent Advances in Bioengineering, Biorefining and Catalysis. *Angew. Chem. Int. Ed.* **2016**, *55* (29), 8164–8215.

(3)   Sakakibara, A. A Structural Model of Softwood Lignin. *Wood SciTechnol* **1980**, *14* (2), 89–100.

(4)   Chabannes, M.; Ruel, K.; Yoshinaga, A.; Chabbert, B.; Jauneau, A.; Joseleau, J.-P.; Boudet, A.-M. In Situ Analysis of Lignins in Transgenic Tobacco Reveals a Differential Impact of Individual Transformations on the Spatial Patterns of Lignin Deposition at the Cellular and Subcellular Levels. *Plant J.* **2001**, *28* (3), 271–282.

(5)   Jones, L.; Ennos, A. R.; Turner, S. R. Cloning and Characterization of Irregular xylem4 (irx4): A Severely Lignin-Deficient Mutant of Arabidopsis. *Plant J.* **2017**, *26* (2), 205–216.

(6)   Campbell, M. M.; Sederoff, R. R. Variation in Lignin Content and Composition (Mechanisms of Control and Implications for the Genetic Improvement of Plants). *Plant Physiol.* **1996**, *110* (1), 3–13.

(7)   Nguyen, T.; Zavarin, E.; II, E. M. barrall. Thermal Analysis of Lignocellulosic Materials. *J. Macromol. Sci. Part C* **1981**, *20* (1), 1–65.

(8)   Freudenberg, K.; Neish, A. C. *Constitution and Biosynthesis of Lignin*, First.; Springer-Verlag, Heidelberg and New York, **1968**.

(9)   Windeisen, E.; Wegener, G. 10.15 - Lignin as Building Unit for Polymers. In *Polymer Science: A Comprehensive Reference*; Matyjaszewski, K., Möller, M., Eds.; Elsevier: Amsterdam, **2012**; pp 255–265.

(10)   Boudet, A. M.; Lapierre, C.; Grima-Pettenati, J. Biochemistry and Molecular Biology of Lignification. *New Phytol.* **1995**, *129* (2), 203–236.

(11)   Patil, S. V.; Argyropoulos, D. S. Stable Organic Radicals in Lignin: A Review. *ChemSusChem* **2017**, *10* (17), 3284–3303.

(12)   Upton, B. M.; Kasko, A. M. Strategies for the Conversion of Lignin to High-Value Polymeric Materials: Review and Perspective. *Chem Rev* **2016**, *116* (4), 2275–2306.

(13)   Heitner, C.; Dimmel, D.; Schmidt, J. *Lignin and Lignans: Advances in Chemistry*; CRC Press, **2016**.

(14)   Ralph, J.; Lundquist, K.; Brunow, G.; Lu, F.; Kim, H.; Schatz, P. F.; Marita, J. M.; Hatfield, R. D.; Ralph, S. A.; Christensen, J. H.; et al. Lignins: Natural Polymers from Oxidative Coupling of 4-Hydroxyphenyl- Propanoids. *Phytochem. Rev.* **2004**, *3* (1–2), 29–60.

(15)   Adler, E. Lignin Chemistry—past, Present and Future. *Wood Sci. Technol.* **1977**, *11* (3), 169–218.

(16)   Constant, S.; J. Wienk, H. L.; E. Frissen, A.; de Peinder, P.; Boelens, R.; Es, D. S. van; H. Grisel, R. J.; M. Weckhuysen, B.; J. Huijgen, W. J.; A. Gosselink, R. J.; et al. New Insights into the Structure and Composition of Technical Lignins: A Comparative Characterisation Study. *Green Chem.* **2016**, *18* (9), 2651–2665.

(17)   McDonough, T. J. The Chemistry of Organosolv Delignification. *TAPPI J.* **1993**, *76* (8), 186.

(18)   Strassberger, Z.; Tanase, S.; Rothenberg, G. The Pros and Cons of Lignin Valorisation in an Integrated Biorefinery. *RSC Adv.* **2014**, *4* (48), 25310–25318.

(19)   Lora, J. Chapter 10 - Industrial Commercial Lignins: Sources, Properties and Applications. In *Monomers, Polymers and Composites from Renewable Resources*; Belgacem, M. N., Gandini, A., Eds.; Elsevier: Amsterdam, **2008**; pp 225–241.

(20)   Abächerli, A.; Doppenberg, F. *Method for Preparing Alkaline Solutions Containing Aromatic Polymers*; Google Patents, **2001**.

(21)   Lora, J. H.; Wu, C. F.; Pye, E. K.; Balatinecz, J. J. Characteristics and Potential Applications of Lignin Produced by an Organosolv Pulping Process. In *Lignin*; ACS Symposium Series; American Chemical Society, **1989**; Vol. 397, pp 312–323.

(22)   Pan, X.; Saddler, J. N. Effect of Replacing Polyol by Organosolv and Kraft Lignin on the Property and Structure of Rigid Polyurethane Foam. *Biotechnol. Biofuels* **2013**, *6*, 12.

(23)   Axegaard, P.; Wiken, J. E. (Svenska T. Delignification Studies - Factors Affecting the Amount Of "residual Lignin." *Sven. Papperstidning Swed.* **1983**, 178–184.

(24)   Sjöström, E. Chapter 4 - LIGNIN. In *Wood Chemistry (Second Edition)*; Academic Press: San Diego, **1993**; pp 71–89.

(25)   Tomani, P. The Lignoboost Process. *Cellul. Chem. Technol.* **2010**, *44* (1–3), 53–58.

(26)   Kouisni, L.; Gagné, A.; Maki, K.; Holt-Hindle, P.; Paleologou, M. LignoForce System for the Recovery of Lignin from Black Liquor: Feedstock Options, Odor Profile, and Product Characterization. *ACS Sustain. Chem. Eng.* **2016**, *4* (10), 5152–5159.

(27)   Imhoff, M. L.; Bounoua, L.; Ricketts, T.; Loucks, C.; Harriss, R.; Lawrence, W. T. Global Patterns in Human Consumption of Net Primary Production. *Nature* **2004**, *429* (6994), 870.

(28)   Shaw, L.; K. Somisara, D. M. U.; C. How, R.; J. Westwood, N.; A. Bruijnincx, P. C.; M. Weckhuysen, B.; J. Kamer, P. C. Electronic and Bite Angle Effects in Catalytic C–O Bond Cleavage of a Lignin Model Compound Using Ruthenium Xantphos Complexes. *Catal. Sci. Technol.* **2017**, *7* (3), 619–626.

(29)   Briens, C.; Piskorz, J.; Berruti, F. Biomass Valorization for Fuel and Chemicals Production -- A Review. *Int. J. Chem. React. Eng.* **2008**, *6* (1).

(30)   Espinoza-Acosta, J. L.; Torres-Chávez, P. I.; Ramírez-Wong, B.; López-Saiz, C. M.; Montaño-Leyva, B. Antioxidant, Antimicrobial, and Antimutagenic Properties of Technical Lignins and Their Applications. *BioResources* **2016**, *11* (2), 5452–5481.

(31)   Silva, E. A. B. da; Zabkova, M.; Araújo, J. D.; Cateto, C. A.; Barreiro, M. F.; Belgacem, M. N.; Rodrigues, A. E. An Integrated Process to Produce Vanillin and Lignin-Based Polyurethanes from Kraft Lignin. *Chem. Eng. Res. Des.* **2009**, *87* (9), 1276–1292.

(32)   Gellerstedt, G. Softwood Kraft Lignin: Raw Material for the Future. *Ind. Crops Prod.* **2015**, *77* (Supplement C), 845–854.

(33)   Laurichesse, S.; Avérous, L. Chemical Modification of Lignins: Towards Biobased Polymers. *Prog. Polym. Sci.* **2014**, *39* (7), 1266–1290.

(34)   Keilen, J. J.; Pollak, A. Lignin for Reinforcing Rubber. *Ind. Eng. Chem.* **1947**, *39* (4), 480–483.

(35)   Baumberger, S.; Lapierre, C.; Monties, B.; Valle, G. D. Use of Kraft Lignin as Filler for Starch Films. *Polym. Degrad. Stab.* **1998**, *59* (1), 273–277.

(36)   Košíková, B.; Gregorová, A.; Osvald, A.; Krajčovičová, J. Role of Lignin Filler in Stabilization of Natural Rubber–based Composites. *J. Appl. Polym. Sci.* **2007**, *103* (2), 1226–1231.

(37)   Sadeghifar, H.; Argyropoulos, D. S. Correlations of the Antioxidant Properties of Softwood Kraft Lignin Fractions with the Thermal Stability of Its Blends with Polyethylene. *ACS Sustain. Chem. Eng.* **2015**, *3* (2), 349–356.

(38)   Qian, Y.; Qiu, X.; Zhu, S. Lignin: A Nature-Inspired Sun Blocker for Broad-Spectrum Sunscreens. *Green Chem.* **2015**, *17* (1), 320–324.

(39)   De Chirico, A.; Armanini, M.; Chini, P.; Cioccolo, G.; Provasoli, F.; Audisio, G. Flame Retardants for Polypropylene Based on Lignin. *Polym. Degrad. Stab.* **2003**, *79* (1), 139–145.

(40)   Huber, G. W.; Iborra, S.; Corma, A. Synthesis of Transportation Fuels from Biomass: Chemistry, Catalysts, and Engineering. *Chem. Rev.* **2006**, *106* (9), 4044–4098.

(41)   Barth, T.; Kleinert, M. Motor Fuels from Biomass Pyrolysis. *Chem. Eng. Technol.* **2008**, *31* (5), 773–781.

(42)   Gardner, D. J.; Schultz, T. P.; McGinnis, G. D. The Pyrolytic Behavior of Selected Lignin Preparations. *J. Wood Chem. Technol.* **1985**, *5* (1), 85–110.

(43)   Ferdous, D.; Dalai, A. K.; Bej, S. K.; Thring, R. W. Pyrolysis of Lignins: Experimental and Kinetics Studies. *Energy Fuels* **2002**, *16* (6), 1405–1412.

(44)   Várhegyi, G.; Antal, M. J.; Jakab, E.; Szabó, P. Kinetic Modeling of Biomass Pyrolysis. *J. Anal. Appl. Pyrolysis* **1997**, *42* (1), 73–87.

(45)   Kang, S.; Li, X.; Fan, J.; Chang, J. Hydrothermal Conversion of Lignin: A Review. *Renew. Sustain. Energy Rev.* **2013**, *27*, 546–558.

(46)   Leonowicz, A.; Matuszewska, A.; Luterek, J.; Ziegenhagen, D.; Wojtaś-Wasilewska, M.; Cho, N.-S.; Hofrichter, M.; Rogalski, J. Biodegradation of Lignin by White Rot Fungi. *Fungal Genet. Biol.* **1999**, *27* (2), 175–185.

(47)   Pandey, M. P.; Kim, C. S. Lignin Depolymerization and Conversion: A Review of Thermochemical Methods. *Chem Eng Technol* **2011**, *34* (1), 29–41.

(48)   Sharma, R. K.; Wooten, J. B.; Baliga, V. L.; Lin, X.; Geoffrey Chan, W.; Hajaligol, M. R. Characterization of Chars from Pyrolysis of Lignin. *Fuel* **2004**, *83* (11–12), 1469–1482.

(49)   Yang, H.; Yan, R.; Chen, H.; Lee, D. H.; Zheng, C. Characteristics of Hemicellulose, Cellulose and Lignin Pyrolysis. *Fuel* **2007**, *86* (12), 1781–1788.

(50)   Wang, S.; Lin, H.; Ru, B.; Sun, W.; Wang, Y.; Luo, Z. Comparison of the Pyrolysis Behavior of Pyrolytic Lignin and Milled Wood Lignin by Using TG–FTIR Analysis. *J. Anal. Appl. Pyrolysis* **2014**, *108*, 78–85.

(51)   Kawamoto, H. Lignin Pyrolysis Reactions. *J. Wood Sci.* **2017**, *63* (2), 117–132.

(52)   Liu, Q.; Wang, S.; Zheng, Y.; Luo, Z.; Cen, K. Mechanism Study of Wood Lignin Pyrolysis by Using TG–FTIR Analysis. *J. Anal. Appl. Pyrolysis* **2008**, *82* (1), 170–177.

(53)   Wang, S.; Ru, B.; Lin, H.; Sun, W.; Luo, Z. Pyrolysis Behaviors of Four Lignin Polymers Isolated from the Same Pine Wood. *Bioresour. Technol.* **2015**, *182*, 120–127.

(54)   Liu, C.; Hu, J.; Zhang, H.; Xiao, R. Thermal Conversion of Lignin to Phenols: Relevance between Chemical Structure and Pyrolysis Behaviors. *Fuel* **2016**, *182*, 864–870.

(55)   Ben, H.; Ragauskas, A. J. NMR Characterization of Pyrolysis Oils from Kraft Lignin. *Energy Fuels* **2011**, *25* (5), 2322–2332.

(56)   Pinto, P. C. R.; Costa, C. E.; Rodrigues, A. E. Oxidation of Lignin from Eucalyptus Globulus Pulping Liquors to Produce Syringaldehyde and Vanillin. *Ind. Eng. Chem. Res.* **2013**, *52* (12), 4421–4428.

(57)   Wang, Y.; Sun, S.; Li, F.; Cao, X.; Sun, R. Production of Vanillin from Lignin: The Relationship between β-O-4 Linkages and Vanillin Yield. *Ind. Crops Prod.* **2018**, *116*, 116–121.

(58)   Tarabanko, V. E.; Kaygorodov, K. L.; Skiba, E. A.; Tarabanko, N.; Chelbina, Y. V.; Baybakova, O. V.; Kuznetsov, B. N.; Djakovitch, L. Processing Pine Wood into

Vanillin and Glucose by Sequential Catalytic Oxidation and Enzymatic Hydrolysis. *J. Wood Chem. Technol.* **2017**, *37* (1), 43–51.

(59)   Fache, M.; Boutevin, B.; Caillol, S. Vanillin Production from Lignin and Its Use as a Renewable Chemical. *ACS Sustain. Chem. Eng.* **2016**, *4* (1), 35–46.

(60)   Araújo, J. D. P.; Grande, C. A.; Rodrigues, A. E. Vanillin Production from Lignin Oxidation in a Batch Reactor. *Chem. Eng. Res. Des.* **2010**, *88* (8), 1024–1032.

(61)   Hocking, M. B. Vanillin: Synthetic Flavoring from Spent Sulfite Liquor. *J. Chem. Educ.* **1997**, *74* (9), 1055.

(62)   Villar, J. C.; Caperos, A.; García-Ochoa, F. Oxidation of Hardwood Kraft-Lignin to Phenolic Derivatives with Oxygen as Oxidant. *Wood Sci. Technol.* **2001**, *35* (3), 245–255.

(63)   Villar, J. C.; Caperos, A.; García-Ochoa, F. Oxidation of Hardwood Kraft-Lignin to Phenolic Derivatives. Nitrobenzene and Copper Oxide as Oxidants. *J. Wood Chem. Technol.* **1997**, *17* (3), 259–285.

(64)   Mahmood, N.; Yuan, Z.; Schmidt, J.; Xu, C. (Charles). Hydrolytic Depolymerization of Hydrolysis Lignin: Effects of Catalysts and Solvents. *Bioresour. Technol.* **2015**, *190*, 416–419.

(65)   Huang, S.; Mahmood, N.; Tymchyshyn, M.; Yuan, Z.; Xu, C. (Charles). Reductive de-Polymerization of Kraft Lignin for Chemicals and Fuels Using Formic Acid as an in-Situ Hydrogen Source. *Bioresour. Technol.* **2014**, *171*, 95–102.

(66)   Adler, E.; Brunow, G.; Lundquist, K. Investigation of the Acid-Catalysed Alkylation of Lignins by Means of NMR Spectroscopic Methods. *Holzforsch. - Int. J. Biol. Chem. Phys. Technol. Wood* **1987**, *41* (4), 199–207.

(67)   Li, Y.; Sarkanen, S. Alkylated Kraft Lignin-Based Thermoplastic Blends with Aliphatic Polyesters. *Macromolecules* **2002**, *35* (26), 9707–9715.

(68)   Biberstein, J.; Das, S.; Umbach, J.; Boyer, R.; Sutton, K.; Czepizak, M. *Production of Dimethyl Sulfide from Lignin*; Gaylord Chemical, **2010**.

(69)   Calvo-Flores, F. G.; Dobado, J. A. Lignin as Renewable Raw Material. *ChemSusChem* **2010**, *3* (11), 1227–1235.

(70)   Liu, Y.; Li, K. Preparation and Characterization of Demethylated Lignin-Polyethylenimine Adhesives. *J. Adhes.* **2006**, *82* (6), 593–605.

(71)   Pizzi, A. Recent Developments in Eco-Efficient Bio-Based Adhesives for Wood Bonding: Opportunities and Issues. *J. Adhes. Sci. Technol.* **2006**, *20* (8), 829–846.

(72)   Mansouri, N. E.; Pizzi, A.; Salvadó, J. Lignin-Based Wood Panel Adhesives without Formaldehyde. *Holz Als Roh- Werkst.* **2007**, *65* (1), 65.

(73)   Mansouri, N.-E. E.; Pizzi, A.; Salvado, J. Lignin-Based Polycondensation Resins for Wood Adhesives. *J. Appl. Polym. Sci.* **2007**, *103* (3), 1690–1699.

(74)   Alonso, M. V.; Rodríguez, J. J.; Oliet, M.; Rodríguez, F.; García, J.; Gilarranz, M. A. Characterization and Structural Modification of Ammonic Lignosulfonate by Methylolation. *J. Appl. Polym. Sci.* **2001**, *82* (11), 2661–2668.

(75)   Alonso, M. V.; Oliet, M.; Rodríguez, F.; Astarloa, G.; Echeverría, J. M. Use of a Methylolated Softwood Ammonium Lignosulfonate as Partial Substitute of Phenol in Resol Resins Manufacture. *J. Appl. Polym. Sci.* **2004**, *94* (2), 643–650.

(76)   Arend, M.; Westermann, B.; Risch, N. Modern Variants of the Mannich Reaction. *Angew. Chem. Int. Ed.* **1998**, *37* (8), 1044–1070.

(77)   Matsushita, Y.; Yasuda, S. Reactivity of a Condensed–type Lignin Model Compound in the Mannich Reaction and Preparation of Cationic Surfactant from Sulfuric Acid Lignin. *J Wood Sci* **2003**, *49* (2), 166–171.

(78)   Yue, X.; Chen, F.; Zhou, X. Improved interfacial bonding of pvc/wood-flour composites by lignin amine modification. *BioResources* **2011**, *6* (2), 2022–2044.

(79)   Zhang, L.; Huang, J. Effects of Hard-Segment Compositions on Properties of Polyurethane–nitrolignin Films. *J. Appl. Polym. Sci.* **2001**, *81* (13), 3251–3259.

(80)   Huang, J.; Zhang, L. Effects of NCO/OH Molar Ratio on Structure and Properties of Graft-Interpenetrating Polymer Networks from Polyurethane and Nitrolignin. *Polymer* **2002**, *43* (8), 2287–2294.

(81)   Zhang, L.; Huang, J. Effects of Nitrolignin on Mechanical Properties of Polyurethane–nitrolignin Films. *J Appl Polym Sci* **2001**, *80* (8), 1213–1219.

(82)   Argyropoulos, D. S. 31P NMR in Wood Chemistry: A Review of Recent Progress. *Res. Chem. Intermed.* **1995**, *21* (3–5), 373–395.

(83)   Balakshin, M.; Capanema, E. On the Quantification of Lignin Hydroxyl Groups With 31P and 13C NMR Spectroscopy. *J. Wood Chem. Technol.* **2015**, *35* (3), 220–237.

(84)   Faix, O.; Argyropoulos, D. S.; Robert, D.; Neirinck, V. Determination of Hydroxyl Groups in Lignins Evaluation of 1H-, 13C-, 31P-NMR, FTIR and Wet Chemical Methods. *Holzforsch.-Int. J. Biol. Chem. Phys. Technol. Wood* **1994**, *48* (5), 387–394.

(85)   Pu, Y.; Cao, S.; Ragauskas, A. J. Application of Quantitative 31P NMR in Biomass Lignin and Biofuel Precursors Characterization. *Energy Env. Sci* **2011**, *4* (9), 3154–3166.

(86)   Argyropoulos, D. S. Quantitative Phosphorus-31 NMR Analysis of Lignins, a New Tool for the Lignin Chemist. *J. Wood Chem. Technol.* **1994**, *14* (1), 45–63.

(87)   Liu, W.-J.; Jiang, H.; Yu, H.-Q. Thermochemical Conversion of Lignin to Functional Materials: A Review and Future Directions. *Green Chem.* **2015**, *17* (11), 4888–4907.

(88)   Kai, D.; Tan, M. J.; Chee, P. L.; Chua, Y. K.; Yap, Y. L.; Loh, X. J. Towards Lignin-Based Functional Materials in a Sustainable World. *Green Chem.* **2016**, *18* (5), 1175–1200.

(89)   Sivasankarapillai, G.; McDonald, A. G. Synthesis and Properties of Lignin-Highly Branched Poly (Ester-Amine) Polymeric Systems. *Biomass Bioenergy* **2011**, *35* (2), 919–931.

(90)   Luong, N. D.; Binh, N. T. T.; Duong, L. D.; Kim, D. O.; Kim, D.-S.; Lee, S. H.; Kim, B. J.; Lee, Y. S.; Nam, J.-D. An Eco-Friendly and Efficient Route of Lignin Extraction from Black Liquor and a Lignin-Based Copolyester Synthesis. *Polym. Bull.* **2012**, *68* (3), 879–890.

(91)   Sailaja, R. R. N.; Deepthi, M. V. Mechanical and Thermal Properties of Compatibilized Composites of Polyethylene and Esterified Lignin. *Mater. Des.* **2010**, *31* (9), 4369–4379.

(92)   Sivasankarapillai, G.; McDonald, A. G.; Li, H. Lignin Valorization by Forming Toughened Lignin-Co-Polymers: Development of Hyperbranched Prepolymers for Cross-Linking. *Biomass Bioenergy* **2012**, *47*, 99–108.

(93)   Maldhure, A. V.; Ekhe, J. D.; Deenadayalan, E. Mechanical Properties of Polypropylene Blended with Esterified and Alkylated Lignin. *J. Appl. Polym. Sci.* **2012**, *125* (3), 1701–1712.

(94)   Kaewtatip, K.; Thongmee, J. Effect of Kraft Lignin and Esterified Lignin on the Properties of Thermoplastic Starch. *Mater. Des.* **2013**, *49*, 701–704.

(95)   Luo, S.; Cao, J.; McDonald, A. G. Esterification of Industrial Lignin and Its Effect on the Resulting poly(3-Hydroxybutyrate-Co-3-Hydroxyvalerate) or Polypropylene Blends. *Ind. Crops Prod.* **2017**, *97*, 281–291.

(96)   Dehne, L.; Vila Babarro, C.; Saake, B.; Schwarz, K. U. Influence of Lignin Source and Esterification on Properties of Lignin-Polyethylene Blends. *Ind. Crops Prod.* **2016**, *86*, 320–328.

(97)   Hu, L.; Stevanovic, T.; Rodrigue, D. Unmodified and Esterified Kraft Lignin-Filled Polyethylene Composites: Compatibilization by Free-Radical Grafting. *J. Appl. Polym. Sci.* **2015**, *132* (7).

(98)   Guo, Z.-X.; Gandini, A. Polyesters from lignin—2. The Copolyesterification of Kraft Lignin and Polyethylene Glycols with Dicarboxylic Acid Chlorides. *Eur. Polym. J.* **1991**, *27* (11), 1177–1180.

(99)   Guo, Z.-X.; Gandini, A.; Pla, F. Polyesters from Lignin. 1. The Reaction of Kraft Lignin with Dicarboxylic Acid Chlorides. *Polym. Int.* **1992**, *27* (1), 17–22.

(100)   Fang, R.; Cheng, X.; Lin, W. Preparation and application of dimer acid/lignin graft copolymer. *BioResources* **2011**, *6* (3), 2874–2884.

(101)   Gordobil, O.; Moriana, R.; Zhang, L.; Labidi, J.; Sevastyanova, O. Assesment of Technical Lignins for Uses in Biofuels and Biomaterials: Structure-Related Properties, Proximate Analysis and Chemical Modification. *Ind. Crops Prod.* **2016**, *83*, 155–165.

(102)   Saito, T.; H. Brown, R.; A. Hunt, M.; L. Pickel, D.; M. Pickel, J.; M. Messman, J.; S. Baker, F.; Keller, M.; K. Naskar, A. Turning Renewable Resources into Value-Added Polymer : Development of Lignin -Based Thermoplastic. *Green Chem.* **2012**, *14* (12), 3295–3303.

(103)   Thielemans, W.; Wool, R. P. Lignin Esters for Use in Unsaturated Thermosets: Lignin Modification and Solubility Modeling. *Biomacromolecules* **2005**, *6* (4), 1895–1905.

(104)   Effendi, A.; Gerhauser, H.; Bridgwater, A. V. Production of Renewable Phenolic Resins by Thermochemical Conversion of Biomass: A Review. *Renew. Sustain. Energy Rev.* **2008**, *12* (8), 2092–2116.

(105)   Tan, T. T. M. Cardanol–lignin-Based Polyurethanes. *Polym Int* **1996**, *41* (1), 13–16.

(106)   Wu, L. C.-F.; Glasser, W. G. Engineering Plastics from Lignin. I. Synthesis of Hydroxypropyl Lignin. *J. Appl. Polym. Sci.* **1984**, *29* (4), 1111–1123.

(107)   Bernardini, J.; Cinelli, P.; Anguillesi, I.; Coltelli, M.-B.; Lazzeri, A. Flexible Polyurethane Foams Green Production Employing Lignin or Oxypropylated Lignin. *Eur. Polym. J.* **2015**, *64*, 147–156.

(108)   Mahmood, N.; Yuan, Z.; Schmidt, J.; Xu, C. (Charles). Preparation of Bio-Based Rigid Polyurethane Foam Using Hydrolytically Depolymerized Kraft Lignin via Direct Replacement or Oxypropylation. *Eur. Polym. J.* **2015**, *68* (Supplement C), 1–9.

(109)   Kühnel, I.; Saake, B.; Lehnen, R. Oxyalkylation of Lignin with Propylene Carbonate: Influence of Reaction Parameters on the Ensuing Bio-Based Polyols. *Ind. Crops Prod.* **2017**, *101*, 75–83.

(110)   Kühnel, I.; Podschun, J.; Saake, B.; Lehnen, R. Synthesis of Lignin Polyols via Oxyalkylation with Propylene Carbonate. *Holzforschung* **2014**, *69* (5), 531–538.

(111)   Sadeghifar, H.; Cui, C.; Argyropoulos, D. S. Toward Thermoplastic Lignin Polymers. Part 1. Selective Masking of Phenolic Hydroxyl Groups in Kraft Lignins via Methylation and Oxypropylation Chemistries. *Ind Eng Chem Res* **2012**, *51* (51), 16713–16720.

(112)   Wang, J.; Yao, K.; Korich, A. L.; Li, S.; Ma, S.; Ploehn, H. J.; Iovine, P. M.; Wang, C.; Chu, F.; Tang, C. Combining Renewable Gum Rosin and Lignin: Towards Hydrophobic Polymer Composites by Controlled Polymerization. *J. Polym. Sci. Part Polym. Chem.* **2011**, *49* (17), 3728–3738.

(113)   Ismail, T. N. M. T.; Hassan, H. A.; Hirose, S.; Taguchi, Y.; Hatakeyama, T.; Hatakeyama, H. Synthesis and Thermal Properties of Ester-Type Crosslinked Epoxy Resins Derived from Lignosulfonate and Glycerol. *Polym. Int.* **2010**, *59* (2), 181–186.

(114)   Feng, Q.; Li, J.; Cheng, H.; Chen, F.; Xie, Y. Synthesis and Characterization of Porous Hydrogel Based on Lignin and Polyacrylamide. *BioResources* **2014**, *9* (3), 4369–4381.

(115)   Jawerth, M.; Johansson, M.; Lundmark, S.; Gioia, C.; Lawoko, M. Renewable Thiol–Ene Thermosets Based on Refined and Selectively Allylated Industrial Lignin. *ACS Sustain. Chem. Eng.* **2017**, *5* (11), 10918–10925.

Chapter 3

3   UV-Curable Coatings of Modified Lignin

3.1   Introduction

"Lignocellulose" is the biomass derived from dry plant matter,[1] which consists of three major components: cellulose, hemicellulose, and lignin. The importance of lignocellulose as a source of energy and commodity chemicals is hallmarked by the availability of this renewable, carbon-based resource to produce fuels and chemicals that currently, are obtained from petroleum-based sources.[2] Among the main constituents of lignocellulose, lignin is considered the least utilized component. As a complex cross-linked, racemic[3], amorphous heteropolymer that is primarily generated as a by-product of the pulp and paper industry, lignin is utilized on-site as a fuel for recovery boilers in the form of black liquor. However, given the large production volume of 50-55 million tons (and growing) per year, a great amount of the material is under-utilized, with only about 2% of the lignin by-product being utilized for onwards product development.[4,5]

This natural polymer is can be best described as several phenylpropanoid (C9) units that are linked together via different linkages (mainly ether and carbon-carbon),[6] leading to a macromolecular structure that is rich in functional group chemistry (e.g. -OH, -C=O, and -OMe),[7] which can undergo a variety of chemical reactions aimed at converting this industrial by-product into a value-added one. Several processes have been reported in the past with the sole purpose of creating higher value products from this untapped resource such as fragmentation/depolymerization by thermal conversion,[8–14]with the purpose of breaking down the chemical structure of lignin to obtain commodity reagents (e.g. phenolic monomers). On the other hand, processes such as alkylation/de-alkylation,[15–17][14–16] hydroxyalkylation,[18–20] amination,[21,22] and nitration[23] focus on chemically modifying lignin in order to increase its reactivity towards post-modification through the introduction/addition of functional groups. Nevertheless, considering the abundance and diversity of hydroxyl groups within lignin's structure[24], chemical modification of the bulk material through conversion of the hydroxyl groups is considered a highly viable, if not the best, approach to converting lignin into a value-added material. Such modified lignin

will have the ability (depending on the type of modification) to undergo various post-modification processes specifically targeting value-addition. Chemical methods such as esterification,[25–31] phenolation,[32–36] etherification,[37–40] and urethanization[41] are among the commonly used processes reported for modification of lignin *via* the hydroxyl functional groups (Scheme 3-1).
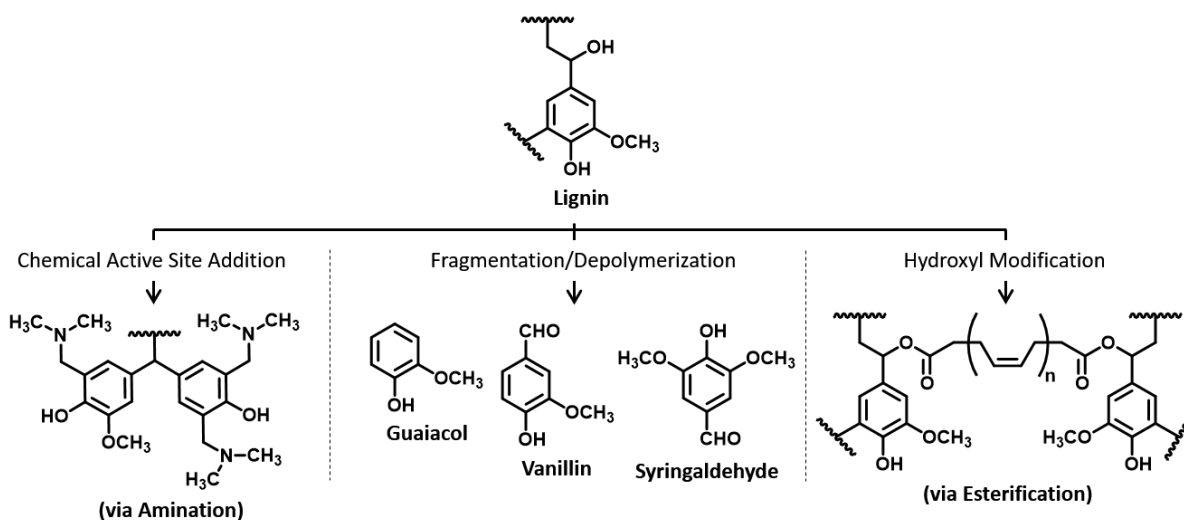
Scheme 3-1 Examples of compounds and materials produced by different lignin modification processes such as amination,[21] fragmentation/depolymerization,[42] and esterification.[26]

Lignin has a significant Ultraviolet- (UV)-absorbing property and therefore, has been incorporated into formulations to impart this property into various systems,[43,44] and therefore, the focus on lignin based coatings has centered on thermally-crosslinked thiol-ene networks[45,46], coatings[47–49], or polyurethane thermosets.[50–53] Nevertheless, utilizing un-purified commercial lignin as a monomer into UV/eb-crosslinkable systems and determining the properties of the coatings remain rare and require the use of photosensitive moieties as grafted co-monomers, multi-step syntheses, or other additives to overcome the inherently UV-absorbing nature of lignin.[54,55] Curing coatings by UV light is widely accepted as the most efficient method for the rapid generation of highly-crosslinked, polymer networks from liquid formulations at ambient temperature.[56] In

comparison to other types of photopolymerization and thermally initiated polymerization, UV-curing has several significant advantages that include lower equipment costs, much lower energy consumption, rapid curing times, and a imparts a substantial improvement on workplace safety as light cured coatings are far less hazardous to manufacture.[56,57]

In this context, kraft lignin (**KL**) was methacrylated using methacrylic anhydride to obtain methacrylated lignin (**ML**). The obtained **ML** was then incorporated into UV-curable formulations (up to 31 wt.% **ML**). The resulting formulations were cured on glass substrates as 15 µm thick coatings. Extent and efficiency of chemical modification of lignin were analyzed using multinuclear magnetic resonance (NMR) and Fourier transform-infrared (FT-IR) spectroscopies. The UV-cured coatings were also characterized and analyzed using FT-IR spectroscopy (Attenuated Total Reflectance; ATR), Thermogravimetric analysis (TGA), and Drop shape analysis (DSA); Pull-off strengths and cohesive/adhesive failures of the prepared coatings were obtained following ASTM D4541-09 standard test.

3.2   Experimental Section

3.2.1 Materials

Kraft lignin (**KL**) was provided by FPInnovations-Thunder Bay Bio-Economy Technology Centre. **KL** samples were crushed into powder using a mortar and pestle and heated at 45ºC for 48 hours *in vacuo* (762 mmHg; C9=180 g). Methacrylic anhydride (MethA; 94%, stabilized with 0.2% 2,4-dimethyl-6-tert-butylphenol), 1-methylimidazole (1MIM; 99%), and triphenylphosphine (Ph$_3$P; 99%) were purchased from Alfa Aesar and used as received. 2,2-Dimethoxy-2-phenylacetophenone (DMPA; 99%), tetra(ethylene glycol)diacrylate (TEGDA; technical grade, contains 150-200 ppm monomethyl ether hydroquinone (MEHQ) as inhibitor; 100-150 ppm hydroquinone as inhibitor), methacrylic acid (MA; 99%, contains 250 ppm MEHQ as inhibitor), 2,2'-biphenol (99%), 4-methoxyphenol (99%), 4-(benzyloxy)phenol (98%), benzyl alcohol (anhydrous, 99.8%), 3-phenyl-1-propanol (98%), 1,2-phenylenediacetic acid (99%), biphenyl-4,4'-dicarboxylic (97%), triethylamine (NEt$_3$; ≥ 99.5%, and chlorodi(isopropyl)phosphine ([CH(CH$_3$)$_2$]$_2$PCl, 96%) were obtained from Sigma-

Aldrich Co. and used as received. 6,6'-methylenebis(2-methoxy-4-methylphenol) was prepared using a literature procedure.[58] Tetrahydrofuran (THF) was purchased from Caledon and dried using an MBraun Solvent Purification System (SPS) for the methacrylation process. The same solvent was stored in the drybox over 4Å molecular sieves for the reaction with chlorodi(isopropyl)phosphine. Dichloromethane (CH_2Cl_2) and hexanes were purchased from Caledon Laboratories and used without further purification. Dimethylsulfoxide-d_6 (DMSO-d_6) was purchased from Cambridge Isotope Laboratories and used without any further purification. 2-[bis(4-hydroxyphenyl)methyl]benzyl alcohol was purchased from Tokyo Chemical Industry Co., Ltd. (TCI America) and used as received.

3.2.2 Methacrylation of **KL**

KL (1.00 g, 5.50 mmol) was added to THF (10 mL) in a round-bottom flask under vigorous stirring. The mixture was stirred for 5 min to obtain a homogeneous dark-brown solution. A mixture of 1-methylimidazole (1MIM, 0.10 mL, 0.10 mg, 1.25 mmol) and methacrylic anhydride (MethA, 0.82 mL, 0.84 g, 5.50 mmol) were then added to the **KL** solution and stirred at 60 ˚C for 60 minutes under an N_2 atmosphere. The brown mixture was then added dropwise into hexanes (100 mL) while stirring to precipitate a light brown powder. The obtained powder was dissolved in CH_2Cl_2 (10 mL) and washed with deionized water (30 mL) to remove the catalyst and any unreacted reagents. The organic phase was then precipitated in hexanes (100 mL) and dried *in vacuo* to give 1.46 g (146 wt% recovered product yield) **ML**. ^{1}H NMR (DMSO-d_6, 600 MHz): δ_H 1.89 (br, 3H, CH_3), 5.82 (br, 1H, vinyl), 6.14 (br, 1H, vinyl).

3.2.3 Product Characterization

Proton NMR spectra were recorded using a Varian INOVA 600 MHz spectrometer on solutions of ca. 5 mg of sample dissolved in 1 g of DMSO-d_6. ^{31}P{^{1}H} NMR spectra were recorded using a Varian INOVA 400 MHz spectrometer on solutions of 50 mg sample, dissolved in 1 g of THF (256 scans, relaxation delay = 5s). All ^{31}P{^{1}H} NMR spectra were referenced using 85% phosphoric acid as an external standard ($\delta_P = 0.0$). FT-IR spectra of samples were performed on a PerkinElmer FT-IR Spectrometer using

the universal attenuated total reflectance mode (UATR), a diamond crystal, as well as the UATR sampling accessory (part number: L1050231). Thermogravimetric analyses (TGA) were carried out on samples weighing 5-6 mg, using the Ramp mode at temperatures increasing from 25 ºC to 600 ºC at the rate of 10 ºC/min on a Q600 SDT TA Instrument and analyzed using TA Universal Analysis. Water contact angles (WCA) were measured placing the coatings on the stage of a Kruss DSA100 Drop Shape Analyzer (KRUSS GmbH, Hamburg, Germany). A static drop shape analyzer was used to determine the water contact angle on the surface.

A modified version of the method reported by Argyropoulos[24,59] was employed for quantitative $^{31}P\{^{1}H\}$ NMR analysis of **KL** compared with **ML** to quantify the OH groups on the **KL** sample, quantitatively determined the extent to which the hydroxyl groups were successfully converted during the methacrylation process. **KL** (0.05 g, 0.28 mmol) was added to THF (2 mL) in a round-bottom flask under vigorous stirring in the dry-box. The mixture was stirred for 5 min. to obtain a dark brown solution. NEt$_3$ (0.19 g, 261 µl, 1.88 mmol) was added to the mixture under stirring and stirred for 1 min. and then chlorodiisopropylphosphine ($[CH(CH_3)_2]_2PCl$; 0.085 g, 90 µl, 0.56 mmol) was added and the reaction mixture was stirred for 10 min at ambient temperature. The reaction mixture was then precipitated in n-pentane (10 mL) and dried *in vacuo* to obtain a light brown powder. The dried powder was swelled in THF (1.7 mL) and inserted into an NMR tube. 50 µL of a 0.05 molar solution of Ph$_3$P (2.5×10^{-6} mols) in THF was transferred into a capillary tube, flame-sealed, and inserted into the NMR tube containing the product and $^{31}P\{^{1}H\}$ NMR spectra were collected. The same procedure was carried out on the obtained **ML** sample and the extent of methacrylation was determined by comparing the integrations of the observed peaks in relative to the external standard. Different regions of the obtained $^{31}P\{^{1}H\}$ NMR spectrum were identified using small molecule, model reactions of corresponding hydroxyl-containing substrates with $[CH(CH_3)_2]_2PCl$.

3.2.4 Small Molecule Reactions

A general procedure was employed for model the reactions of $[CH(CH_3)_2]_2PCl$ with hydroxyl-containing small molecules. Briefly, one molar equivalent of each small molecule was dissolved in THF (5 mL) in the dry-box. Excess NEt$_3$ was added to the

stirred solution, followed by addition of 1 molar equivalent [CH(CH$_3$)$_2$]$_2$PCl. A sample of the reaction mixture was transferred to an NMR tube, and ^{31}P{^{1}H} NMR spectra were obtained.

2,2'-biphenol, 4-methoxyphenol, and 4-(benzyloxy)phenol were used as model small molecules containing uncondensed phenolic hydroxyl groups. ^{31}P{^{1}H} NMR (400 MHz): δ$_P$ = 148.3, [C$_6$H$_4$O**P**(C$_3$H$_7$)$_2$]$_2$; 149.4, CH$_3$O(C$_6$H$_4$)O**P**(C$_3$H$_7$)$_2$; 149.5, (C$_6$H$_5$)CH$_2$O(C$_6$H$_4$)O**P**(C$_3$H$_7$)$_2$.

Benzyl alcohol and 3-phenyl-1-propanol were used to represent aliphatic hydroxyl groups. ^{31}P{^{1}H} NMR (400 MHz): δ$_P$ = 154.6, (C$_6$H$_5$)CH$_2$O**P**(C$_3$H$_7$)$_2$; 151.5, (C$_6$H$_5$)C$_3$H$_6$O**P**(C$_3$H$_7$)$_2$.

2-[bis(4-hydroxyphenyl)methyl]benzyl alcohol was used as a small molecule comprising both aliphatic and uncondensed phenolic hydroxyl groups on its structure. ^{31}P{^{1}H} NMR (400 MHz): δ$_P$ = 154.9, [(C$_6$H$_4$)O**P**(C$_3$H$_7$)$_2$]$_2$CH[(C$_6$H$_4$)CH$_2$O**P**(C$_3$H$_7$)$_2$]; 148.1, [(C$_6$H$_4$)OP(C$_3$H$_7$)$_2$]$_2$CH[(C$_6$H$_4$)CH$_2$O**P**(C$_3$H$_7$)$_2$].

To assign where the chemical shifts for the product of the reaction of COOH groups with [CH(CH$_3$)$_2$]$_2$PCl would be observed, biphenyl-4,4'-dicarboxylic acid was used. ^{31}P{^{1}H} NMR (400 MHz): δ$_P$ = 144.4, [(C$_3$H$_7$)$_2$**P**OC(O)C$_6$H$_4$]$_2$.

Finally, 6,6'-methylenebis(2-methoxy-4-methylphenol) was reacted with [CH(CH$_3$)$_2$]$_2$PCl to assign the peak region of the product of condensed aromatic hydroxyl groups. ^{31}P{^{1}H} NMR (400 MHz): δ$_P$ = 162.1, [CH$_3$(C$_6$H$_5$)(OCH$_3$)(O**P**(C$_3$H$_7$)$_2$)]$_2$.

3.2.5 UV-Cured Coatings of Methacrylate Lignin (**ML**) and Characterization

Mixtures, containing different weight percentages of **ML** (0, 10, 20, and 31 wt.%), equal amounts of photoinitiator (2,2-Dimethoxy-2-phenylacetophenone; DMPA; 5 wt.%), reactive diluent (methacrylic acid; MA 38 wt.%, incorporated into the coating after curing) and corresponding amounts of crosslinker (tetra(ethyleneglycol)diacrylate; TEGDA) were weighed and combined in screw top vials and sonicated at room temperature for 20 min to obtain particulate- and haze-free formulations, which were then

cast on clean glass slides (or stainless steel sheets in case of the coating-to-surface adhesion tests) using a 12-inch meyer rod (AP-JR10, Jr. rod, 12 inch OA, 3/8 inch DIA, 8-1/2 inch EP, #10 wire). Photopolymerization was then performed using a modified UV-curing conveyor system, purchased from UV Process and Supply Inc. with a mercury bulb (UVA: 154 mW/cm^2, 189 mJ/cm^2, UVB: 74 mW/cm^2, 90 mJ/cm^2; as determined by a PP2-H-U Power Puck II purchased from EIT Instrument Markets) by placing the formulation cast surfaces on a conveyor (5.8 cm/s speed) for 25 s and irradiating with UV light to give coatings of 15 µm thickness as measured by a micrometer. Coating-to-surface adhesion for pull-off strengths and cohesive/adhesive failures of the prepared coatings were performed were obtained following ASTM D4541-09^{ε1} standard test, using a PostiTest pull-off adhesion tester (type V, self-aligning), purchased from Defelsko Corporation USA on coatings of 15 µm thickness, applied and cured on 20×15 cm stainless steel sheets. The procedures for determining the coating properties were all carried out in triplicates to ensure reproducibility and the results are reported as mean ± standard deviation.

3.3 Results and Discussion

3.3.1 Methacrylation of **KL**

Methacrylic anhydride (MethA) and 1-methylimidazole (1MIM) were used as the methacrylating reagent and the catalyst, respectively (Figure 3-1a). Samples of the reaction mixture were evaluated by ^{1}H NMR spectroscopy and showed three new signals for the **ML** sample as compared to the **KL** sample. The broad signal at $\delta_H = 1.89$ was assigned to the methyl functionality and the signals at $\delta_H = 5.82$ and 6.14 were attributed to the olefinic protons of the methacrylate group and gave strong evidence for grafted methacrylate groups onto lignin (Figure 3-1b).

FT-IR spectroscopy was performed on **KL** and the prepared **ML** samples (Figure 3-1c). Spectra of **ML** repeatedly showed significantly decreased signals at 3200-3500 cm^{-1} (s, br; O-H) relative to **KL** along with a corresponding increase in in the signal at 1735-1750 cm^{-1} (C=O), providing corroborating evidence for the methacrylation of lignin and the transformation of hydroxyl to acrylate. After methacrylation, IR signals increased in the

ML product at 1000-1320 cm^{-1} and 650-1000 cm^{-1} corresponding to stretching vibrations of C–O (ester) and bending vibrations of the unsaturated C=C groups, respectively. Taken together, these spectroscopic signatures provide strong evidence for the successful grafting of lignin.
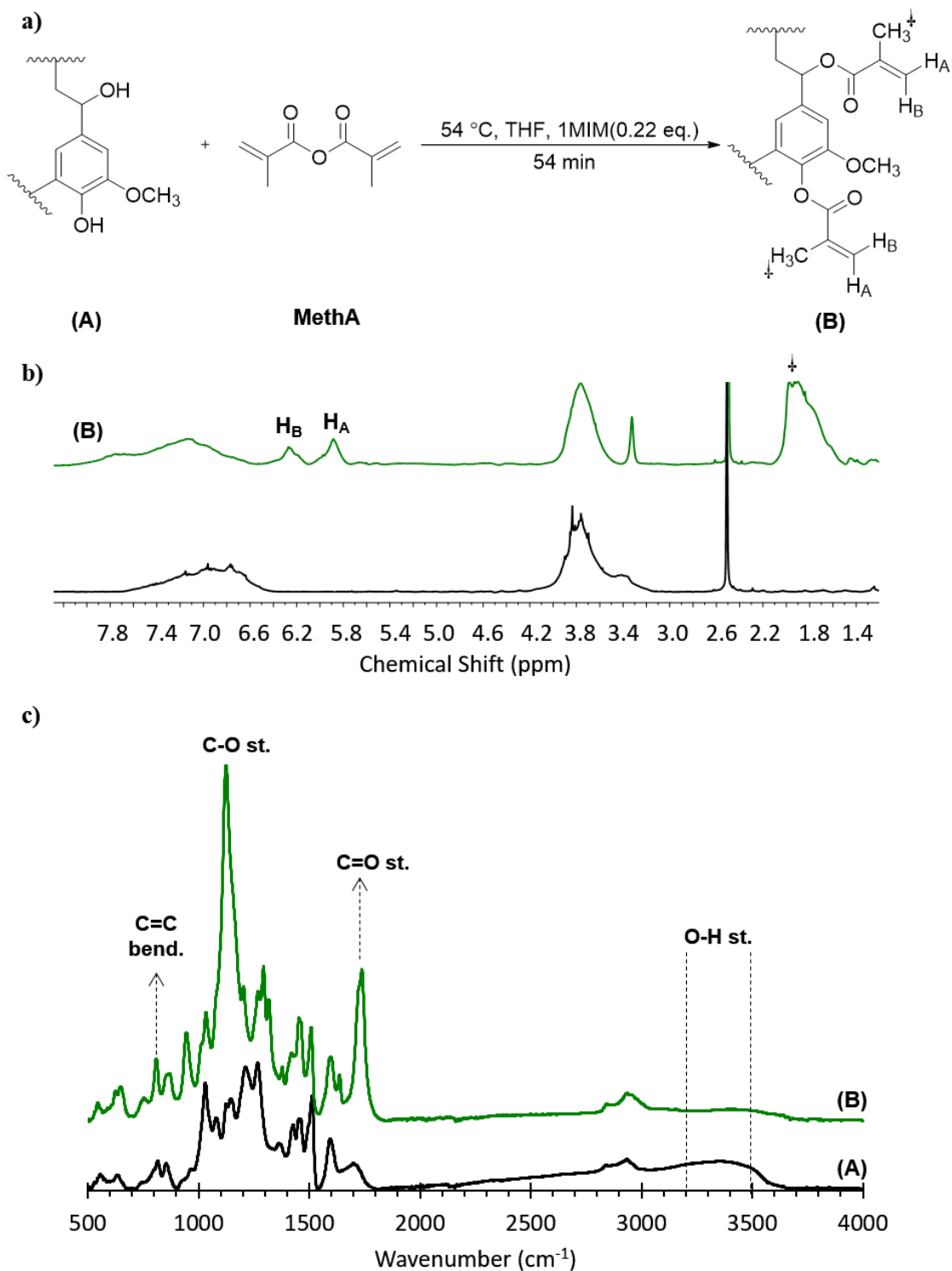
Figure 3-1 Reaction scheme for methacrylation of lignin using methacrylic anhydride (MethA) and 1-methylimidazole (1MIM) (a), along with ^{1}H NMR (b) and FTIR (c) spectra of **KL** (A) and **ML** (B).

3.3.2 Quantification of the Hydroxyl Functionalities of **KL**

Other studies have utilized ^{31}P{^{1}H} NMR spectroscopy for quantifying the hydroxyl-based functional groups in lignin. Such work used 4,4,5,5-tetramethyl-1,2,3-dioxophospholane, in the presence of chromium(III) acetylacetonate (relaxation reagent) to probe a native lignin sample and the modified lignin.[24,59,60] In this current work, chlorodi(isopropyl)phosphine ([CH(CH$_3$)$_2$]$_2$PCl) was used to install a phosphine functional group that aided in the identification and quantification of the hydroxyl environments within the structure of lignin. This is a good mimic for the phospholene employed by Argyropoulos, given the comparable steric and electronic demand. After dehydrohalogen coupling, the various locations of P throughout lignin gave separate signals for the different O-P functional group environments (aliphatic, δ_P = 160-170; uncondensed aromatic, δ_P = 147-150; condensed aromatic, δ_P = 150-160; and carboxyl, δ_P = 136-147). After the lignin has undergone methacrylation (i.e. to form **ML**), the chlorophosphine was again utilized as a probe for residual OH groups that remained unfunctionalized. To correlate ^{31}P{^{1}H} signals arising from the dehydrocoupling reaction promoting the P-O linkage to lignin, benchmark reactions with small molecule models were completed. The stoichiometry of OH groups within lignin was correlated by referencing the signal integrations with a known internal standard, Ph$_3$P. In a typical reaction of either small molecule or lignin itself (Scheme 3-2), corresponding signals appear in the ^{31}P{^{1}H} spectra that resulted from the dehydrohalogen coupling.
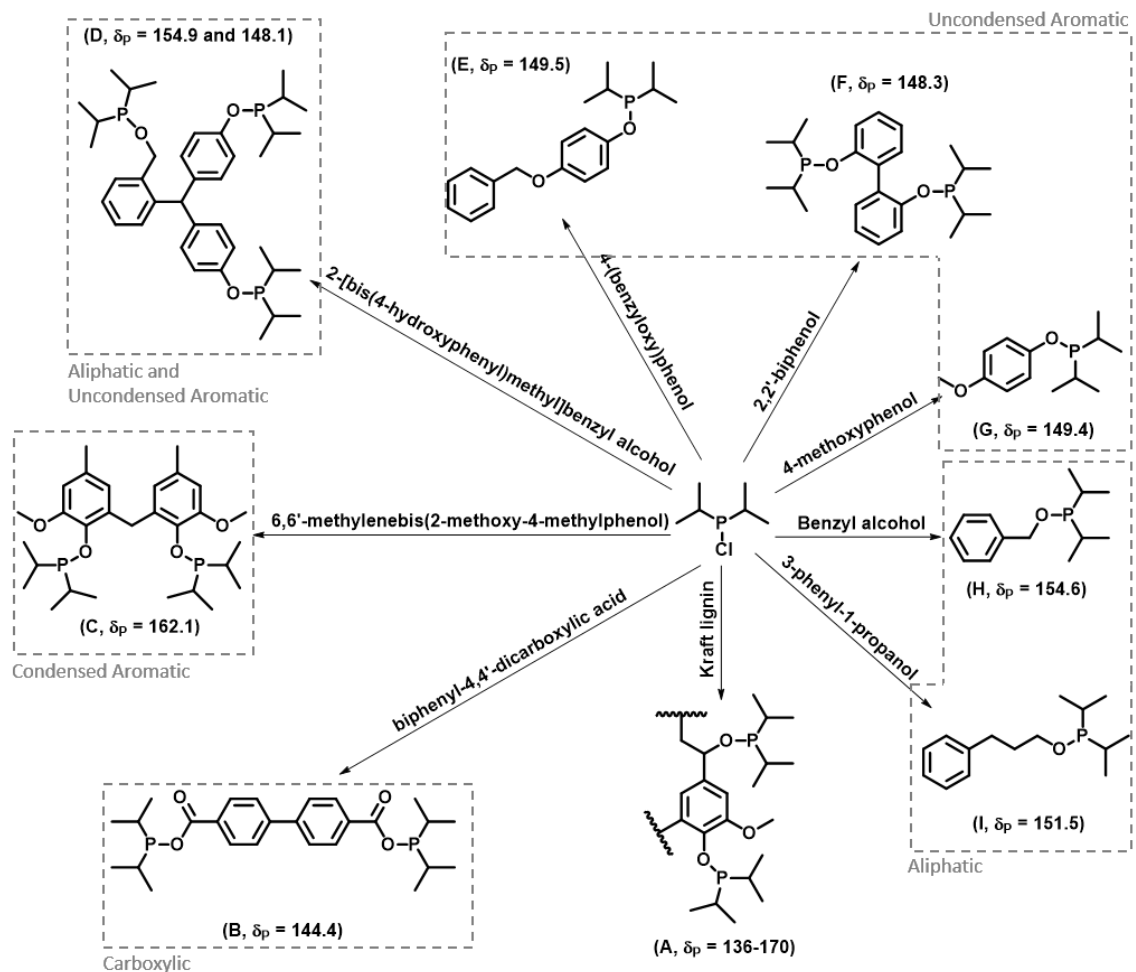
Scheme 3-2 Reaction scheme of kraft lignin and small molecules representing different hydroxyl functionalities with chlorodi(isopropyl)phosphine along with the corresponding chemical shifts of the products. Chemical shifts of the structural motifs were in good agreement with related molecular architectures.[61,62,63]

Spectroscopic signals ranging from $\delta_P = 136\text{-}170$ were observed and the obtained signals were used to identify four regions corresponding to different types of O-P environments and by extension we identified the -OH functionalities within the **KL** sample (Figure 3-2). The signal range was then integrated in comparison with the external standard (Ph$_3$P, 2.5×10^{-6} mols, $\delta_P = -4$) to determine the amount of -OP functionalities within 0.05 g of the sample.

$$2.5 \times 10^{-6} mol\ Ph_3P \times \frac{int.\ \boldsymbol{KL - Pi}}{1.00\ int.\ Ph_3P} \times \frac{180g\ \boldsymbol{KL}}{0.05\ g\ \boldsymbol{KL} \times C9} \times \frac{1mol\ OH}{1mol\ \boldsymbol{KL - Pi}}$$

$$\cong 1.5 \pm 0.2\ \frac{mol\ OH}{C9} \hspace{4cm} \textbf{Equation S-1}$$

Thus, it was determined that each C9 unit within the **KL** sample, contained an average of 1.5 ± 0.2 mol hydroxyl functionalities. This process was carried out in triplicate to confirm its reproducibility. The breakdown of each of the regions gave the corresponding amounts of each type of hydroxyl functionality Once the corresponding regions were identified, this information was used along with the Ph₃P standard to identify and quantify the number and type of O-P functionalities within **KL** and **ML** samples per gram of sample (Figure 3-3). The **KL** sample contained 0.86 mmol·g⁻¹ aliphatic hydroxyl groups, 0.70 mmol·g⁻¹ uncondensed phenolic hydroxyl groups, 1.76 mmol·g⁻¹ condensed phenolic groups, and 0.85 mmol.g⁻¹ carboxylic groups, on average. Furthermore, we determined that on average, every C9 unit on lignin contains 1.5 ± 0.2 molar equivalents of hydroxyl functionalities. The ³¹P{¹H} NMR spectroscopic analyses were performed in triplicate.
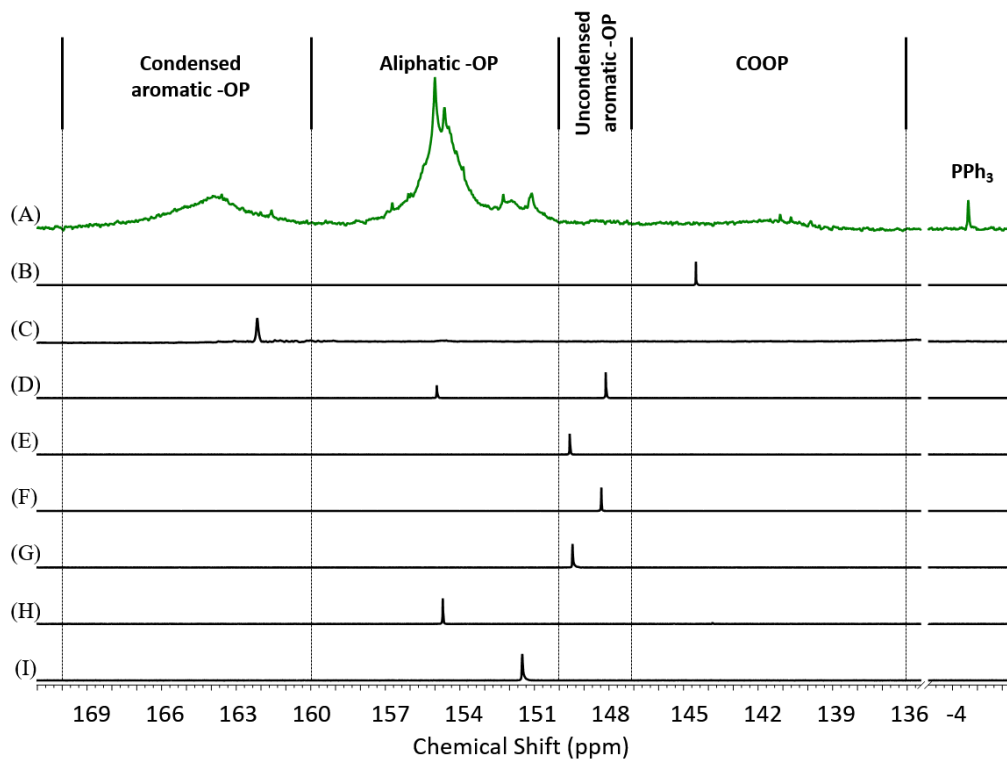
Figure 3-2 $^{31}P\{^1H\}$ NMR spectra of products (Scheme 3-2) obtained from reaction of chlorodi(isopropyl)phosphine with kraft lignin (A), biphenyl-4,4'-dicarboxylic acid (B; $\delta_p = 144.4$), 6,6'-methylenebis(2-methoxy-4-methylphenol) (C; $\delta_p = 162.1$), 2-[bis(4-hydroxyphenyl)methyl]benzyl alcohol (D; $\delta_p = 154.9$, uncondensed aromatic, $\delta_p = 148.1$, aliphatic), 4-(benzyloxy)phenol (E; $\delta_p = 149.5$), 2,2'-biphenol (F; $\delta_p = 148.3$), 4-methoxyphenol (G; $\delta_p = 149.4$), benzyl alcohol (H; $\delta_p = 154.6$), and 3-phenyl-1-propanol (I; $\delta_p = 151.5$).

3.3.3 Extent of Methacrylation

To determine the EOM, **ML** was reacted with $[CH(CH_3)_2]_2PCl$ using the same reaction conditions and parameters as previously described for reacting the **KL** sample with $[CH(CH_3)_2]_2PCl$. Using the same amount of Ph_3P as the external standard while obtaining the $^{31}P\{^1H\}$ spectrum of the product of reacting **ML** with $[CH(CH_3)_2]_2PCl$ (Figure 3-3), we were able to quantify residual hydroxyl functionalities on the **ML** sample that were not converted in the methacrylation process. Using this approach, the EOM was found to be $70 \pm 1.7\%$, where all carboxylic and uncondensed aromatic hydroxyls, as well as

72.27% and 44.48% of the aliphatic and the condensed aromatic hydroxyls were respectively determined to be completely converted through this process.
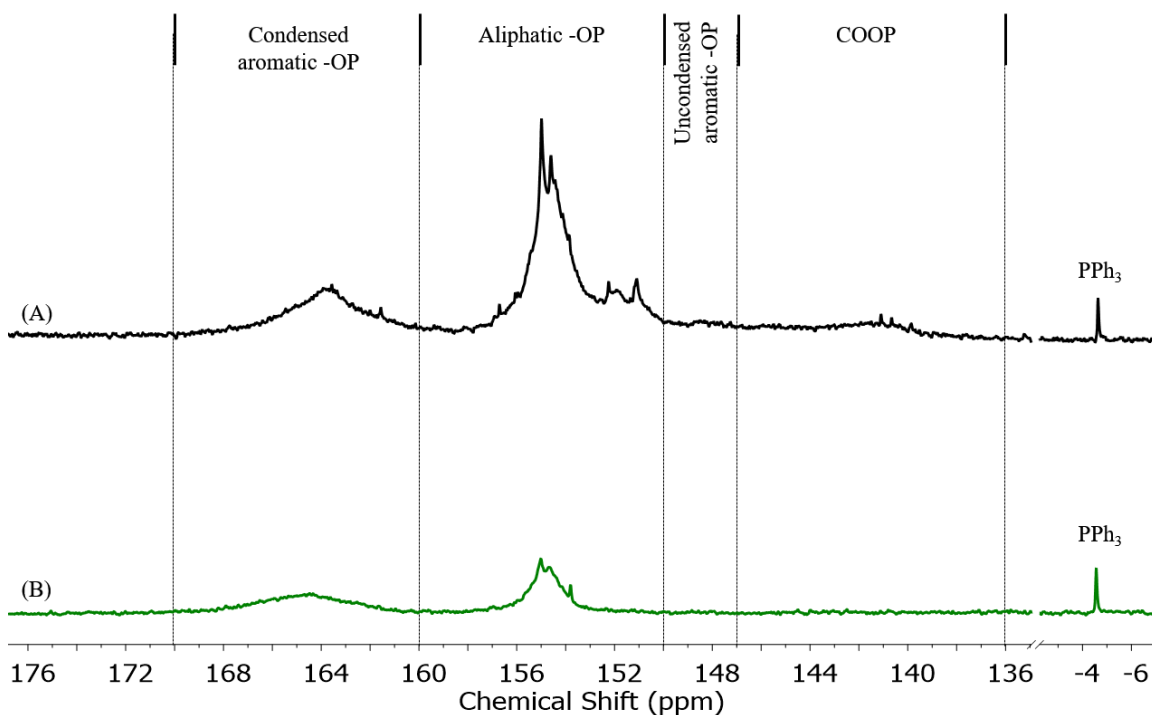
Figure 3-3 ^{31}P{^{1}H} NMR spectra of products obtained from the reaction of **KL** (A) and **ML** (B) with [CH(CH$_3$)$_2$]$_2$PCl.

3.3.4 Preparation and Characterization of UV-Cured Coatings Using ML

While the KL sample had a naturally dark brown color and limited solubility in common organic solvents, the ML sample had a much better solubility profile, making UV-curing more facile. **ML**-based UV-cured coatings were prepared using formulations consisting of **ML**, photoinitiator (DMPA; 5 wt.%), reactive diluent (MethAcid, 38 wt.%), and corresponding amounts of crosslinker (TEGDA) as described in Table 3-1. The cast formulations were applied onto the corresponding surfaces (glass or stainless steel) using a Meyer rod, and cured on a UV-curing conveyor (Scheme 3-3). Coatings containing more than 31 wt.% **ML** were not curable under UV-light, likely due to the decreased transparency of the formulations at higher **ML** loadings, preventing effective penetration of the coatings by UV light.
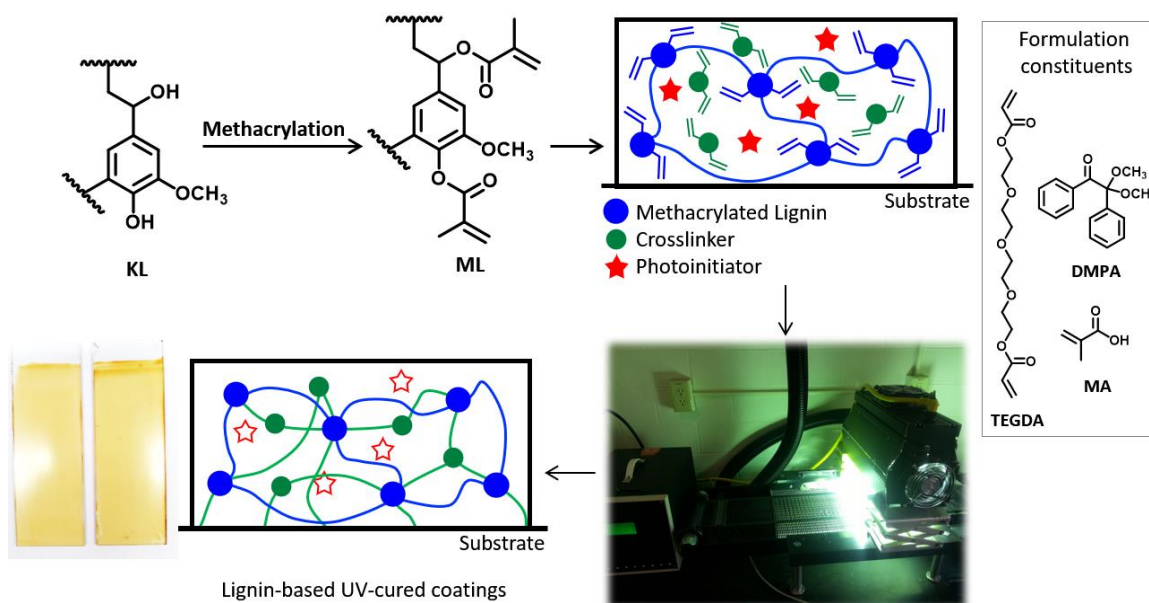
Scheme 3-3 Process description for incorporating lignin into UV-cured coatings (TEGDA = tetraethyleneglycoldiacrylate; MA = methacrylic acid; DMPA (photoinitiator) = 2,2-Dimethoxy-2-phenylacetophenone.

ATR-FTIR spectra were obtained before curing and for freshly prepared coatings after removing from the surface with a scalpel and grinding into powder form using a mortar and pestel. The peak corresponding to C=O (1720 cm^{-1}) was used as an internal standard as its intensity does not change upon curing. The C=C (1620-1680 cm^{-1}) peak was devoncoluted from the adjacent C=O peak in each spectra, the corresponding intensity was compared to the intensity of the internal standard peak before and after curing and the cure percentage was calculated as the percent decrease in the relative intensity of the C=C peak (Figure 3-4, 100% corresponding to zero C=C functionality remaining). Figure 3-5a shows the cure percentages corresponding to the wt.% of **ML** in each coating. It was determined that more of the liquid formulation was cured as the amount of **ML** was increased in the formulation (Table 3-1), which was attributed to the inherently high cross-link density provided by the **ML**
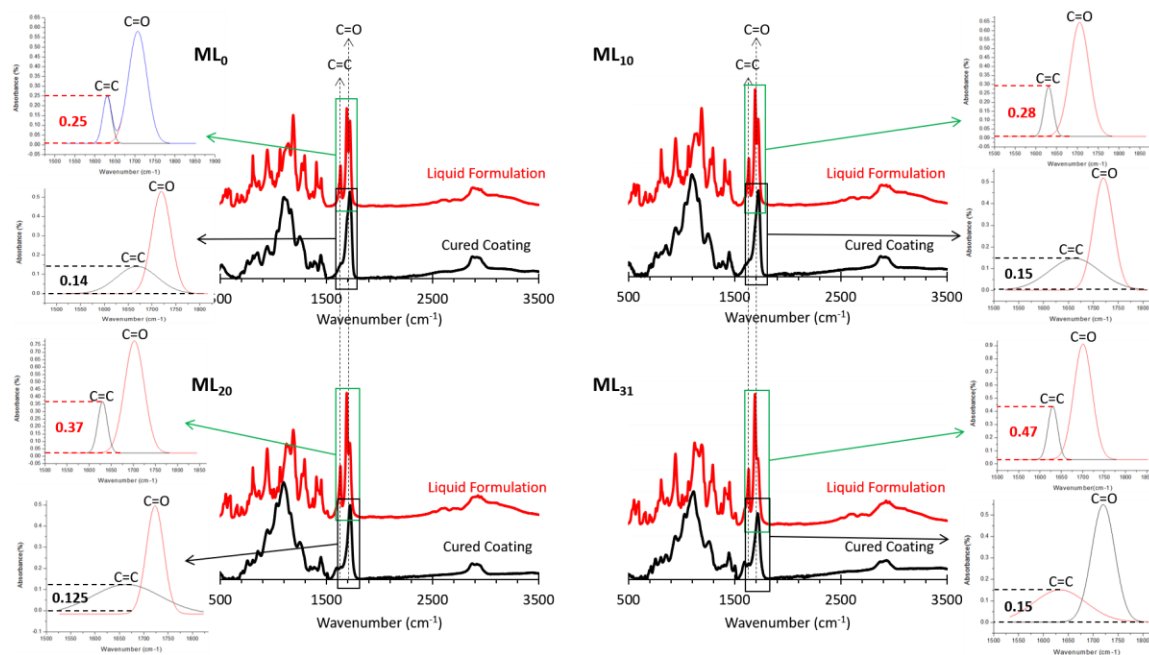
Figure 3-4 ATR-FTIR spectra of the prepared liquid formulations and cured coatings, highlighting the reduction in the intensity of the C=C peak (corresponding to the cure percentage). Values shown on the deconvoluted peaks represent the peak intensities used for determining corresponding cure percentages.

Drop shape analysis was used to determine the effect of the **ML**-incorporation on the hydrophobicity of the prepared UV-cured coatings (Figure 3-5b). It was determined that the incorporation of **ML** into the prepared coatings increased their hydrophobicity, with the measured water contact angle of the **ML₀** and the **ML₃₁** being 43.1 ± 0.3 and 51.2 ± 0.6 degrees, respectively (Table 3-1). The obtained values are in-line with the hydrophobic nature of lignin or lignin derivatives[27,64,65] and comparable to the same values reported for thermally cured lignin-based coatings.[66]

Pull-off adhesion tests were performed on the prepared coatings to determine the actual pull-off force (F) required to detach a steel dolly (14 mm diameter) that was affixed to coatings cured on stainless steel substrates (Figure 3-5c). Liquid formulations containing known amounts of **ML** (0, 10, 20, and 31 wt.%) were applied to clean steel plates (approximately 12 cm by 24 cm) and cured under UV-light. Coated surfaces were degreased using acetone to remove any oil, moisture, or dust. the surfaces were then

abraded using a 3M abrasive pad to promote adhesion between the surface and the dollies. A mixture of Loctite 907 Hysol adhesive was prepared according to the standard procedure and applied on the bases of 14mm dollies (approximately 50-100 microns thick); Dollies were then placed on the coated surfaces and pushed carefully to avoid any sliding. Any excess adhesive around the edges of the dolly was removed with cotton swabs. The dollies were then left for 3 days to let the adhesive cure completely. After 3 days, the dollies were connected to the tester using the provided actuator assembly. Following the manufacturer's instructions, tests were carried out at MPa rates of 0.40, 0.70, 1.40, 2.00, and 2.50 to obtain the pressure required for pulling the attached dolly off the coated surface. Each coating was tested in triplicate and the results were reported as mean ± standard deviation. The required force for each coating was calculated according to the equation provided in the standard test procedure: $X = \frac{4F}{\pi d^2}$; where X represents greatest mean pull-off stress applied during a pass/fail test, or the pull-off strength achieved at failure (both have units of MPa); F represents the actual force applied to the test surface (N); and d stands for the equivalent diameter of the original surface area stressed (mm). It was determined that increasing the amount of **ML** in the coating formulation up to 31 wt.%, increased the force required for pulling the corresponding coating off the surface by 278 N (Table 3-1).
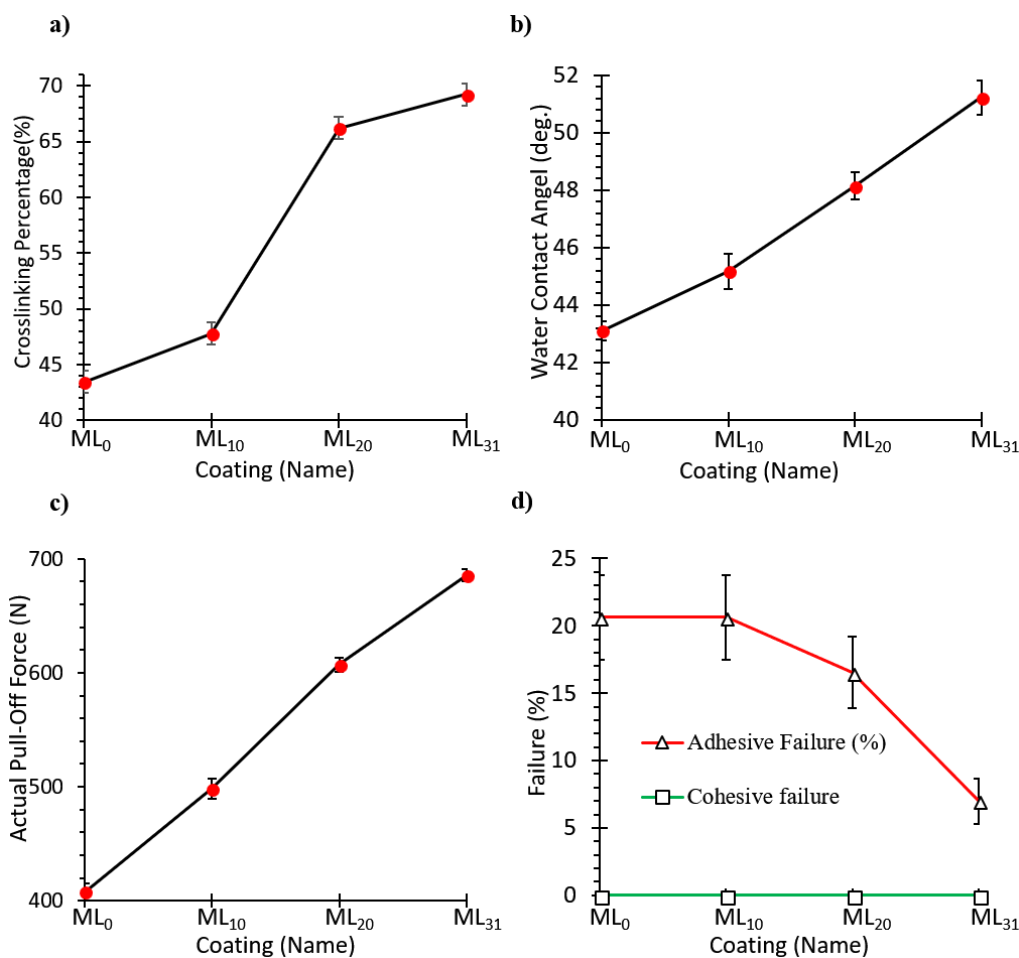
Figure 3-5 Determined cure percentages (a), water contact angles (b), actual pull-off forces (c), and adhesive/cohesive failures (d) of the **ML**-based UV-cured coatings.

Percentages of adhesive and cohesive failures were calculated by determining the respective areas on the dollies representing adhesive (area of the coating attached to the dolly after pull-off) and cohesive failures (area of the coating with visibly lost cohesiveness; Figure 3-5d). During the pull-off adhesion test, each tested surface was monitored to measure the cohesive and adhesive failures. Adhesive failure refers to the percentage of the coating which fails to stick on the surface, whereas the cohesive failure refers to the percentage of the coating that fails to keep its entirety and is divided into two layers (i.e. one sticking to the dolly and one to the surface). The area of the dolly was measured prior to the test (*b*). The area of coating attached to the dolly after the pull-off test was measured as well (*a*). Comparing these two recorded values gave the adhesive

failures as: $A.F. = \frac{a}{b} \times 100$. If the coatings were to detach from the surface in a non-cohesive manner (losing its entirety), the area of non-cohesive coating left on the dolly would be recorded (c). Comparing this area with the total surface of the dolly (b) would then give the cohesive failure as: $C.F. = \frac{c}{b} \times 100$. Each measurement was carried out in triplicate to ensure its reproducibility. As no cohesive failure was observed for any of the coatings, no mean and standard deviation was reported for the cohesive failures. While none of the coatings showed any signs of cohesive failure, the percentage of adhesive failure decreased as the amount of **ML** was increased in the coating formulation (Table 3-1).

Table 3-1 Formulation details for ML-based UV-cured coatings.

Composition or property	ML_0	ML_{10}	ML_{20}	ML_{31}
ML (wt.%)	0	10	20	31
DMPA (wt.%)	5	5	5	5
MA (wt.%)	38	38	38	38
TEGDA (wt.%)	57	47	37	27
Cure percentage (%)	43.4 ± 1.7	47.7 ± 2.3	66.2 ± 1.2	69.2 ± 1.1
Water contact angle (°)	43.1 ± 0.3	45.2 ± 0.6	48.2 ± 0.5	51.2 ± 0.6
Pull-off force (N)	407.7 ± 7.8	498.5 ± 8.7	607.2 ± 6.1	685.7 ± 5.1
Adhesive failure (%)	20.6 ± 3.1	20.6 ± 3.1	16.5 ± 2.6	7.0 ± 1.6
Cohesive failure (%)	0	0	0	0
T_d onset (°C)	86.2 ± 1.7	140.5 ± 1.0	160.9 ± 0.8	165.3 ± 0.9
Wt.% at 600 °C	3.7 ± 1.3	13.3 ± 1.8	15.9 ± 1.5	21.9 ± 1.0

After casting and curing the formulations on glass slides, each coating was scraped off the glass surface using a scalpel and crushed using a mortar and pestle. Each crushed sample was heated at 40 °C *in vacuo* for 24 h before measuring its thermal properties. Thermogravimetric analyses were then performed on the crushed coating samples to examine the effect of **ML**-incorporation on the thermal stability of the coatings at high temperatures (Figure 5). It was observed that the methacrylation of lignin, along with the incorporation of **ML** into the prepared coatings, impacted the T_d onset temperatures of the coatings. The T_d onset values of the **KL** sample (99.2 ± 0.9 °C) increased by 60.6 °C upon methacrylation (159.8 ± 1.7 °C for **ML**). While increasing the amount of **ML** in the UV-cured coatings the T_d onset temperatures increased to 86.2 ± 1.7, 140.5 ± 1.0, 160.9 ± 0.8, and 165.3 ± 0.9°C for the **ML$_0$, ML$_{10}$, ML$_{20}$**, and **ML$_{31}$** coatings, respectively. Similarly increasing **ML** amounts in the coatings increased the retained weight at 600 °C, i.e., increased char formation, resulting from the presence of lignin with inherently crosslinked structure that promotes char formation.[10,66]
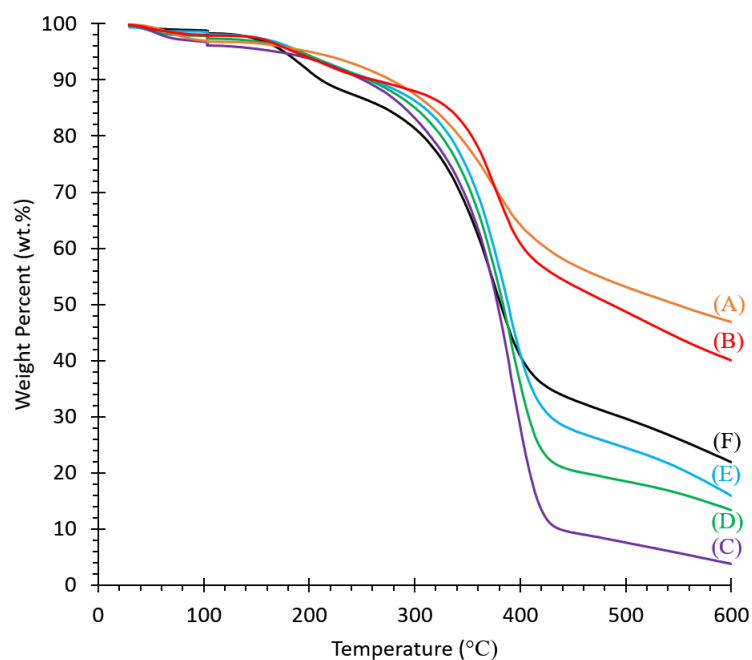
Figure 3-6 Thermogravimetric analysis of the **KL**(A) and **ML**(B) samples, along with the **ML$_0$** (C), **ML$_{10}$** (D), **ML$_{20}$** (E), and **ML$_{31}$** (F) coatings, representing the obtained

thermograms under N_2, as well as the onset decomposition temperatures (T_d onset) and the retained weights (char) at 600 °C (wt.%) for each sample.

3.4 References

(1)   Carroll, A.; Somerville, C. Cellulosic Biofuels. *Annu. Rev. Plant Biol.* **2009**, *60* (1), 165–182.

(2)   Luterbacher, J. S.; Alonso, D. M.; Dumesic, J. A. Targeted Chemical Upgrading of Lignocellulosic Biomass to Platform Molecules. *Green Chem.* **2014**, *16* (12), 4816–4838.

(3)   Ralph, J.; Peng, J.; Lu, F.; Hatfield, R. D.; Helm, R. F. Are Lignins Optically Active? *J. Agric. Food Chem.* **1999**, *47* (8), 2991–2996.

(4)   Bruijnincx, P.; Weckhuysen, B.; Gruter, G.-J.; Engelen-Smeets, E. *Lignin Valorisation: The Importance of a Full Value Chain Approach*; 2016.

(5)   Silva, E. A. B. da; Zabkova, M.; Araújo, J. D.; Cateto, C. A.; Barreiro, M. F.; Belgacem, M. N.; Rodrigues, A. E. An Integrated Process to Produce Vanillin and Lignin-Based Polyurethanes from Kraft Lignin. *Chem. Eng. Res. Des.* **2009**, *87* (9), 1276–1292.

(6)   Windeisen, E.; Wegener, G. 10.15 - Lignin as Building Unit for Polymers. In *Polymer Science: A Comprehensive Reference*; Matyjaszewski, K., Möller, M., Eds.; Elsevier: Amsterdam, 2012; pp 255–265.

(7)   Morandim-Giannetti, A. A.; Agnelli, J. A. M.; Lanças, B. Z.; Magnabosco, R.; Casarin, S. A.; Bettini, S. H. P. Lignin as Additive in Polypropylene/Coir Composites: Thermal, Mechanical and Morphological Properties. *Carbohydr. Polym.* **2012**, *87* (4), 2563–2568.

(8)   Kang, S.; Li, X.; Fan, J.; Chang, J. Hydrothermal Conversion of Lignin: A Review. *Renew. Sustain. Energy Rev.* **2013**, *27*, 546–558.

(9)   Liu, C.; Hu, J.; Zhang, H.; Xiao, R. Thermal Conversion of Lignin to Phenols: Relevance between Chemical Structure and Pyrolysis Behaviors. *Fuel* **2016**, *182*, 864–870.

(10)   Sharma, R. K.; Wooten, J. B.; Baliga, V. L.; Lin, X.; Geoffrey Chan, W.; Hajaligol, M. R. Characterization of Chars from Pyrolysis of Lignin. *Fuel* **2004**, *83* (11–12), 1469–1482.

(11)   Patwardhan, P. R.; Brown, R. C.; Shanks, B. H. Understanding the Fast Pyrolysis of Lignin. *ChemSusChem* **2011**, *4* (11), 1629–1636.

(12)   Cheng, S.; Yuan, Z.; Leitch, M.; Anderson, M.; Xu, C. (Charles). Highly Efficient de-Polymerization of Organosolv Lignin Using a Catalytic Hydrothermal Process and Production of Phenolic Resins/Adhesives with the Depolymerized Lignin as a Substitute for Phenol at a High Substitution Ratio. *Ind. Crops Prod.* **2013**, *44* (Supplement C), 315–322.

(13)   Yang, H.; Yan, R.; Chen, H.; Lee, D. H.; Zheng, C. Characteristics of Hemicellulose, Cellulose and Lignin Pyrolysis. *Fuel* **2007**, *86* (12), 1781–1788.

(14)   Liu, Q.; Wang, S.; Zheng, Y.; Luo, Z.; Cen, K. Mechanism Study of Wood Lignin Pyrolysis by Using TG–FTIR Analysis. *J. Anal. Appl. Pyrolysis* **2008**, *82* (1), 170–177.

(15)   Kim, K. H.; Dutta, T.; Walter, E. D.; Isern, N. G.; Cort, J. R.; Simmons, B. A.; Singh, S. Chemoselective Methylation of Phenolic Hydroxyl Group Prevents Quinone

Methide Formation and Repolymerization During Lignin Depolymerization. *ACS Sustain. Chem. Eng.* **2017**, *5* (5), 3913–3919.

(16)   Liu, Y.; Li, K. Preparation and Characterization of Demethylated Lignin-Polyethylenimine Adhesives. *J. Adhes.* **2006**, *82* (6), 593–605.

(17)   Biberstein, J.; Das, S.; Umbach, J.; Boyer, R.; Sutton, K.; Czepizak, M. *Production of Dimethyl Sulfide from Lignin*; Gaylord Chemical, 2010.

(18)   Hu, L.; Pan, H.; Zhou, Y.; Zhang, M. Methods to Improve Lignin's Reactivity as a Phenol Substitute and as Replacement for Other Phenolic Compounds: A Brief Review. *BioResources* **2011**, *6* (3), 3515–3525.

(19)   Alonso, M. V.; Oliet, M.; Rodríguez, F.; Astarloa, G.; Echeverría, J. M. Use of a Methylolated Softwood Ammonium Lignosulfonate as Partial Substitute of Phenol in Resol Resins Manufacture. *J. Appl. Polym. Sci.* **2004**, *94* (2), 643–650.

(20)   Alonso, M. V.; Rodríguez, J. J.; Oliet, M.; Rodríguez, F.; García, J.; Gilarranz, M. A. Characterization and Structural Modification of Ammonic Lignosulfonate by Methylolation. *J. Appl. Polym. Sci.* **2001**, *82* (11), 2661–2668.

(21)   Matsushita, Y.; Yasuda, S. Reactivity of a Condensed–type Lignin Model Compound in the Mannich Reaction and Preparation of Cationic Surfactant from Sulfuric Acid Lignin. *J. Wood Sci.* **2003**, *49* (2), 166–171.

(22)   Yue, X.; Chen, F.; Zhou, X. IMPROVED INTERFACIAL BONDING OF PVC/WOOD-FLOUR COMPOSITES BY LIGNIN AMINE MODIFICATION. *BioResources* **2011**, *6* (2), 2022–2044.

(23)   Zhang, L.; Huang, J. Effects of Nitrolignin on Mechanical Properties of Polyurethane–nitrolignin Films. *J. Appl. Polym. Sci.* **2001**, *80* (8), 1213–1219.

(24)   Argyropoulos, D. S. Quantitative Phosphorus-31 NMR Analysis of Lignins, a New Tool for the Lignin Chemist. *J. Wood Chem. Technol.* **1994**, *14* (1), 45–63.

(25)   Thielemans, W.; Wool, R. P. Lignin Esters for Use in Unsaturated Thermosets: Lignin Modification and Solubility Modeling. *Biomacromolecules* **2005**, *6* (4), 1895–1905.

(26)   Saito, T.; H. Brown, R.; A. Hunt, M.; L. Pickel, D.; M. Pickel, J.; M. Messman, J.; S. Baker, F.; Keller, M.; K. Naskar, A. Turning Renewable Resources into Value-Added Polymer : Development of Lignin -Based Thermoplastic. *Green Chem.* **2012**, *14* (12), 3295–3303.

(27)   Gordobil, O.; Herrera, R.; Llano-Ponte, R.; Labidi, J. Esterified Organosolv Lignin as Hydrophobic Agent for Use on Wood Products. *Prog. Org. Coat.* **2017**, *103*, 143–151.

(28)   Guo, Z.-X.; Gandini, A. Polyesters from lignin—2. The Copolyesterification of Kraft Lignin and Polyethylene Glycols with Dicarboxylic Acid Chlorides. *Eur. Polym. J.* **1991**, *27* (11), 1177–1180.

(29)   Fang, R.; Cheng, X.; Lin, W. PREPARATION AND APPLICATION OF DIMER ACID/LIGNIN GRAFT COPOLYMER. *BioResources* **2011**, *6* (3), 2874–2884.

(30)   Luo, S.; Cao, J.; McDonald, A. G. Esterification of Industrial Lignin and Its Effect on the Resulting poly(3-Hydroxybutyrate-Co-3-Hydroxyvalerate) or Polypropylene Blends. *Ind. Crops Prod.* **2017**, *97*, 281–291.

(31)   Dehne, L.; Vila Babarro, C.; Saake, B.; Schwarz, K. U. Influence of Lignin Source and Esterification on Properties of Lignin-Polyethylene Blends. *Ind. Crops Prod.* **2016**, *86*, 320–328.

(32)   Jiang, X.; Liu, J.; Du, X.; Hu, Z.; Chang, H.; Jameel, H. Phenolation to Improve Lignin Reactivity toward Thermosets Application. *ACS Sustain. Chem. Eng.* **2018**, *6* (4), 5504–5512.

(33)   Podschun, J.; Stücker, A.; Saake, B.; Lehnen, R. Structure–Function Relationships in the Phenolation of Lignins from Different Sources. *ACS Sustain. Chem. Eng.* **2015**, *3* (10), 2526–2532.

(34)   Younesi-Kordkheili, H.; Pizzi, A.; Niyatzade, G. Reduction of Formaldehyde Emission from Particleboard by Phenolated Kraft Lignin. *J. Adhes.* **2016**, *92* (6), 485–497.

(35)   Tan, T. T. M. Cardanol–lignin-Based Polyurethanes. *Polym. Int.* **1996**, *41* (1), 13–16.

(36)   Podschun, J.; Saake, B.; Lehnen, R. Reactivity Enhancement of Organosolv Lignin by Phenolation for Improved Bio-Based Thermosets. *Eur. Polym. J.* **2015**, *67*, 1–11.

(37)   Duval, A.; Avérous, L. Cyclic Carbonates as Safe and Versatile Etherifying Reagents for the Functionalization of Lignins and Tannins. *ACS Sustain. Chem. Eng.* **2017**, *5* (8), 7334–7343.

(38)   Ahvazi, B.; Wojciechowicz, O.; Ton-That, T.-M.; Hawari, J. Preparation of Lignopolyols from Wheat Straw Soda Lignin. *J. Agric. Food Chem.* **2011**, *59* (19), 10505–10516.

(39)   Nadji, H.; Bruzzèse, C.; Belgacem, M. N.; Benaboura, A.; Gandini, A. Oxypropylation of Lignins and Preparation of Rigid Polyurethane Foams from the Ensuing Polyols. *Macromol. Mater. Eng.* **2005**, *290* (10), 1009–1016.

(40)   Sadeghifar, H.; Cui, C.; Argyropoulos, D. S. Toward Thermoplastic Lignin Polymers. Part 1. Selective Masking of Phenolic Hydroxyl Groups in Kraft Lignins via Methylation and Oxypropylation Chemistries. *Ind Eng Chem Res* **2012**, *51* (51), 16713–16720.

(41)   Hatakeyama, H.; Hirogaki, A.; Matsumura, H.; Hatakeyama, T. Glass Transition Temperature of Polyurethane Foams Derived from Lignin by Controlled Reaction Rate. *J. Therm. Anal. Calorim.* **2013**, *114* (3), 1075–1082.

(42)   Pandey, M. P.; Kim, C. S. Lignin Depolymerization and Conversion: A Review of Thermochemical Methods. *Chem Eng Technol* **2011**, *34* (1), 29–41.

(43)   Liu, X.; Wang, J.; Li, S.; Zhuang, X.; Xu, Y.; Wang, C.; Chu, F. Preparation and Properties of UV-Absorbent Lignin Graft Copolymer Films from Lignocellulosic Butanol Residue. *Ind. Crops Prod.* **2014**, *52*, 633–641.

(44)   Hambardzumyan, A.; Foulon, L.; Chabbert, B.; Aguié-Béghin, V. Natural Organic UV-Absorbent Coatings Based on Cellulose and Lignin: Designed Effects on Spectroscopic Properties. *Biomacromolecules* **2012**, *13* (12), 4081–4088.

(45)   Jawerth, M.; Johansson, M.; Lundmark, S.; Gioia, C.; Lawoko, M. Renewable Thiol–Ene Thermosets Based on Refined and Selectively Allylated Industrial Lignin. *ACS Sustain. Chem. Eng.* **2017**, *5* (11), 10918–10925.

(46)   Buono, P.; Duval, A.; Averous, L.; Habibi, Y. Lignin-Based Materials Through Thiol–Maleimide "Click" Polymerization. *ChemSusChem 10* (5), 984–992.

(47)   Li, S.; Xie, W.; Wilt, M.; Willoughby, J. A.; Rojas, O. J. Thermally Stable and Tough Coatings and Films Using Vinyl Silylated Lignin. *ACS Sustain. Chem. Eng.* **2018**, *6* (2), 1988–1998.

(48)   Hult, E.-L.; Koivu, K.; Asikkala, J.; Ropponen, J.; Wrigstedt, P.; Sipilä, J.; Poppius-Levlin, K. Esterified Lignin Coating as Water Vapor and Oxygen Barrier for Fiber-Based Packaging. *Holzforschung* **2013**, *67* (8), 899–905.

(49)   Hult, E.-L.; Ropponen, J.; Poppius-Levlin, K.; Ohra-Aho, T.; Tamminen, T. Enhancing the Barrier Properties of Paper Board by a Novel Lignin Coating. *Ind. Crops Prod.* **2013**, *50*, 694–700.

(50)   Bernardini, J.; Cinelli, P.; Anguillesi, I.; Coltelli, M.-B.; Lazzeri, A. Flexible Polyurethane Foams Green Production Employing Lignin or Oxypropylated Lignin. *Eur. Polym. J.* **2015**, *64*, 147–156.

(51)   Bonini, C.; D'Auria, M.; Emanuele, L.; Ferri, R.; Pucciariello, R.; Sabia, A. R. Polyurethanes and Polyesters from Lignin. *J. Appl. Polym. Sci.* **2005**, *98* (3), 1451–1456.

(52)   Cateto, C. A.; Barreiro, M. F.; Rodrigues, A. E.; Brochier-Salon, M. C.; Thielemans, W.; Belgacem, M. N. Lignins as Macromonomers for Polyurethane Synthesis: A Comparative Study on Hydroxyl Group Determination. *J Appl Polym Sci* **2008**, *109* (5), 3008–3017.

(53)   Laurichesse, S.; Huillet, C.; Avérous, L. Original Polyols Based on Organosolv Lignin and Fatty Acids: New Bio-Based Building Blocks for Segmented Polyurethane Synthesis. *Green Chem.* **2014**, *16* (8), 3958–3970.

(54)   Wang, C.; Venditti, R. A. UV Cross-Linkable Lignin Thermoplastic Graft Copolymers. *ACS Sustain. Chem. Eng.* **2015**, *3* (8), 1839–1845.

(55)   Yan, R.; Yang, D.; Zhang, N.; Zhao, Q.; Liu, B.; Xiang, W.; Sun, Z.; Xu, R.; Zhang, M.; Hu, W. Performance of UV Curable Lignin Based Epoxy Acrylate Coatings. *Prog. Org. Coat.* **2018**, *116*, 83–89.

(56)   Decker, C. The Use of UV Irradiation in Polymerization. *Polym. Int.* **1998**, *45* (2), 133–141.

(57)   Christian Decker. UV-radiation Curing Chemistrynull. *Pigment Resin Technol.* **2001**, *30* (5), 278–286.

(58)   Meylemans, H. A.; Groshens, T. J.; Harvey, B. G. Synthesis of Renewable Bisphenols from Creosol. *ChemSusChem* **2012**, *5* (1), 206–210.

(59)   Argyropoulos, D. S. 31P NMR in Wood Chemistry: A Review of Recent Progress. *Res. Chem. Intermed.* **1995**, *21* (3–5), 373–395.

(60)   Capanema, E. A.; Balakshin, M. Y.; Kadla, J. F. A Comprehensive Approach for Quantitative Lignin Characterization by NMR Spectroscopy. *J. Agric. Food Chem.* **2004**, *52* (7), 1850–1860.

(61)   Nifantiev, E. E.; Grachev, M. K.; Burmistrov, S. Y. Amides of Trivalent Phosphorus Acids as Phosphorylating Reagents for Proton-Donating Nucleophiles. *Chem. Rev.* **2000**, *100* (10), 3755–3800.

(62)   Bolaño, S.; Bravo, J.; Carballo, R.; Freijanes, E.; García-Fontán, S.; Rodríguez-Seoane, P. Oxorhenium(V) Complexes with Bis-Phosphinite Chelating Coligands. The Crystal Structure of [ReOCl2(OMe)L1], [ReOCl3L2], [ReOCl2(OEt)L2] and [ReOCl2{Ph2PO(CH2)2O}{PPh2(OEt)}] [L1=Cy2PO(CH2)2OPCy2, L2=Ph2PO(CH2)2OPPh2]. *Polyhedron* **2003**, *22* (13), 1711–1717.

(63)   Bedford, R. B.; Limmert, M. E. Catalytic Intermolecular Ortho-Arylation of Phenols. *J. Org. Chem.* **2003**, *68* (22), 8669–8682.

(64)   Da Cunha C.; Deffieux A.; Fontanille M. Synthesis and Polymerization of Lignin-based Macromonomers. III. Radical Copolymerization of Lignin-based Macromonomers with Methyl Methacrylate. *J. Appl. Polym. Sci.* **2003**, *48* (5), 819–831.

(65)   Liu, X.; Xu, Y.; Yu, J.; Li, S.; Wang, J.; Wang, C.; Chu, F. Integration of Lignin and Acrylic Monomers towards Grafted Copolymers by Free Radical Polymerization. *Int. J. Biol. Macromol.* **2014**, *67*, 483–489.

(66)   Jakab, E.; Faix, O.; Till, F. Thermal Decomposition of Milled Wood Lignins Studied by Thermogravimetry/Mass Spectrometry. *J. Anal. Appl. Pyrolysis* **1997**, *40*, 171–186.

Chapter 4

4 Methacrylation of Kraft Lignin for UV-Curable Coatings: Process Optimization Using Response Surface Methodology

4.1 Introduction

Lignin is a complex, racemic,[1] and aromatic heteropolymer, composed of mainly three phenylpropanoid (C9) units: *p*-coumaryl alcohol, coniferyl alcohol, and synapyl alcohol containing zero, one, and two methoxy functionalities, respectively, linked mainly by ether bonds (β-O-4 or α-O-4) and C-C (5-5) linkages.[2,3] Lignin as the main component in lignocellulosic biomass is an abundant natural polymer second only to cellulose. It is currently produced in large quantities as technical lignin, such as kraft lignin (**KL**), byproduct from the pulping processes, which is however utilized mainly as low-value solid fuel for heat production and for regeneration of pulping chemicals in recovery boilers.[4] As such, lignin is an under-utilized sustainable resource.

Lignin's chemical structure, particularly the relative abundance of hydroxyl functionalities,[5] provides the potential for the macromolecule to undergo various chemical modification processes for the production of high-value bio-based products.[6–8] The chemical modification of hydroxyl functionalities has been the subject of many studies, aiming to convert lignin into a material that is suitable for post-modification and subsequent incorporation into various products that are currently produced from fossil-resources. Such chemical modifications have also proved to improve lignin's limited solubility in common organic solvents and subsequently, increase the possibility of incorporating lignin into different supramolecular systems.[8–10] Tan[11] reported that phenolation of the aliphatic hydroxyl functionalities within lignin with excess amounts of cardanol, a natural alkyl phenol, for 6 h at 60 °C, resulting in the addition of phenolic hydroxyls in lignin and making it a more suitable polyol for the preparation of bio-based polyurethane coatings. Sadeghifar *et al.*[12] reported oxypropylation (i.e., etherification of phenolic hydroxyl functionalities with propylene oxide) of kraft lignin at 40 °C for 18 h, using excess amounts of propylene oxide. Wang *et al.*[13] reported that esterification of

lignin's hydroxyl functionalities with 2-boromoisobutyryl bromide (BiBB). They subsequently employed the synthesized lignin-Br material as an atom transfer radical polymerization (ATRP) macroinitiator with 2-methacryloxyethyl dehydroabieticcarboxylate (MAEDA), 2-acryloyloxyethyl dehydroabieticcarboxylate (AEDA), and 4-acryloxybutyl dehydroabieticcarboxylate (ABDA), respectively, to prepare corresponding MAEDA-, AEDA-, and ABDA-polymer grafted lignin materials with increased water contact angles as spin-cast films.[13] In a separate study, Wang *et al.*[14] reported conversion of lignin to lignin-Br, using excess amounts of BiBB for 25 h at 0 °C, which yielded ca. 65% lignin-Br material as an ATRP macroinitiator to synthesize lignin-*graft*-polystyrene (lignin-*g*-PS) and lignin-*graft*-poly(styrene-*co*-acryloyl benzophenone) (lignin-*g*-poly(styrene-*co*-ABP) co-polymers. Thielemans and Wool[15] reported that esterifying lignin with excess amounts of methacrylic anhydride for 18 h at 50 °C resulted in metacrylation of both the aliphatic and the phenolic hydroxyl functionalities within its chemical structure, yielding 55% of esterified lignin products as a suitable candidate for incorporation into unsaturated thermoset systems.

Although the reported studies on the chemical modification of lignin present very interesting chemistry, some major setbacks of the reported process of lignin modification are: (1) all were on a lab-scale; (2) the majority of the reported processes do not operate under optimized conditions; and (3) to the best of our knowledge, most chemical modification processes for lignin generally need excess amounts of reagents, as well as relatively long reaction times, yielding relatively low amounts of final products.[15–17] While a shorter reaction time is always desirable for industrially-feasible processes, the use of excess reagent amounts can harm the process's feasibility both in terms of its upfront costs, and the work-up costs of the process to recycle the unreacted reagent. Although lignin's low cost and renewability make it an appealing starting material to produce high-value bioproducts, an expensive, complicated, and low-yield process would lead to expensive final products, regardless of the price of the starting material. To take full advantage of the sustainability that lignin offers, processes aiming at converting lignin into value-added products must be optimized, to achieve the highest possible efficiency for up-scale production.

Response surface methodology (RSM) comprises a set of mathematical and statistical techniques capable of obtaining an adequate functional relationship between a response and several associated input variables. Although unknown, this relationship can be approximately depicted depending on the complexity of the system. Among the available RSM designs, central composite design (CCD) is the most commonly employed. CCD starts with a first order design (fitting a first-degree model) and uses additional points to fit the second-degree model, which can be depicted by the following equation.[18,19]

$$Y = \beta_0 + \sum_{i=1}^{K} \beta_i X_i + \sum_{i=1}^{K} \beta_{ii} X_i^2 + \sum_{i=1}^{K=1} \sum_{j=i+1}^{K} \beta_{ij} X_i X_j + \varepsilon$$

Equation 4-1

Where Y is the response in the study and X_i and X_j are independent variables, ε corresponds to the noise/error component in the response and β_0, β_i, β_{ii}, and β_{ij} represent the regression coefficients of the intercept, linear, quadratic and interaction parameters, respectively.[19]

The present work aimed at transforming lignin - the under-utilized sustainable resource into a methacrylated lignin (**ML**) for UV-curable coatings. The process parameters (i.e. reaction time, reaction temperature, and the reagent/lignin molar ratio) for the methacrylation of kraft lignin (**KL**) were optimized using response surface methodology with a central composite design to maximize the mass yield of the synthesized methacrylated lignin (**ML**). The obtained **ML** material was then incorporated into a UV-curable formulation at 30 wt.% and cast as a 25 µm thick coating film on a glass slide subject to UV-curing. The obtained coating was then characterized with respect to its thermal stability, water contact angle, and crosslinking percentage.

4.2   Materials and Methods

4.2.1 Materials

Kraft lignin (**KL**) was provided by FPInnovations, produced by FPInnovations-Thunder Bay Bio-Economy Technology Centre (M_w ~10,000 g/mol, based on GPC-*UV* analysis;

0.57 wt.% ash; and 5.2 wt.% sulfur on a dry ash free basis). The **KL** samples were crushed into powder using a mortar and pestle and heated at 45ºC for 48 hours under vacuum (-762 mmHg; C9=180 g). Methacrylic anhydride (**MethA**; 94%, stabilized with ca. 0.2% 2,4-dimethyl-6-tert-butylphenol) and 1-methylimidazole (**1MIM**; 99%) were purchased from Alfa Aesar and used as received. Chlorodi(isopropyl)phosphine ($[CH(CH_3)_2]_2PCl$, 96%) and 2-hydroxy-2-methylpropiophenone (**HDMAP**; 97%) were obtained from Sigma-Aldrich Co. and used as recieved. EBERCYL® 1360 (**EB-1360**, a hexafunctional silicone hexaacrylate resin from Allnex company) as a crosslinker for UV curing was purchased from Allnex Belgium SA. and used as received. Tetrahydrofuran (THF) was purchased from Caledon and dried using an MBraun Solvent Purification System (SPS) for the methacrylation process. The same solvent was stored in the drybox over 4 Å molecular sieves for the reaction with chlorodi(isopropyl) phosphine. Dichloromethane and hexanes were purchased from Caledon Laboratories and used without further purification. Dimethylsulfoxide-d_6 (DMSO-d_6) was purchased from Cambridge Isotope Laboratories and was used without any further purification.

4.2.2 Characterization Methods

^1H NMR spectra were recorded using a Varian INOVA 600 MHz spectrometer (^1H, 599.5 MHz; ^{13}C, 150.8 MHz; ^{31}P, 242.6 MHz) and referenced to residual DMSO (2.5 ppm). $^{31}P\{^1H\}$ NMR spectra were recorded using a Varian INOVA 400 MHz spectrometer (^1H, 400 MHz; ^{13}C, 158 MHz; and $^{31}P\{^1H\}$, 162 MHz) and referenced using an external standard (85% H_3PO_4; $\delta_P = 0$). FT-IR spectra of samples were performed on a PerkinElmer FT-IR Spectrometer using the universal attenuated total reflectance mode (UATR), a diamond crystal, as well as the UATR sampling accessory (part number: L1050231). Thermogravimetric analyses were carried out on samples weighing ca. 5-6 mg, using the Ramp mode at temperatures increasing from 25 ºC to 800 ºC at the rate of 10 ºC/min on a Q600 SDT TA Instrument and analyzed using TA Universal Analysis. Crosslinking percentages were calculated by comparing the signal intensity at 800 cm^{-1}, corresponding to the C=C bending vibrations in the FTIR spectra of the liquid UV-curable formulation (before curing) and the solid UV-cured coating samples. Water contact angles (WCA) were measured using a Kruss DSA100 Drop Shape Analyzer. UV-curing was performed using

a modified UV-curing conveyor system, purchased from UV Process and Supply Inc. with a mercury bulb (UVA: 154 mW/cm^2, 189 mJ/cm^2, UVB: 74 mW/cm^2, 90 mJ/cm^2; as determined by a PP2-H-U Power Puck II purchased from EIT Instrument Markets).

4.2.3 Methacrylation of **KL**

The methacrylation processes were carried out in 10 mL round-bottom flasks by reacting **KL** with **MethA** in THF sovlent in the presence of **1MIM** as catalyst at 40-80°C for 20-100 min. In a typical run (the center point of the CCD as shown in Table 1: 60 °C, 60 min and **1MIM/KL** = 0.22), dried **KL** (200 mg, 1.1 mmol) was added to 2 mL THF in the round-bottom flask under vigorous stirring. The mixture was stirred for ca. 5 min to obtain a homogeneous dark-brown solution. A mixture of **1MIM** (19 µL, 19 mg, 0.24 mmol) and **MethA** (165 µL, 171 mg, 1.1 mmol) was then added to the previous solution and stirred at 60 ˚C for 1 h under N$_2$ atmosphere. The brown mixture was then added dropwise to 20 mL hexanes under stirring to precipitate a light brown powder. The obtained powder was dissolved in DCM and washed with water to remove the catalyst and any unreacted reagent. The organic phase was then precipitated in 20 mL hexanes and dried under vacuum to give **ML**. ^{1}H NMR (DMSO-d_6, 600 MHz): δ$_H$ 1.89 (br, 3H, CH$_3$), 5.82 (br, 1H, vinyl), 6.14 (br, 1H, vinyl). The obtained powder was then weighed to determine the reaction yield. The recovered mass yield was calculated as follows:

$$Recovered\ Mass\ Yield\ (wt.\%) = \frac{m_{ML}}{m_{KL}} \times 100 \qquad \textbf{Equation 4-2}$$

Where $\boldsymbol{m_{KL}}$ is the weight of **KL** as starting material and $\boldsymbol{m_{ML}}$ is the weight of the final product.

4.2.4 Experiment Design

A central composite design (CCD), incorporating 3 independent variables (i.e., reaction time (min), reaction temperature (°C), and **KL**/**1MIM** molar ratio) was used to optimize the **KL** methacrylation process. The design contained 8 cube points, 6 axial points, and 1 center point and consisted of 20 runs, including 6 replicate runs to examine the reproducibility of the center point conditions. Ranges for the three variables in this design

were chosen based on our preliminary experiments and the literature.[15,20] The variables and their corresponding levels are detailed in Table 4-1. Response surface methodology was implemented, and the results were interpereted using MiniTab 17. The response surface design was analyzed to optimize the synthesis condition of **ML** and probe the relative or interactive effects of **KL/1MIM** molar ratio, reaction temperature, and reaction time on the amount of obtained product from the methacrylation reaction.

Table 4-1 Independent variables and their levels in the central composite design.

Variables	Unit	Term	Coded level of variables				
			-1.682	-1	0	1	1.682
Reaction temperature	°C	X_1	43	50	60	70	77
Reaction time	min	X_2	26	40	60	80	94
1MIM/KL	mol/mol	X_3	0.186	0.200	0.220	0.240	0.253

4.2.5 Preparation of **ML**-based UV-Cured Coatings

In 2 separate vials, two mixtures containing 0 and 30 wt.% **ML**, equal amounts of photoinitiator (5 wt.% HDMAP), corresponding amounts of the crosslinker (95 and 65 wt.% EB-1360), and 100 mg CH_2Cl_2 were mixed and sonicated for ca. 15 min to obtain particulate- and haze-free solutions. The obtained formulations were then cast on clean glass slides, using a 12-inch meyer rod (AP-JR30, 12-inch OA, 3/8-inch DIA, 8-1/2-inch EP, #30 wire) and placed on the UV-curing conveyor system and irradiated with UV-light to give coatings of ca. 76 µm thickness.

4.3 Results and Discussion

4.3.1 Modelling and Analysis of Variance

Detailed values of the performed reactions and their corresponding mass yields are reported in Table 4-2. The obtained results show that the amount of obtained product is dependent

on the amount of catalyst in use, reaction time, and reaction temperature. To find the best fitting model to the experimental responses, various functions such as linear, quadratic and cubic models were developed. A quadratic equation based on the coded values of the variables was determined to have the best fit to the experimental responses. Coefficient significances were evaluated according to a 95% confidence interval (P-value $> \alpha=0.05$). Any coefficient with P-value < 0.05 has a statistically significant effect on the responses and *vice ver*sa. The final model to predict the methacrylation recovered mass yield is as follows:

$$Yield\ (wt.\%) = 141.16 - 14.34X_1 - 12.37X_2 + 3.62X_3 - 12.30X_1^2 \quad \textbf{Equation 4-3}$$
$$- 8.76X_2^2 - 9.12X_3^2 - 4.81X_1X_2 - 8.56X_1X_3$$
$$+ 12.06X_2X_3$$

Where X_1, X_2, and X_3 represent the coded values for reaction temperature, reaction time and **1MIM/KL** molar ratio, respectively. A positive term is indicative of a synergistic effect on the response and a negative term indicates an antagonistic effect on the response. The complex model for the methacrylation mass yield shows that all the terms including linear, square and interaction factors are significant. The model also depicts that the linear factor of **1MIM/KL** molar ratio (X_3) and the interaction term of reaction time and the **1MIM/KL** molar ratio (X_2X_3) are the only two coefficients that have a positive effect on the response, while all other coefficients have negative effects on it. Thus, lower reaction times and reaction temperature, along with employment of more catalyst will lead to a higher mass yield for the methacrylation process of **KL**. However, the model predicts that decreasing the reaction temperature and reaction time will have a greater effect on the mass yield than increasing the catalyst amount, which can be worth considering in an industrial setting.

Table 4-2 The central composite matrix and output responses for methacrylation of **KL**.

| | | Parameters and levels | | | | | | Output responses | |
| | | Coded values | | | Real-time value | | | | |
Std.	Run #	X_1	X_2	X_3	Temp. (°C)	Time (min)	**1MIM/KL** (mol/mol)	Product mass	Mass yield (wt.%)
1	18	-1	-1	-1	50	40	0.200	0.262	131
2	8	1	-1	-1	70	40	0.200	0.26	130
3	9	-1	1	-1	50	80	0.200	0.18	90
4	3	1	1	-1	70	80	0.200	0.143	71.5
5	6	-1	-1	1	50	40	0.240	0.268	134
6	10	1	-1	1	70	40	0.240	0.201	100.5
7	12	-1	1	1	50	80	0.240	0.286	143
8	5	1	1	1	70	80	0.240	0.177	88.5
9	13	-1.682	0	0	43	60	0.220	0.265	132.5
10	4	1.682	0	0	77	60	0.220	0.16	80
11	7	0	-1.682	0	60	26	0.220	0.272	136
12	1	0	1.682	0	60	94	0.220	0.193	96.5
13	20	0	0	-1.682	60	60	0.186	0.227	113.5
14	2	0	0	1.682	60	60	0.253	0.234	117

15	15	0	0	0	60	60	0.220	0.286	143
16	16	0	0	0	60	60	0.220	0.278	139
17	11	0	0	0	60	60	0.220	0.284	142
18	19	0	0	0	60	60	0.220	0.288	144
19	14	0	0	0	60	60	0.220	0.27	135
20	17	0	0	0	60	60	0.220	0.288	144

Analysis of variance (ANOVA) and F-test were carried out on the regression model to evaluate its suitability and precision (Table 4-3).

Table 4-3 ANOVA results of the quadratic model for methacrylation of KL[a]

Source	Deg. of freedom	Sum of squares	Mean squares	F-value	P-value (prob > F)
Model	9	10783.5	1198.16	80.97	0.000
Lack of fit	5	85.1	17.03	1.36	0.373
Pure error	5	62.8	1.00	—	—
Total	19	10931.5	—	—	—

[a] $R^2 = 0.9865$; $adjusted\ R^2 = 0.9743$; $predicted\ R^2 = 0.9323$

The P-value < 0.05 for the regression model was taken as evidence for the significance and appropriateness of it for accurately predicting the reaction yields according to its

parameters. Moreover, The *F*-value of 1.36 and *P*-value of 0.373 (larger than confidence interval) for the "lack of fit" confirmed its insignificance in the developed model, further proving its good fitting. As well, the coefficient of determination (R^2) for the mass yield of methacrylation was 0.9865, meaning 98.65% of the mass yield variations can be explained by the independent variables based on the developed model, while the adjusted R^2 value was 0.9743, confirming that the model was not over-fitted. Additionally, the predicted R^2 value of 0.9323 showed a good agreement between the values predicted by the model and the real-time experimental responses. Moreover, the normal probability plot (Figure 4-1a) showed a normal distribution of errors, indicating a good prediction of the responses by the model, while the residual plot (Figure 4-1b), depicting the relationship between the residual values and the fitted values for each response, showed random scattering of the residuals around the zero line, further demonstrating the competence of the developed model.
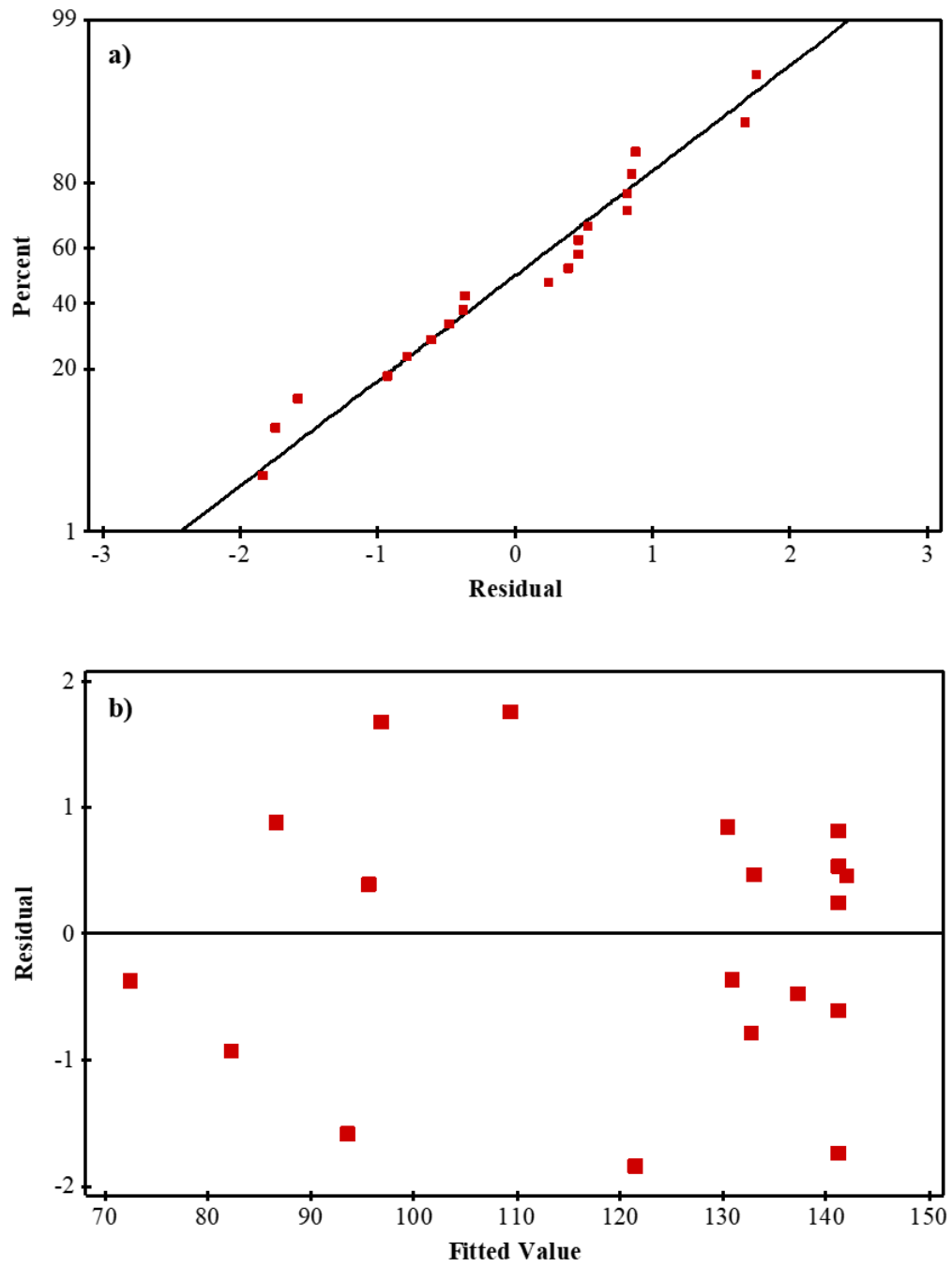
Figure 4-1 The normal probability plot (a) and residual plot (b) of the obtained model.

4.3.2 Response Surface Plot and Optimization of Variables

The response surface plots (Figure 4-2a-c) and contour plots (Figure 4-2d-f) of the methacrylation of **KL** show a good agreement with the developed regression model. The developed plots and regression model were then employed to determine the maximum possible response of the reaction (recovered mass yield) obtainable from the minimum possible amounts of the reaction parameters. Following the predictions of the regression model and the depictions of the developed plots, it was determined that the response (mass yield) can reach values higher than 140 wt.% by keeping the reaction temperature between 50 °C and 60 °C, while having a **1MIM/KL** molar ratio between 0.22 and 0.25 (Figure 4-2a and 4-2d). Moreover, Figures 4-2b and 4-2e suggest that for the same response value range, the reaction time must be under 60 min, while Figures 4-2c and 4-2e give predictions in-line with the mentioned observations. On the other hand, the circular shape of the center of the contour plot, corresponding to mass yield (wt.%) > 140%, suggested that changes in each variable must be in a certain range and moving past said range will have a negative effect on the reaction mass yield (Figure 4-2d, 4-2e, and 4-2f). Thus, the process optimization was carried out via the response surface methodology to maximize the methacrylation mass yield, while minimizing the reaction parameters without negatively affecting the mass yield. The result suggested a methacrylation reaction run at 54 °C for 54 minutes, with **1MIM/KL** molar ratio of 0.225. The predicted mass yield for such reaction was 148.13 wt.%. Given the recommended reaction conditions, a new reaction was carried out, which yielded 146.5 wt.% **ML** and thus, the predicted values and experimental results were proven to be in a very good agreement. Considering the maximum theoretical yield of 150.25 such a high product mass yield is significant.
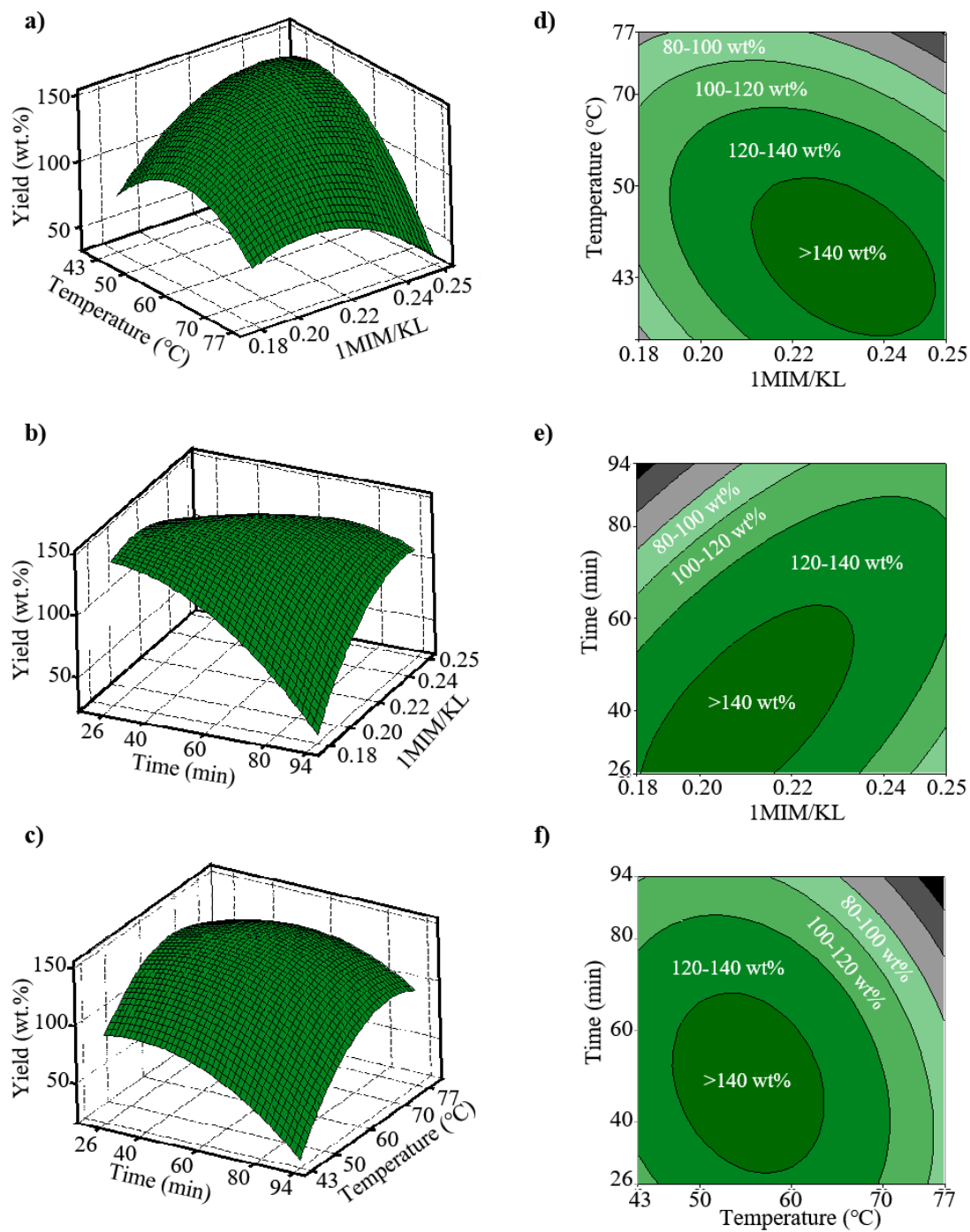
**Figure 4-2** Response surface plots and contour plots of different variable values vs. recovered mass yield: effects of **1MIM/KL** molar ratio and reaction temperature (a, d); effects of **1MIM/KL** molar ratio and reaction time (b, e); and effects of reaction time and reaction temperature (c, f).

4.3.3 Optimized Product Characterization

The **ML** obtained via the optimized reaction conditions (Figure 4-3-I) was characterized in comparison with **KL** by ^{1}H NMR and FTIR (Figure 4-3-II). Three new broad signals were observed in the ^{1}H NMR spectrum of **ML** as compared to **KL**, with chemical shifts of δ_H = 1.89, 5.82, and 6.14 which were attributed to the methyl functionalities and the methacrylate group's two olefinic groups. Moreover, the FTIR spectrum of **ML** showed a decrease at 3200-3500 cm^{-1} (s, br) relative to **KL**, corresponding to significant removal of hydroxyl groups, as well as increases in the esters' C=O stretching vibrations (1735-1750 cm^{-1}), C-O stretching vibrations (1000-1320 cm^{-1}) and C=C bending vibration regions (650-1000 cm^{-1}), suggesting successful grafting of methacrylate groups on lignin's structure. Finally, the extent of methacrylation was determined by a modified version of the method reported by Argyropolous[22] in 1994 for the quantification of lignin's hydroxyl groups. The most significant alterations were the change in the halo-phosphine reagent ($[CH(CH_3)_2]_2PCl$), the base ($N(Et)_3$), and the use of an external standard (PPh_3) for quantification purposes. Equal amounts of **KL** and **ML** were reacted with $[CH(CH_3)_2]_2PCl$ separately in presence of excess amounts of $N(Et)_3$ at room temperature. The extent of methacrylation was then determined by comparing the integrations of resulting -OP regions in $^{31}P\{^1H\}$ NMR spectra to an external standard solution of PPh_3 (Figure 4). Based on the obtained results, we determined that on average ca. 70% of the hydroxyl groups on **KL** were converted to methacrylate groups in **ML**.
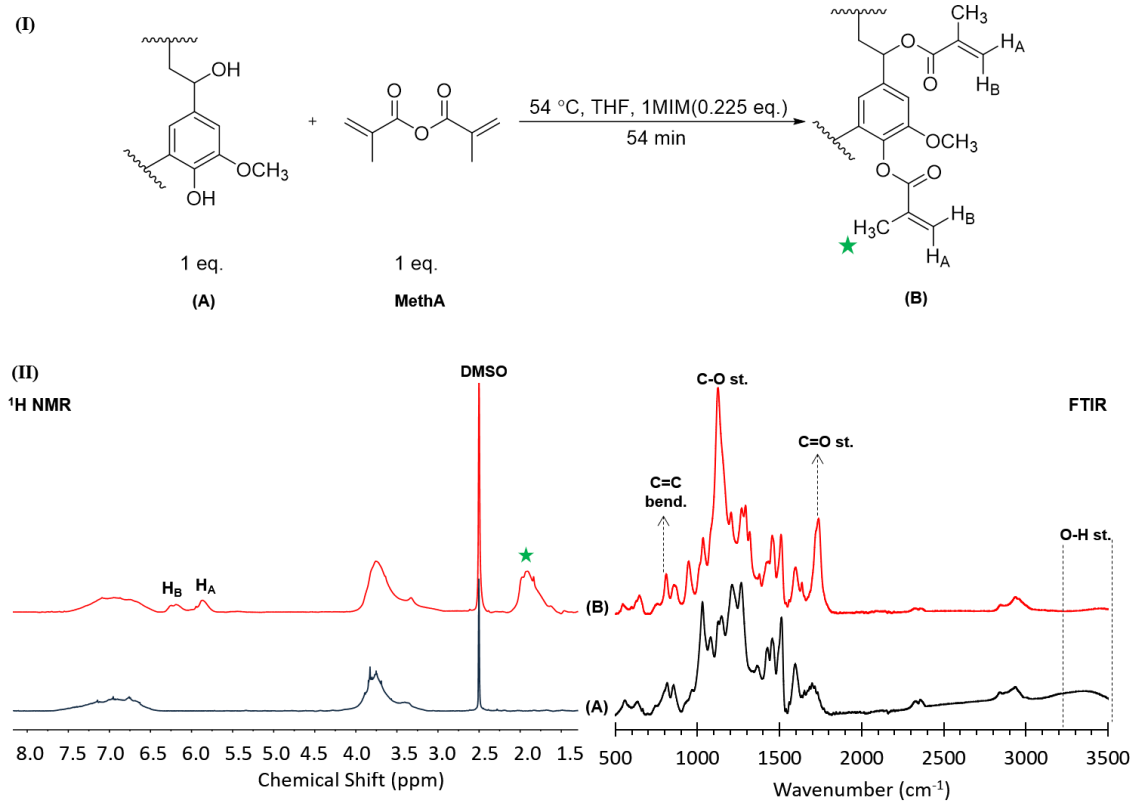
Figure 4-3 I) The methacrylation scheme under optimized reaction conditions and **II)** ¹H NMR and FTIR spectra of (A) **KL** and (B) **ML** synthesized under the optimized reaction conditions.
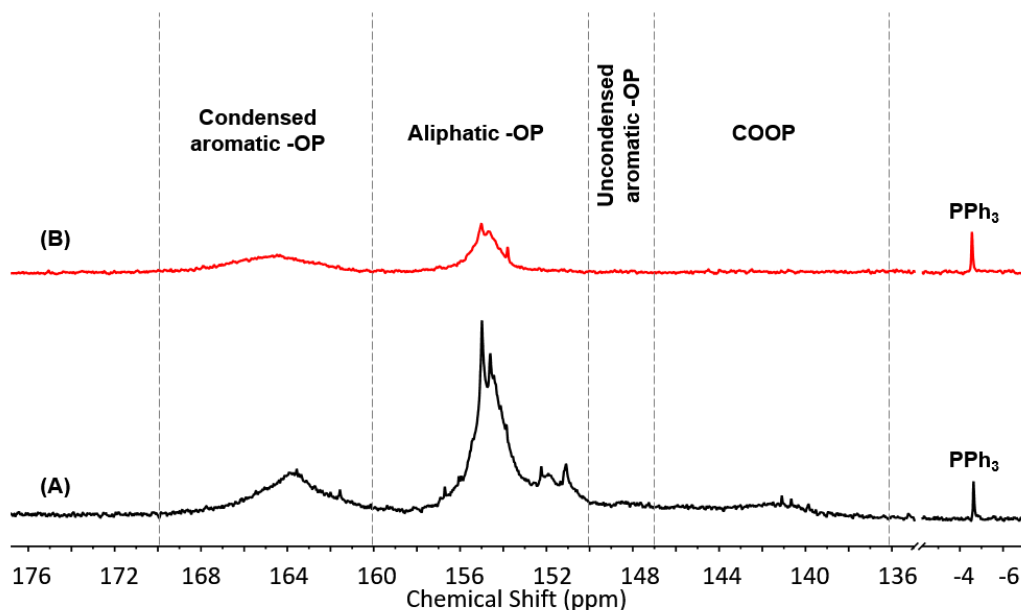
Figure 4-4 ^{31}P{^{1}H} NMR spectra of products obtained from the reaction of (A) **KL** and (B) **ML** with [CH(CH$_3$)$_2$]$_2$PCl. All peak regions were integrated according to peak at -4.6 ppm, corresponding to the external standard used in this procedure (PPh$_3$).

4.3.4 Characterization of the **ML**-based UV-Cured Coatings

ML (30 wt.%) was incorporated into a UV-cured coating sample as discussed before, containing **EB-1360**, a hexafunctional siloxane-based crosslinker (65 wt.%), **HDMAP** (5 wt.%) as the photoinitiator. To determine the effect of such incorporation, a UV-cured coating sample containing no **ML** was prepared as a reference through the same process (with 95 wt.% **EB-1360** and 5 wt.% **HDMAP**) and the coatings were characterized in conjugate with each other.

Drop shape analysis was employed to evaluate the effect of introducing **ML** as a hydrophobic component into the coating system, as siloxane-based systems are known for their relatively low hydrophobicity and lignin was known to reduce the wettability of the system in which it is incorporated.[16,23,24] It was determined that while the **ML**-free coating sample had a water contact angle of 60.4 ± 1.8 degrees, such value was increased to 82.6

± 1.9 degrees in the **ML**-based coating. This increase in the hydrophobicity of the coating was attributed to the incorporation of **ML** into the coating system as a hydrophobic moiety.

To determine the crosslinking percentages of the coating, the FTIR spectrum of each cured coating sample was compared to that of the corresponding liquid formulation of the said coating before UV-curing, particularly with regards to the signal intensity at ca. 800 cm^{-1} (C=C bending vibrations). It was determined that while the crosslinking percentage of the **ML**-free coating was ca. 35.8%, the same value for the **ML**-based coatings as ca. 64.1%, suggesting better crosslinking in the coating system with the incorporation of the **ML** moiety. Finally, to compare the thermal stabilities of the prepared coatings, each cured coating sample was scraped off the glass surface using a surgical-grade scalpel and fully crushed by a mortar and a pestle. The obtained crushed coatings were then heated *in vacuo* at 40 °C for 24 h, at which point, thermogravimetric analyses were performed on the samples. Moreover, the thermal stability of the **KL** and **ML** samples were also evaluated for references. It was determined that **KL** had an onset decomposition temperature of 200 °C, and it was lowered to 189 °C in **ML** and similarly, **ML**'s residual weight percent at 800 °C was ca. 36.7 wt.%, slightly lower than that of **KL** (40.1 wt.%). Consequently, it was determined that the **ML**-free and the **ML**-based coatings decomposed at 239 and 246 °C, respectively, while the residual weight percentage at 800 °C was 3.3 wt.% and 13.8 wt.% for the **ML**-free and the **ML**-based coatings, respectively. The above results suggest that the introduction of **ML** into the UV coating system had a positive effect on the coating's thermal stability (Figure 4-5), likely attributed to the improved crosslinking percentages of the coating by the **ML**, which aligns well with the resulted reported in many literature studies on the positive effects of lignin on char formation.[25–27]
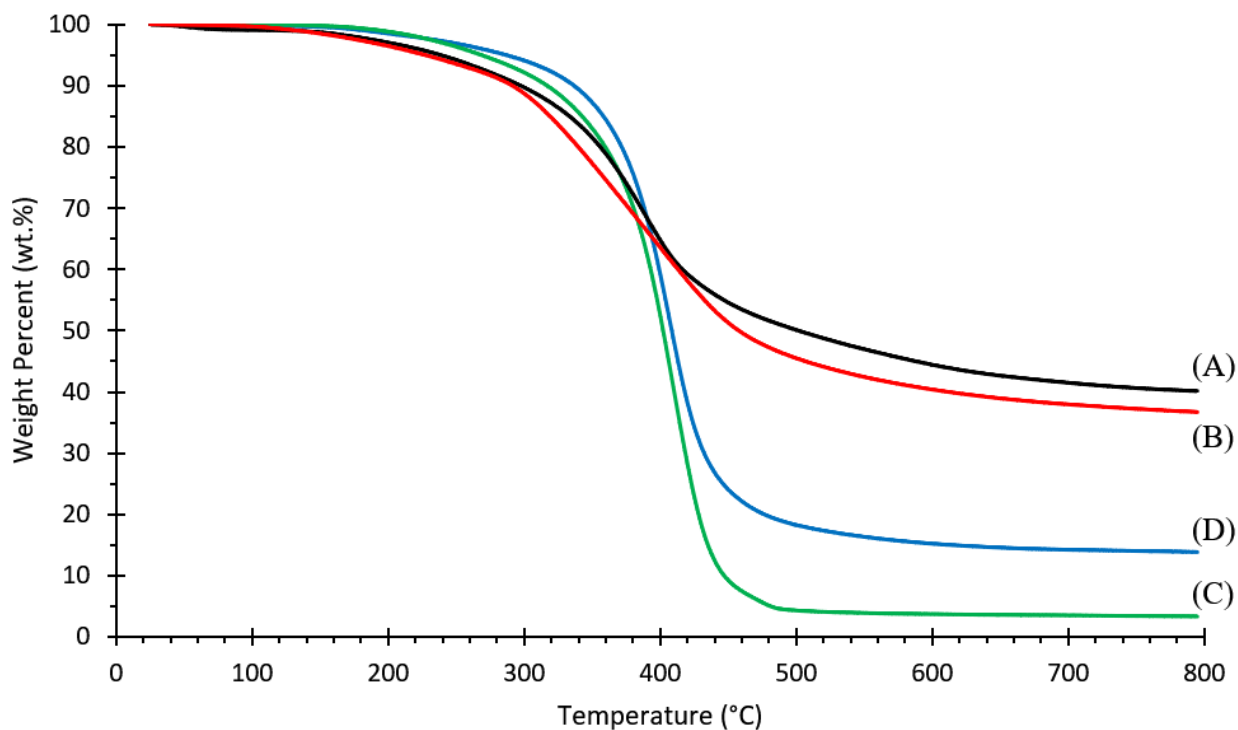
Figure 4-5 Thermogravimetric analysis of **KL** (A), **ML** (B), plus **ML**-free (C) and **ML**-based (D) UV-cured coatings.

4.4 Conclusions

Kraft lignin was chemically modified via a methacrylation process. The process parameters (reaction time, reaction temperature, and **1MIM/KL** molar ratio) for the lignin methacrylation were optimized through central composite design and response surface methodology to maximize the methacrylated lignin (**ML**) product yield. The optimum conditions for the lignin methacrylation, determined from the study, are as follows: 54 minutes at 54 °C with 0.225 **1MIM/KL** molar ratio, resulting in an **ML** mass yield of 146.5 wt.%. The obtained **ML** demonstrated to be curable in a UV-cured coating system, with positive effects on the hydrophobicity, crosslinking percentage, and thermal stability of the coating system in which it was incorporated. Thus, this work realized optimized chemical modification of lignin by methacrylation, demonstrated promising application of the methacrylated lignin as an environmentally friendly UV-curable material for UV-cured coatings.

4.5 References

(1)   Ralph, J.; Peng, J.; Lu, F.; Hatfield, R. D.; Helm, R. F. Are Lignins Optically Active? *J Agric Food Chem* **1999**, *47* (8), 2991–2996.

(2)   Freudenberg, K.; Neish, A. C. *Constitution and Biosynthesis of Lignin*, First.; Springer-Verlag, Heidelberg and New York, **1968**.

(3)   Boerjan, W.; Ralph, J.; Baucher, M. Lignin Biosynthesis. *Annu. Rev. Plant Biol.* **2003**, *54* (1), 519–546.

(4)   Phillips, M. The Chemistry of Lignin. *Chem. Rev.* **1934**, *14* (1), 103–170.

(5)   Morandim-Giannetti, A. A.; Agnelli, J. A. M.; Lanças, B. Z.; Magnabosco, R.; Casarin, S. A.; Bettini, S. H. P. Lignin as Additive in Polypropylene/Coir Composites: Thermal, Mechanical and Morphological Properties. *Carbohydr. Polym.* **2012**, *87* (4), 2563–2568.

(6)   Laurichesse, S.; Avérous, L. Chemical Modification of Lignins: Towards Biobased Polymers. *Prog. Polym. Sci.* **2014**, *39* (7), 1266–1290.

(7)   Mahmood, N.; Yuan, Z.; Schmidt, J.; Xu, C. (Charles). Preparation of Bio-Based Rigid Polyurethane Foam Using Hydrolytically Depolymerized Kraft Lignin via Direct Replacement or Oxypropylation. *Eur. Polym. J.* **2015**, *68* (Supplement C), 1–9.

(8)   Ferdosian, F.; Yuan, Z.; Anderson, M.; Xu, C. (Charles). Sustainable Lignin-Based Epoxy Resins Cured with Aromatic and Aliphatic Amine Curing Agents: Curing Kinetics and Thermal Properties. *Thermochim. Acta* **2015**, *618* (Supplement C), 48–55.

(9)   Liu, W.-J.; Jiang, H.; Yu, H.-Q. Thermochemical Conversion of Lignin to Functional Materials: A Review and Future Directions. *Green Chem.* **2015**, *17* (11), 4888–4907.

(10)   Kai, D.; Tan, M. J.; Chee, P. L.; Chua, Y. K.; Yap, Y. L.; Loh, X. J. Towards Lignin-Based Functional Materials in a Sustainable World. *Green Chem.* **2016**, *18* (5), 1175–1200.

(11)   Tan, T. T. M. Cardanol–lignin-Based Polyurethanes. *Polym Int* **1996**, *41* (1), 13–16.

(12)   Sadeghifar, H.; Cui, C.; Argyropoulos, D. S. Toward Thermoplastic Lignin Polymers. Part 1. Selective Masking of Phenolic Hydroxyl Groups in Kraft Lignins via Methylation and Oxypropylation Chemistries. *Ind Eng Chem Res* **2012**, *51* (51), 16713–16720.

(13)   Wang, J.; Yao, K.; Korich, A. L.; Li, S.; Ma, S.; Ploehn, H. J.; Iovine, P. M.; Wang, C.; Chu, F.; Tang, C. Combining Renewable Gum Rosin and Lignin: Towards Hydrophobic Polymer Composites by Controlled Polymerization. *J. Polym. Sci. Part Polym. Chem.* **2011**, *49* (17), 3728–3738.

(14)   Wang, C.; Venditti, R. A. UV Cross-Linkable Lignin Thermoplastic Graft Copolymers. *ACS Sustain. Chem Eng* **2015**, *3* (8), 1839–1845.

(15)   Thielemans, W.; Wool, R. P. Lignin Esters for Use in Unsaturated Thermosets: Lignin Modification and Solubility Modeling. *Biomacromolecules* **2005**, *6* (4), 1895–1905.

(16)   Liu, Y.; Li, K. Preparation and Characterization of Demethylated Lignin-Polyethylenimine Adhesives. *J. Adhes.* **2006**, *82* (6), 593–605.

(17)   Passauer, L.; Salzwedel, K.; Struch, M.; Herold, N.; Appelt, J. Quantitative Analysis of the Etherification Degree of Phenolic Hydroxyl Groups in Oxyethylated Lignins: Correlation of Selective Aminolysis with FTIR Spectroscopy. *ACS Sustain. Chem Eng* **2016**.

(18)   Khuri, A. I.; Mukhopadhyay, S. Response Surface Methodology. *Wiley Interdiscip. Rev. Comput. Stat.* **2010**, *2* (2), 128–149.

(19)   Montgomery, D. C.; Runger, G. C. *Applied Statistics and Probability for Engineers*; John Wiley & Sons, **2010**.

(20)   Ferdosian, F.; Yuan, Z.; Anderson, M.; Xu, C. (Charles). Synthesis of Lignin-Based Epoxy Resins: Optimization of Reaction Parameters Using Response Surface Methodology. *RSC Adv.* **2014**, *4* (60), 31745–31753.

(21)   Fox, S. C.; McDonald, A. G. Chemical and Thermal Characterization of Three Industrial Lignins and Their Corresponding Lignin Esters. *Bioresources* **2010**, *5* (2), 990–1009.

(22)   Argyropoulos, D. S. Quantitative Phosphorus-31 NMR Analysis of Lignins, a New Tool for the Lignin Chemist. *J. Wood Chem. Technol.* **1994**, *14* (1), 45–63.

(23)   Da Cunha C.; Deffieux A.; Fontanille M. Synthesis and Polymerization of Lignin-based Macromonomers. III. Radical Copolymerization of Lignin-based Macromonomers with Methyl Methacrylate. *J. Appl. Polym. Sci.* **2003**, *48* (5), 819–831.

(24)   Gordobil, O.; Herrera, R.; Llano-Ponte, R.; Labidi, J. Esterified Organosolv Lignin as Hydrophobic Agent for Use on Wood Products. *Prog. Org. Coat.* **2017**, *103*, 143–151.

(25)   Li, J.; Li, B.; Zhang, X.; Su, R. The Study of Flame Retardants on Thermal Degradation and Charring Process of Manchurian Ash Lignin in the Condensed Phase. *Polym. Degrad. Stab.* **2001**, *72* (3), 493–498.

(26)   Li, B.; Zhang, X.; Su, R. An Investigation of Thermal Degradation and Charring of Larch Lignin in the Condensed Phase: The Effects of Boric Acid, Guanyl Urea Phosphate, Ammonium Dihydrogen Phosphate and Ammonium Polyphosphate. *Polym. Degrad. Stab.* **2002**, *75* (1), 35–44.

(27)   Sadeghifar, H.; Argyropoulos, D. S. Correlations of the Antioxidant Properties of Softwood Kraft Lignin Fractions with the Thermal Stability of Its Blends with Polyethylene. *ACS Sustain. Chem. Eng.* **2015**, *3* (2), 349–356.

Chapter 5

5 "Lignophines": Lignin-based Tertiary Phosphines with Metal-Scavenging Ability

Lignin is a biopolymer that is a natural component of wood and a by-product from the pulp and paper industry. This material is naturally present in the secondary cell walls of plants, resulting from an *in vivo* enzyme-mediated dehydrogenation polymerization (lignification) of three hydroxycinnamyl alcohol monomers that include *p*-coumaryl, sinapyl, and coniferyl alcohol units (monolignols; Scheme 5-1a).[1,2] Of the almost 50 million tons per year of lignin produced globally, only 2% is utilized for conversion to specialty products, while the rest is used either as low value heating fuel at the site of manufacture or it is disposed of as waste (published data from 2010).[3] New outlets for up conversion and repurposing of this biopolymer need to be established. Lignin is a renewable resource that could be leveraged for a broad range of materials applications given the rich functional group chemistry present within the biopolymer, including hydroxyl, ether, carbonyl, and carboxylic acids, that can be accessed and transformed into value-added products.[4,5]

Both the aromatic and aliphatic hydroxyl groups on lignin have been utilized as key reactivity outlets for valorization. For example, lignin's phenolic hydroxyl groups have been selectively methylated using dimethyl sulfide or oxypropylated with propylene oxide[6], while acyl anhydrides and acyl chlorides have been employed to cap both aliphatic and aromatic hydroxyl groups.[7,8] The key outlets of modified lignins include bio-based epoxy resins[9–11], thermo- and UV-cured graft copolymers[12–15], and flexible and rigid polyurethanes.[16–19] However, the strategies for up-converting lignin have shifted towards developing novel materials with specific applications in recent years, such as cathode-active materials in primary lithium batteries[20,21] and non-toxic bio-degradable nanoparticles with potential applications in drug delivery and pharmaceuticals.[22–25]

a)

| A | B | C | KL |

b)

P(MMA-*co*-MAPC₁(OH)₂)
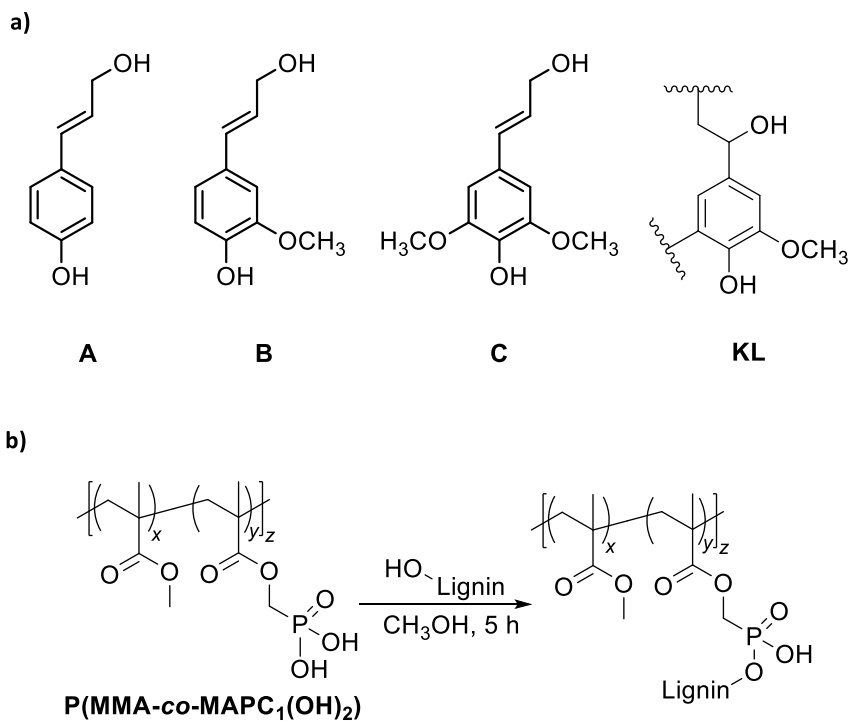
Scheme 5-1 a) The three standard monolignols of *p*-coumaryl (A), coniferyl (B), and sinapyl (C) alcohol as the building blocks of lignin (**KL**, representative structure of lignin) and **b)** the reaction scheme for grafting lignin with hydrolysed **MMA/MAPC1** copolymer **P(MMA-*co*-MAPC₁(OH)₂)** as reported by Ferry et al.

Despite the headway made in upconverting lignin, the elemental diversity installed into the material is woefully narrow and therefore, limits other potential outlets for an inexpensive, sustainable, and abundant biopolymer.

Polymerizable fragments (e.g. olefins,[7] amides,[26] and carboxyls[9]), which contain unsaturated functional groups have been installed into lignin's structure and they can be exploited to build elemental diversity into the material, offering further opportunity in creating a usable, value-added product. Because olefins are easily modified via E-H bond addition, impressive opportunities exist for adding B-H, Si-H, S-H, and P-H across the double bond, creating Lewis acidic or basic bio-based polymers.

Our group has been particularly interested in utilizing transformations of P-H bonds to prepare highly functional phosphorus-based polymeric materials, including self-healing

polyphosphonium ionic networks,[27] P-based interpenetrated polymer networks (IPNs),[28] and highly crosslinked phosphorus photopolymer networks, which have been applied as effective antimicrobial agents,[29] targeted anion self-assembly,[30] and in metal scavenging applications.[31]

Reported procedures on grafting phosphorus-containing compounds onto lignin's structure, to this date, have solely focused on exploiting the hydroxyl functionalities on lignin for the formation of P-O functionalities along the macromolecule's structure. Argyropolous *et al.* have studied such exploitation in detail to develop a procedure capable of quantifying lignin's hydroxyl functionalitites through grafting these P-O functionalities.[32] Ferry *et al.* reported a graft co-polymer of lignin using hydrolyzed methylmethacrylate/dimethyl(methacryloxy)-methyl phosphonate (MMA/MAPC1) copolymer (Scheme 1b), which introduced phosphorus atoms onto lignin via P-O linkages. They then blended the synthesized copolymer with polybutylene succinate (PBS) pellets using compression molding to improve the fire behavior of PBS.[33] However, there have been no reports on the preparation of polymer networks that contain lignin as the backbone and phosphorus as a substituent bound to the network via P-C linkages, which can expand lignin's utility by exploiting the diverse chemistry of phosphorus in derivatizing the network after polymerization.[34] In this context, we have utilized methacrylated lignin in a phosphane-ene click reaction with $PH_3(g)$. The resulting product is rich in P-H bonds, which can be used in subsequent phosphane-ene chemistry with substituted olefins. This creates an array of tertiary alkyl phosphines on the lignin scaffold, which behaves as a polyphosphine and is amenable to metal coordination and metal scavenging. These results represent a major shift in the immense, unlocked potential for lignin as a commodity chemical, rather than negative value waste.[33,35]

Methacrylated lignin (**ML**, 200 mg, synthesized and quantified following the same prcedure as reported in chapter 4) was swelled in CH_3CN (100 mL). Azobis(isobutyronitrile) (**AIBN**; 6 mg, 3 wt.%) was added to the swelled **ML** and the mixture was transferred to a 300 mL autoclave reactor. The autoclave was then degassed by purging N_2 for ca. 10 min and pressurized with phosphine gas (PH_3, 80 psi). The vessel was then stirred for 1 h, at which point it was re-pressurized with PH_3 and heated to 50 °C

under stirring for 24 h. Afterward, the pressurized PH_3 was released in a controlled environment, where it was ignited and burned. Subsequently, the vessel was brought into the glovebox, opened, and the mixture (swelled light-brown substance in solvent) was centrifuged and dried *in vacuo* to obtain **MLPH₂** in the form of a light-brown powder (112.5 % recovered mass yield). A sample of the product was re-swelled in CH_3CN and the $^{31}P\{^1H\}$ NMR spectrum of the sample (Figure 5-1) showed a signal at δ_P = -148 consistent with molecular primary phosphines and the FT-IR spectrum of the same sample showed the clear presence of P-H functional groups (2300 cm^{-1}; P-H stretch; Figure 5-1) and therefore the product was assigned asassigned as the primary phosphine (**MLPH₂**), with 66% of the acrylate groups on **ML** successfully functionalized.
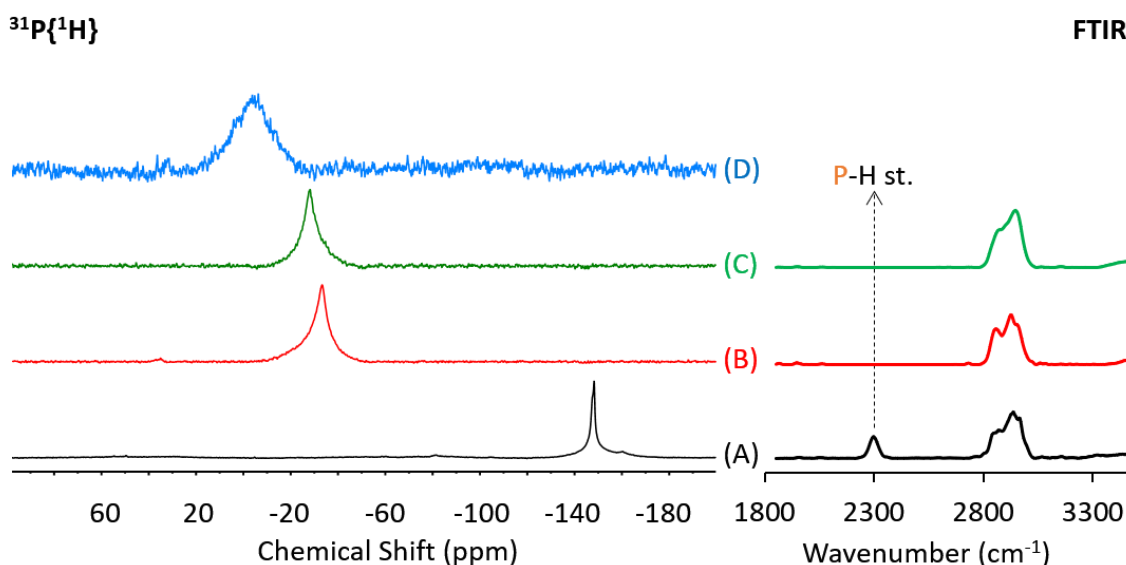
Figure 5-1 $^{31}P\{^1H\}$ NMR and FTIR spectra of **MLPH₂** (A), **MLP^Hex** (B), **MLP^RFn** (C), and the $^{31}P\{^1H\}$ NMR spectrum of **MLP^Ag**.

The hydrophosphination percentage (EOHP) was calculated using a modified version of the quantification process as reported by Argyropoulos.[36] **MLPH₂** (20 mg) was swelled in CH_3CN (2 mL) and transferred into an NMR tube. Separately, 40 µl of a 0.025 mol/L solution of PPh_3 in CH_3CN was transferred to a capillary tube, which was then flame sealed

and inserted into the NMR tube containing the **MLPH₂** sample and the $^{31}P\{^1H\}$ NMR spectrum of the mentioned tube was recorded (Figure 5-2).
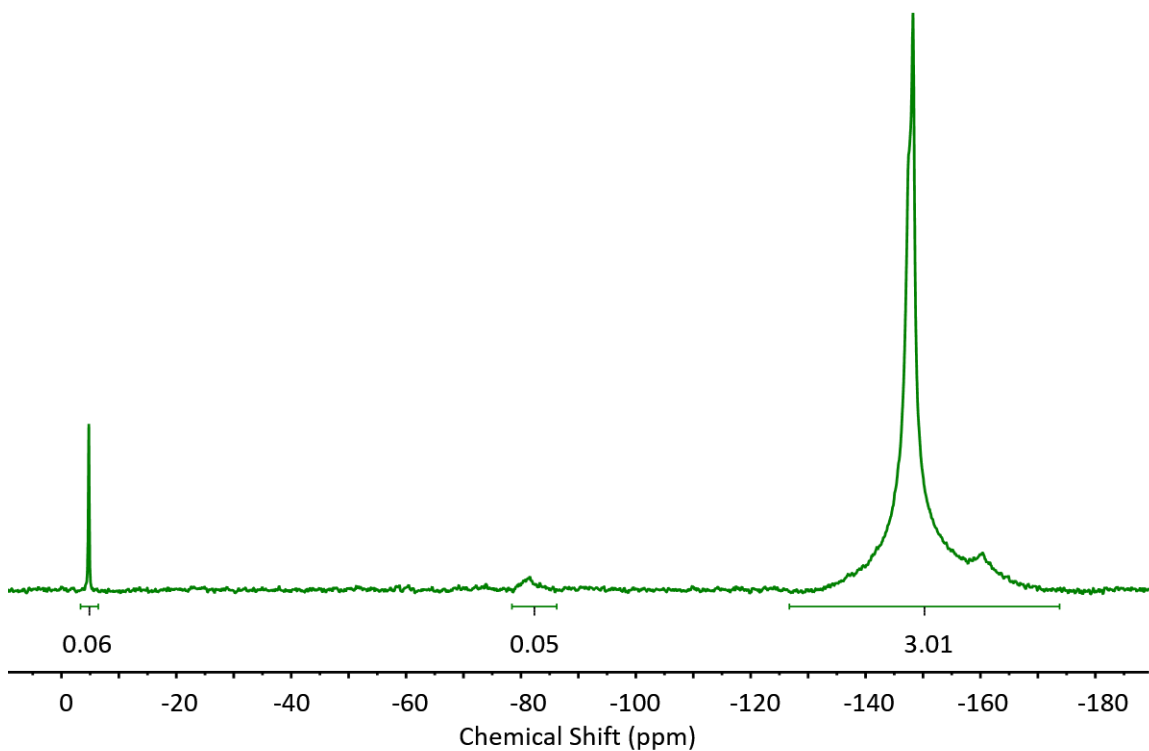
Figure 5-2 $^{31}P\{^1H\}$ NMR spectrum of **MLPH₂** in comparison with PPh₃P as external standard (δ_P = -4 ppm).

Another peak was observed at δ_P = -82 ppm, consistent with molecular secondary phosphines, which was attributed to the result of two methacrylate groups linking to one phosphorus atom and forming a secondary lignophine (**MLPH₁**). The amount of the **MLPH₁** formed was determined to be ca. 3%, which was considered negligible in

determining the obtained material as primary lignophine (**MLPH₂**). The EOHP was determined as described below:

Considering ca. 70% of the -OH functionalities were methacrylated in **ML**:

$$1 mol\ \boldsymbol{KL} \times 1.5 \frac{mol\ OH}{mol\ \boldsymbol{1}} \times 70\% = 1.05\ mol\ methacrylate\ on\ one\ C9$$

$$mod.\ C9 = 180g + \left(1.05\ mol\ meth. \times 85.03 \frac{g}{mol}\right) - \left(1.05\ mol\ H \times 1.008 \frac{g}{mol}\right)$$
$$= 268.24\ g$$

Considering the integration of the peak at δ_P = -148 ppm:

$$10^{-3} mmol\ PPh_3 \times \frac{3.01}{0.06} \times \frac{268.24}{20} = 0.6727\ mol$$

Thus, approximately 0.6727 mol of the methacrylate groups on **ML** were capped.

Considering the integration of the peak at δ_P = -82 ppm:

$$10^{-3} mmol\ PPh_3 \times \frac{0.05}{0.06} \times \frac{268.24}{20} \times \frac{2\ mol\ meth.}{1 mol\ \boldsymbol{MLPH1}} = 0.0222$$

Thus, approximately 0.0222 mol of the methacrylate groups on the **ML** were capped.

Finally, to determine the EOHP:

$$EOHP(\%) = \frac{0.6727 + 0.222}{1.05} \times 100 = 66\%$$

The resulting **MLPH₂** was then heated with excess 1-hexene or 1H,1H,2H-perfluoro-1-hexene in the presence of AIBN at 40 °C to obtain tertiary alkyl or fluoroalkyl lignophine (Scheme 5-2), respectively (**MLP^Hex**; **MLP^RF4**). Both reaction mixtures were filtered, the precipitates washed and then dried *in vacuo* to give light brown solids in all cases. ³¹P{¹H} NMR spectra of the swelled isolated materials each showed one signal at δ_P = -33 and -29, respectively and consistent with the preparation of tertiary phosphines. Moreover, the FT-

IR spectra of the isolated material showed no P-H vibration confirming the absence of P-H functional groups (Figure 5-1).
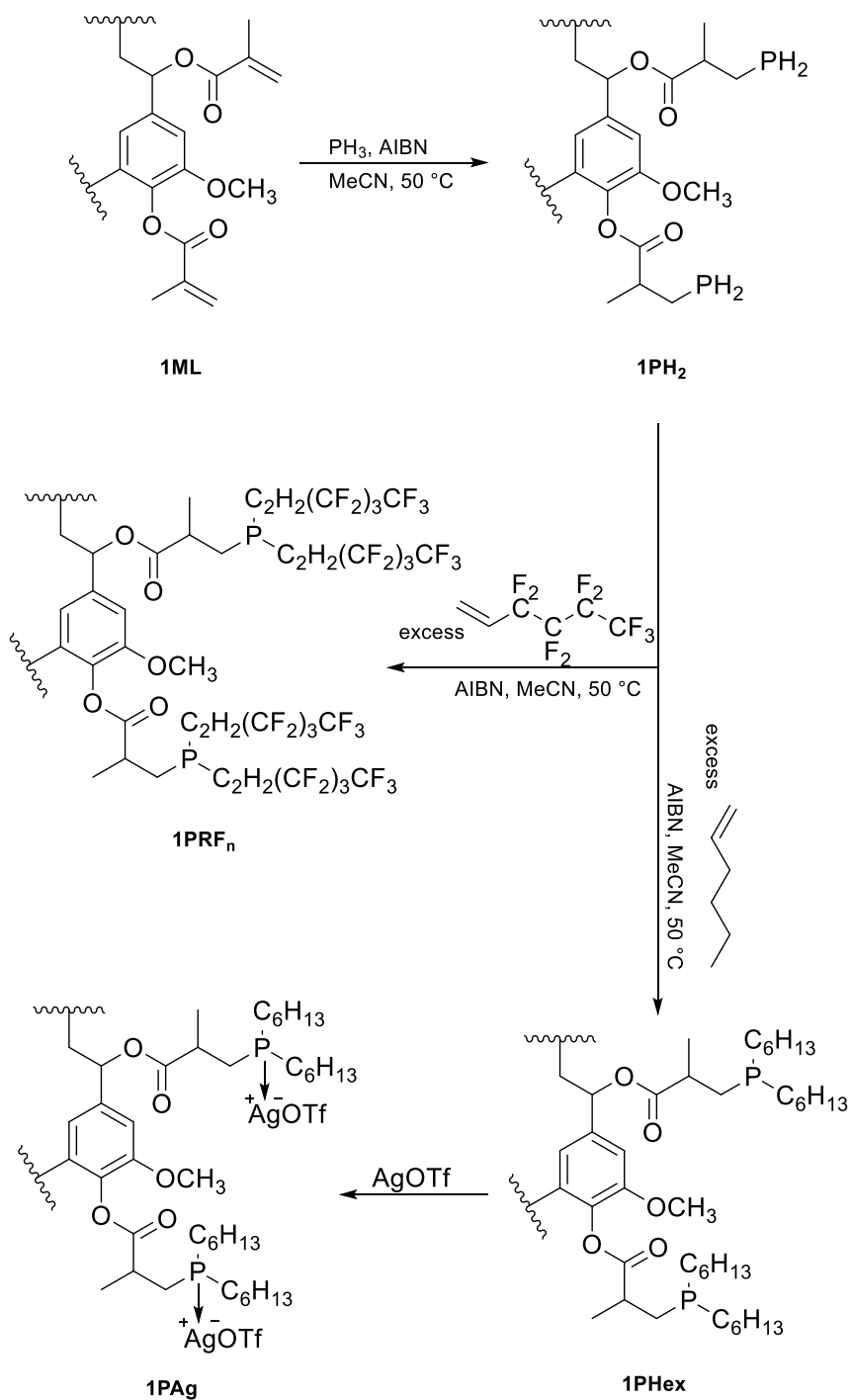
Scheme 5-2 Reaction schemes for the synthesis of **MLPH₂**, **MLP^{RFn}**, **MLP^{Hex}**, and coordination of **MLP^{Hex}** to AgOTf.

Thermal gravimetric analysis of **ML**, **MLPH₂**, **MLP^Hex**, and **MLP^RFn** showed that the **MLPH₂** and **MLP^Hex** samples retained more of their respective weights at high temperatures in comparison with the **ML** sample (43 wt.% for **MLP^Hex**, 40 wt.% for **MLPH₂**, and 34 wt.% retained weight at 900 °C for **ML**), whereas the retained weight for the **MLP^RFn** sample was almost equal to that of the **ML** sample (Figure 5-3).
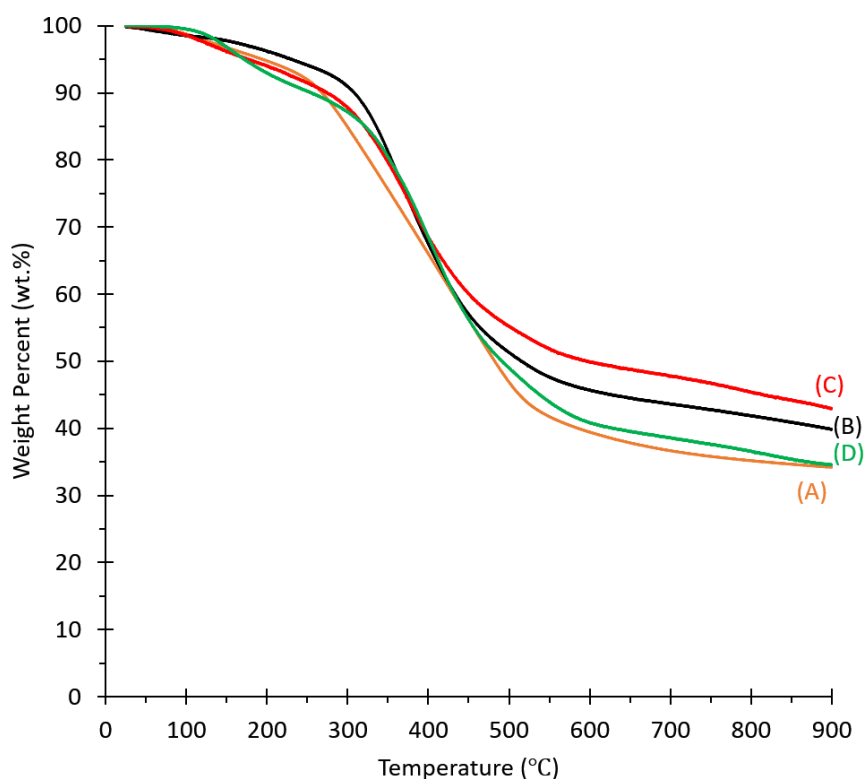
Figure 5-3 TGA thermograms of **ML** (A), **MLPH₂** (B), **MLP^Hex** (C), and **MLP^RFn** (D).

To ascertain whether or not the Lignophine materials are amenable for metal coordination, a sample of **MLP^Hex** was then added to a solution of AgOTf in CH_3CN (Scheme 2). The resulting mixture was then filtered, washed with CH_3CN and dried *in vacuo* to obtain a light brown powder. A swelled sample of the isolated material showed a new signal at δ_P = -4 in the $^{31}P\{^1H\}$ NMR spectrum, a $\Delta\delta_P$ of 31 downfield from **MLP^Hex** that was consistent with metal coordination at phosphorus, giving **MLP^Ag** (Figure 5-1). The $^{19}F\{^1H\}$ NMR spectrum of **MLP^Ag** was considerably broadened at δ_F = -77.5 and is consistent with an associated triflate ion (Figure 5-4).
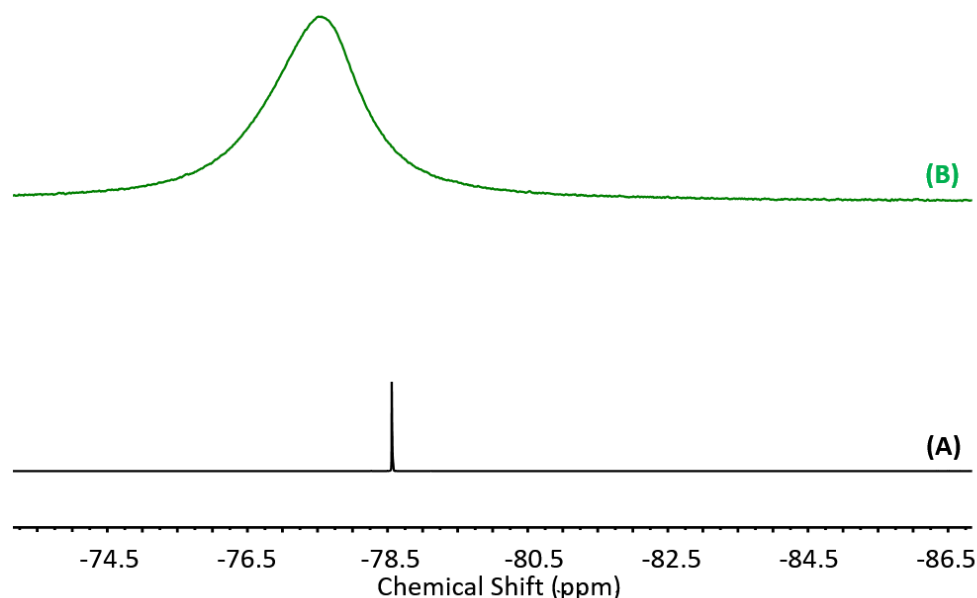
Figure 5-4 ^{31}F{^{1}H} NMR spectra of AgOTf (A) and **MLP^{Ag}** (B).

Given the ability of the lignophine to bind Ag$^+$, we considered that the material could be readily utilized as a metal-scavenger in catalytic reactions to sequester homogeneous catalysts from solution. As a proof of principle and using the methodology reported by Cuthbert *et al.*,[31] scavenging of the homogeneous metathesis catalyst Grubbs I (**GI**) was carried out (Figure 5-5a). Under the standard ring closing metathesis (RCM) conditions[37] **GI** converts 76% of diethyl diallylmalonate (**2**) to product **3** within 35 min (Figure 5-5b, Trace A). In separate reaction vessels, **GI** was first stirred with excess **MLP^{Hex}** (5 mg/0.5 mg **GI** and 10 mg/0.5 mg **GI**) for the incubation periods of 1 h and 24 h. These suspensions were then treated with RCM substrate **2**, where conversions of 11% and 8% were observed for the 5 mg/0.5 mg (**MLP^{Hex}**/**GI**) incubations for 1 h and 24 h, respectively, while the same values for the 10 mg/0.5 mg (**MLP^{Hex}**/**GI**) incubations of 1 h and 24 h were 5% and 0%, respectively (Figure 5-5b). The arrested catalytic conversion shows that **GI** is successfully sequestered from solution by **MLP^{Hex}** and that maximum sequestration of **GI** can be achieved by pre-incubation with **MLP^{Hex}** (10 mg/0.5 mg **GI**) for 24 h. In a separate experiment, **MLP^{Hex}** was pre-functionalized with **GI** and the resulting solid was isolated and used as the catalyst in the RCM of 2. No RCM product was observed, which indicates

both that the sequestered metal is not catalytically active and that the **GI** is not released into the solution in appreciable amounts to intitiate catalysis. This also confirms that the minor RCM conversions at short incubation times and less **MLP^{Hex}** amounts (B-D, Figure 5-5b) were due to incompletely sequestered **GI**.
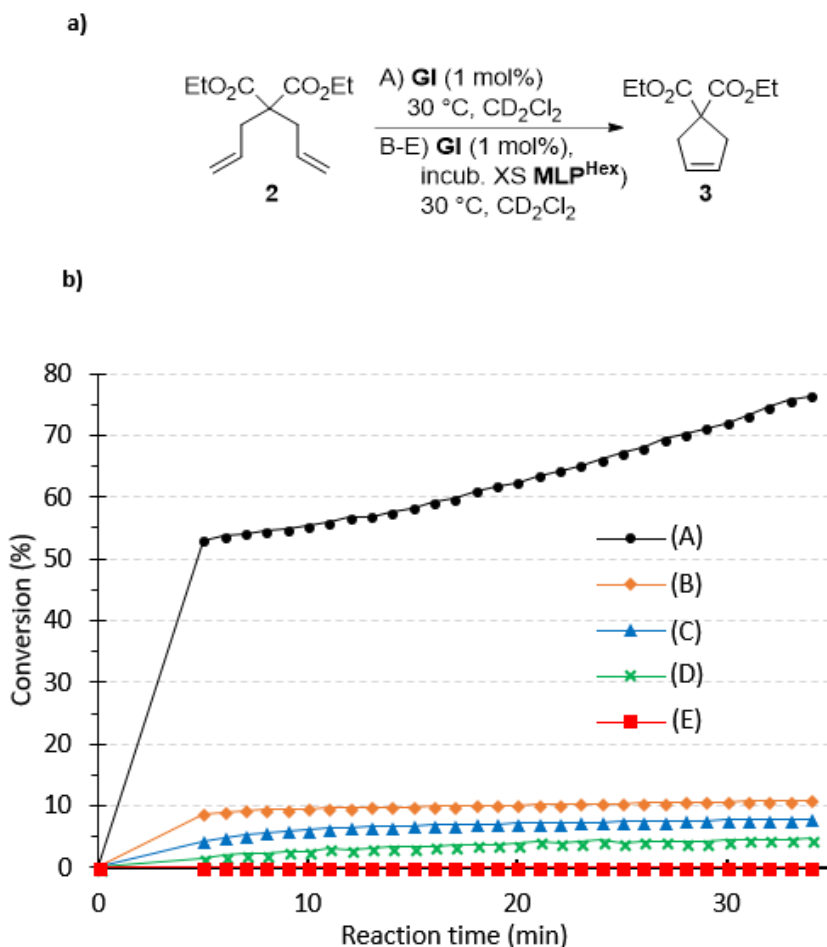
Figure 5-5 Reaction scheme of the RCM of **2** with **GI** without metal-scavenger (A) and with pre-incubated **GI** with **MLP^{Hex}** (B-E) and **b)** conversion (%) of **2** in the RCM reaction in the presence of **GI** without metal-scavenger (A), **GI** pre-incubated with 5 mg **MLP^{Hex}** for 1 h (B) and 24 h (C), and **GI** pre-incubated with 10 mg **1P^{Hex}** for 1 h (D) and 24 h (E).

In conclusion, tertiary lignophine was successfully synthesized through the reaction of methacrylated lignin (**ML**) with phosphine gas and subsequent reaction with 1-hexene

(resulting in **MLP^{Hex}**) and 1H,1H,2H-perfluoro-1-hexene (resulting in **MLP^{RFn}**). The obtained primary and tertiary lignophines were characterized by ^{31}P{^{1}H}, ^{19}F{^{1}H} (for **MLP^{RFn}**), and FT-IR spectroscopy. Thermal gravimetric analysis was then performed on **ML**, **MLPH₂**, and **MLP^{Hex}** and it was concluded that the lignophines exhibited higher retained weight and more char formation at 900 °C in comparison with the **ML** sample. The ability of the obtained **MLP^{Hex}** sample to coordinate to transition metals was probed using AgOTf and it was concluded (via ^{31}P{^{1}H} ^{19}F{^{1}H} NMR spectroscopy) that the synthesized tertiary lignophine has the ability to coordinate to the silver atom in AgOTf. The addition of lignophine to RCM reactions catalyzed by **GI** shows nearly complete catalyst quenching. This indicates that the polymer is an effective metal scavenger and opens a new door for opportunities with lignin a renewable bioresource.

5.1 References

(1)   Patil, S. V.; Argyropoulos, D. S. Stable Organic Radicals in Lignin: A Review. *ChemSusChem 10* (17), 3284–3303.

(2)   Zakzeski, J.; Bruijnincx, P. C. A.; Jongerius, A. L.; Weckhuysen, B. M. The Catalytic Valorization of Lignin for the Production of Renewable Chemicals. *Chem. Rev.* **2010**, *110* (6), 3552–3599.

(3)   Upton, B. M.; Kasko, A. M. Strategies for the Conversion of Lignin to High-Value Polymeric Materials: Review and Perspective. *Chem Rev* **2016**, *116* (4), 2275–2306.

(4)   Bruijnincx, P.; Weckhuysen, B.; Gruter, G.-J.; Engelen-Smeets, E. *Lignin Valorisation: The Importance of a Full Value Chain Approach*; 2016.

(5)   Silva, E. A. B. da; Zabkova, M.; Araújo, J. D.; Cateto, C. A.; Barreiro, M. F.; Belgacem, M. N.; Rodrigues, A. E. An Integrated Process to Produce Vanillin and Lignin-Based Polyurethanes from Kraft Lignin. *Chem. Eng. Res. Des.* **2009**, *87* (9), 1276–1292.

(6)   Sadeghifar, H.; Cui, C.; Argyropoulos, D. S. Toward Thermoplastic Lignin Polymers. Part 1. Selective Masking of Phenolic Hydroxyl Groups in Kraft Lignins via Methylation and Oxypropylation Chemistries. *Ind Eng Chem Res* **2012**, *51* (51), 16713–16720.

(7)   Thielemans, W.; Wool, R. P. Lignin Esters for Use in Unsaturated Thermosets: Lignin Modification and Solubility Modeling. *Biomacromolecules* **2005**, *6* (4), 1895–1905.

(8)   Gordobil, O.; Moriana, R.; Zhang, L.; Labidi, J.; Sevastyanova, O. Assesment of Technical Lignins for Uses in Biofuels and Biomaterials: Structure-Related Properties, Proximate Analysis and Chemical Modification. *Ind. Crops Prod.* **2016**, *83*, 155–165.

(9)   Ismail, T. N. M. T.; Hassan, H. A.; Hirose, S.; Taguchi, Y.; Hatakeyama, T.; Hatakeyama, H. Synthesis and Thermal Properties of Ester-Type Crosslinked Epoxy Resins Derived from Lignosulfonate and Glycerol. *Polym. Int.* **2010**, *59* (2), 181–186.

(10)   Ferdosian, F.; Yuan, Z.; Anderson, M.; Xu, C. (Charles). Sustainable Lignin-Based Epoxy Resins Cured with Aromatic and Aliphatic Amine Curing Agents: Curing Kinetics and Thermal Properties. *Thermochim. Acta* **2015**, *618* (Supplement C), 48–55.

(11)   Sun, G.; Sun, H.; Liu, Y.; Zhao, B.; Zhu, N.; Hu, K. Comparative Study on the Curing Kinetics and Mechanism of a Lignin-Based-Epoxy/Anhydride Resin System. *Polymer* **2007**, *48* (1), 330–337.

(12)   Fang, R.; Cheng, X.; Lin, W. PREPARATION AND APPLICATION OF   . *BioResources* **2011**, *6* (3), 2874–2884.

(13)   Wang, C.; Venditti, R. A. UV Cross-Linkable Lignin Thermoplastic Graft Copolymers. *ACS Sustain. Chem Eng* **2015**, *3* (8), 1839–1845.

(14)   Wang, J.; Yao, K.; Korich, A. L.; Li, S.; Ma, S.; Ploehn, H. J.; Iovine, P. M.; Wang, C.; Chu, F.; Tang, C. Combining Renewable Gum Rosin and Lignin: Towards Hydrophobic Polymer Composites by Controlled Polymerization. *J. Polym. Sci. Part Polym. Chem.* **2011**, *49* (17), 3728–3738.

(15)   Liu, X.; Wang, J.; Li, S.; Zhuang, X.; Xu, Y.; Wang, C.; Chu, F. Preparation and Properties of UV-Absorbent Lignin Graft Copolymer Films from Lignocellulosic Butanol Residue. *Ind. Crops Prod.* **2014**, *52*, 633–641.

(16)   Tan, T. T. M. Cardanol–lignin-Based Polyurethanes. *Polym. Int.* **1996**, *41* (1), 13–16.

(17)   Pan, X.; Saddler, J. N. Effect of Replacing Polyol by Organosolv and Kraft Lignin on the Property and Structure of Rigid Polyurethane Foam. *Biotechnol. Biofuels* **2013**, *6*, 12.

(18)   Cateto, C. A.; Barreiro, M. F.; Rodrigues, A. E.; Brochier-Salon, M. C.; Thielemans, W.; Belgacem, M. N. Lignins as Macromonomers for Polyurethane Synthesis:

A Comparative Study on Hydroxyl Group Determination. *J Appl Polym Sci* **2008**, *109* (5), 3008–3017.

(19)   Mahmood, N.; Yuan, Z.; Schmidt, J.; Xu, C. (Charles). Preparation of Bio-Based Rigid Polyurethane Foam Using Hydrolytically Depolymerized Kraft Lignin via Direct Replacement or Oxypropylation. *Eur. Polym. J.* **2015**, *68* (Supplement C), 1–9.

(20)   Gnedenkov, S. V.; Opra, D. P.; Zemnukhova, L. A.; Sinebryukhov, S. L.; Kedrinskii, I. A.; Patrusheva, O. V.; Sergienko, V. I. Electrochemical Performance of Klason Lignin as a Low-Cost Cathode-Active Material for Primary Lithium Battery. *J. Energy Chem.* **2015**, *24* (3), 346–352.

(21)   Gnedenkov, S. V.; Sinebryukhov, S. L.; Opra, D. P.; Zemnukhova, L. A.; Tsvetnikov, A. K.; Minaev, A. N.; Sokolov, A. A.; Sergienko, V. I. Electrochemistry of Klason Lignin. *Procedia Chem.* **2014**, *11*, 96–100.

(22)   Frangville, C.; Rutkevičius, M.; Richter, A. P.; Velev, O. D.; Stoyanov, S. D.; Paunov, V. N. Fabrication of Environmentally Biodegradable Lignin Nanoparticles. *ChemPhysChem 13* (18), 4235–4243.

(23)   Figueiredo, P.; Lintinen, K.; Kiriazis, A.; Hynninen, V.; Liu, Z.; Bauleth-Ramos, T.; Rahikkala, A.; Correia, A.; Kohout, T.; Sarmento, B.; et al. In Vitro Evaluation of Biodegradable Lignin-Based Nanoparticles for Drug Delivery and Enhanced Antiproliferation Effect in Cancer Cells. *Biomaterials* **2017**, *121*, 97–108.

(24)   Li, Y.; Qiu, X.; Qian, Y.; Xiong, W.; Yang, D. pH-Responsive Lignin-Based Complex Micelles: Preparation, Characterization and Application in Oral Drug Delivery. *Chem. Eng. J.* **2017**, *327*, 1176–1183.

(25)   Yiamsawas, D.; Beckers, S. J.; Lu, H.; Landfester, K.; Wurm, F. R. Morphology-Controlled Synthesis of Lignin Nanocarriers for Drug Delivery and Carbon Materials. *ACS Biomater. Sci. Eng.* **2017**, *3* (10), 2375–2383.

(26)   Feng, Q.; Li, J.; Cheng, H.; Chen, F.; Xie, Y. Synthesis and Characterization of Porous Hydrogel Based on Lignin and Polyacrylamide. *BioResources* **2014**, *9* (3), 4369–4381.

(27)   Cuthbert, T. J.; Jadischke, J. J.; de Bruyn, J. R.; Ragogna, P. J.; Gillies, E. R. Self-Healing Polyphosphonium Ionic Networks. *Macromolecules* **2017**, *50* (14), 5253–5260.

(28)   J. Cuthbert, T.; D. Harrison, T.; J. Ragogna, P.; R. Gillies, E. Synthesis, Properties, and Antibacterial Activity of Polyphosphonium Semi-Interpenetrating Networks. *J. Mater. Chem. B* **2016**, *4* (28), 4872–4883.

(29)   J. Cuthbert, T.; Guterman, R.; J. Ragogna, P.; R. Gillies, E. Contact Active Antibacterial Phosphonium Coatings Cured with UV Light. *J. Mater. Chem. B* **2015**, *3* (8), 1474–1478.

(30)   Hisey, B.; Ragogna, P. J.; Gillies, E. R. Phosphonium-Functionalized Polymer Micelles with Intrinsic Antibacterial Activity. *Biomacromolecules* **2017**, *18* (3), 914–923.

(31)   Cuthbert, T. J.; Evoy, E.; Bow, J. P. J.; Guterman, R.; Stubbs, J. M.; Gillies, E. R.; Ragogna, P. J.; Blacquiere, J. M. CapturePhos – A Phosphorus-Rich Polymer as a Homogeneous Catalyst Scavenger. *Catal. Sci. Technol.* **2017**, *7* (13), 2685–2688.

(32)   Argyropoulos, D. S. 31P NMR in Wood Chemistry: A Review of Recent Progress. *Res. Chem. Intermed.* **1995**, *21* (3–5), 373–395.

(33)   Ferry, L.; Dorez, G.; Taguet, A.; Otazaghine, B.; Lopez-Cuesta, J. M. Chemical Modification of Lignin by Phosphorus Molecules to Improve the Fire Behavior of Polybutylene Succinate. *Polym. Degrad. Stab.* **2015**, *113*, 135–143.

(34)   Guterman, R.; Rabiee Kenaree, A.; Gilroy, J. B.; Gillies, E. R.; Ragogna, P. J. Polymer Network Formation Using the Phosphane–ene Reaction: A Thiol–ene Analogue with Diverse Postpolymerization Chemistry. *Chem. Mater.* **2015**, *27* (4), 1412–1419.

(35)   Zhu, H.; Peng, Z.; Chen, Y.; Li, G.; Wang, L.; Tang, Y.; Pang, R.; Haq Khan, Z. U.; Wan, P. Preparation and Characterization of Flame Retardant Polyurethane Foams Containing Phosphorus–nitrogen-Functionalized Lignin. *RSC Adv.* **2014**, *4* (98), 55271–55279.

(36)   Argyropoulos, D. S. Quantitative Phosphorus-31 NMR Analysis of Lignins, a New Tool for the Lignin Chemist. *J. Wood Chem. Technol.* **1994**, *14* (1), 45–63.

(37)   Ritter, T.; Hejl, A.; Wenzel, A. G.; Funk, T. W.; Grubbs, R. H. A Standard System of Characterization for Olefin Metathesis Catalysts. *Organometallics* **2006**, *25* (24), 5740–5745.

Chapter 6

6 "Lignophoniums": Stimuli-Responsive Lignin-based Polyphopshonium Networks for Controlled Drug Delivery

6.1 Introduction

Lignin is the world's second most abundant polymer, after cellulose. Residing mainly in the secondary cell wall, lignin acts as a filler vital to plant life, as it is responsible for giving stiffness, as well as facilitating the transport of water and other nutrients throughout the plants.[1,2] This complex natural polymer originates from the connection of three phenylpropanoid (C9) units (*p*-hydroxyphenyl, **H**; guaiacyl, **G**; and syringyl, **S**) through various, primarily arylglycerol ether, linkages.[3] The C9 units and their respective linkages are resulted from an *in vivo* enzyme-mediated dehydrogenation polymerization (lignification) of three hydroxycinnamyl (*p*-coumaryl, sinapyl, and coniferyl) alcohol monomers called monolignols (Figure 6-1a).[4–6]

As a sustainable resource with the annual global production of 50-55 MT, more than 98% of the produced lignin is used at its manufacturing plants as a fuel for heat or buried in landfills as waste.[7] Such under-utilization, along with a functional group-rich chemical structure has turned the research field of lignin valorization into a highly attractive area for many researchers.[8,9] The up-conversion of lignin has been widely targeted by chemically modifying and incorporating it into different materials such as epoxy resins,[10–13] coatings,[14–16] polyurethanes,[17–20] and adhesives.[21–24] Approaches to lignin valorization strategies have gained substantial interest over the past few years, which aim at converting lignin into materials with more unique applications. For example, lignin has been chemically modified to produce carbon fibers, nanofibers, and highly hydrophobic ATRP-polymerized graft copolymers,[25–33] all hallmarks of the immense potential lignin has in areas such as biomedicine and medicinal chemistry. Lignin has been probed as a component in systems capable of controlled drug release, mainly in the form of nanocarriers[34–37] and hydrogels.[38,39] Such new streams of up-conversion strategies can play

an important role in the future of lignin valorization and become the next step in turning lignin from a negative-value material to a positive-value one.
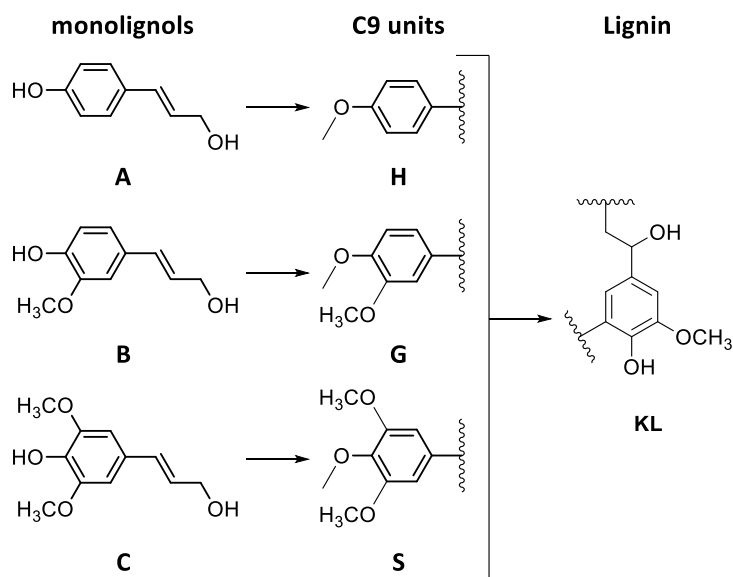
Figure 6-1 The three standard monolignols of *p*-coumaryl (A), coniferyl (B), and sinapyl (C) alcohol and their corresponding *p*-hydroxyphenyl (**H**), guaiacyl (**G**), and syringyl (**S**) C9 units as the building blocks of lignin (**KL**, representative structure of lignin.

Phosphorus chemistry has yet to find its own stream in lignin valorization. While chemical modification of lignin with phosphorus-containing compounds, particularly halophospholanes, has been used extensively since mid-1990s for the purpose of quantifying lignin's hydroxyl functionalities,[40–42] reports on utilizing lignin-based phosphorus containing materials remain rare and generally focus on using phosphates in conjunction with lignin for improved surface area or flame retardancy in the prepared materials.[43–46] Regardless of aiming at valorizing lignin or not, these reports focus on utilizing -O-P functional groups within the structure of lignin, where our group remains the only one examining lignin modification processes through the introduction of -C-P functionalities. A general research stream of our group relies in P-H bond addition reactions to olefinic groups to synthesize highly functional phosphorus-rich materials via phosphane-ene chemistry that have metal and oxygen scavenging abilities,[47,48] self-healing networks,[49] antimicrobial properties,[50–52] and act as ceramic precursors.[53] Recently, we

have synthesized lignophines, lignin-based tertiary polyphosphines, that show effective metal-scavenging ability.

In this context, we have synthesized lignophonium, a lignin-based polyphosphonium salt, from tertiary alkylated lignophine, **MLP^{Hex}**. The isolated lignophonium was then incorporated into siloxane-crosslinked UV-cured thin films, which showed high cure percentages, water contact angles and surface charge density value well over the necessary threshold for antimicrobial films. The swelling degrees were also determined to be suitable for sustained drug release.

6.2   Experimental

6.2.1 Materials and Methods

Lignophine (**MLP^{Hex}**) was synthesized according to the procedure reported in chapter 5 of this thesis. Solvents were purchased from Caledon and dried using an MBraun Solvent Purification System (SPS). EBERCYL 1360 (EB-1360; hexafunctional siloxane-based crosslinker) was purchased from Allnex Belgium SA and used as received. 2-hydroxy-2-methylpropiophenone (HDMAP, 97%), 4-vinylbenzyl chloride (90%), cetyltrimethylammonium chloride (CTAC; 25 wt.% in H$_2$O), and fluorescein (sodium salt) were purchased from Sigma-Aldrich Co. and used as received. Phosphate buffered saline (PBS) (0.15 M) was prepared following a previously reported procedure.[54]

^{31}P{^{1}H} NMR spectra were recorded using a Varian INOVA 600 MHz spectrometer (^{1}H, 599.5 MHz; ^{13}C, 150.8 MHz; ^{31}P, 242.6 MHz) and referenced using an external standard (85% H$_3$PO$_4$; δ_P = 0). FT-IR spectra were recorded using a PerkinElmer FT-IR spectrometer using the universal attenuated total reflectance mode (UATR), a diamond crystal, as well as the UATR sampling accessory (part number: L1050231).

6.2.2 Synthesis of Lignophonium Salt (**MLP$^+$**)

MLP^{Hex} (0.600 g) was added to MeCN (30 mL) under stirring in a 100 mL pressure round-bottom flask in the dry-box and swelled for 10 min. 4-vinylbenzyl chloride (0.300 g, 1.965 mmol) was added to the mixture, the flask was sealed, moved out of the dry-box, and heated in an oil bath at 45 °C for 18 h. The pressure flask was cooled, brought back into the glove

box, and the mixture was centrifuged to obtain a dark brown swelled powder at the bottom of the centrifuge tube. The swelled powder was then washed three times with MeCN (20 mL), centrifuged after each wash, and the solvent was disposed of. Afterward, the swelled powder was transferred into a 50 ml Schlenk round-bottom flask and dried *in vacuo* at room temperature to obtain a light brown powder (109 wt% recovered mass yield).

6.2.3 Preparation of **MLP⁺** UV-Cured Films

MLP⁺ (15 wt.%), EBERCYL 1360 (EB-1360, hexafunctional siloxane-based crosslinker, 80 wt.%), and 2-hydroxy-2-methylpropiophenone (HDMAP, 5 wt.%) were combined and diluted to 50% in *N,N*-dimethylformamide (DMF). 50 µL of the resulting mixture was then deposited on a clean glass slide. A second glass slide, using ~ 170 µm thick electrical tape as a spacer to define the film's thickness, was then placed on top. The slides were passed 5 times at the speed of ~ 0.06 m•s⁻¹ through a modified UV-curing system purchased from UV Process Supply Inc. (Chicago, IL, USA) with a mercury bulb (UVA: 154 mW•cm², 189 mJ•cm², UVB: 74 mW•cm², 90 mJ•cm²; as determined by a PP2-H-U Power Puck II purchased from EIT Instrument Markets). After irradiation, the glass slides were separated, and the resulting film was dried *in vacuo* overnight at 40 °C, resulting in an **MLP⁺** UV-cured film of ~ 150 µm thickness as measured by a micrometer.

6.2.4 Measurement of Cure Percentage

ATR-FTIR spectra were obtained from the liquid formulation before curing and the **MLP⁺** UV-cured film after drying overnight *in vacuo* at 40 °C. The signal corresponding to C=O (~ 1720 cm⁻¹) was used as an internal standard to normalize the obtained spectra, as its intensity does not change after curing. The intensity of the signal corresponding to C=C (~ 810 cm⁻¹) was then compared between the liquid formulation and the UV-cured film. The cure percentage was calculated as the decrease (%) in the relative intensity of the C=C signal (100% corresponding to no C=C functionality remaining in the film's ATR-FTIR spectra). The cure percentage was measured in triplicate and the results are reported as the mean ± standard deviation.

6.2.5 Measurement of Gel Content

The **MLP**[+] UV-cured film from the cure percentage analysis were used to calculate the gel content. The **MLP**[+] UV-cured film was accurately weighed and immersed in excess MeCN (10 mL) for 18 h. The solvent was removed, and the film was dried *in vacuo* at 40 °C for 18 h and re-weighed. Gel content was then calculated as the percentage of mass (%) remaining relative to the initial mass of the film. The gel content was calculated in triplicate and the results are reported as the mean ± standard deviation.

6.2.6 Measurement of water contact angle

The **MLP**[+] UV-cured film from the cure percentage analysis were used to measure the water contact angle. The **MLP**[+] UV-cured film was placed on a glass slide and placed on the stage of a Kruss DSA100 Drop Shape Analyzer (KRUSS GmbH, Hamburg, Germany). Afterward, a 5 µL drop of deionized water was placed on the surface and a static drop shape analyzer was used to measure the water contact angle on the film's surface. Water contact angle was measured in triplicate and the result is reported as the mean ± standard deviation.

6.2.7 Charge density determination

The charge density was determined following a previously reported procedure.[55] After incubating the **MLP**[+] UV-cured film in MeCN (as described above for the measurement of gel content) and drying the film *in vacuo* at 40 °C for 18 h, the **MLP**[+] UV-cured film (0.28 cm^2) was immersed in 10 mL of a 1% w/v aqueous sodium fluorescein solution for 18 h. The film was then immersed in 10 mL deionized water for 4 h and immersed in 10 mL of a 0.1% v/v aqueous cetyltrimethylammonium chloride (CTAC) solution. At different time points, the film was transferred to a fresh CTAC solution, while 10 mM, pH 8 phosphate buffer (100 µL) was added to the previous CTAC solution and its absorbance at 501 nm was measured. The concentration of accessible charges on the surface was then determined according to the extinction coefficient of fluorescein (ε = 54,760 M^{-1}•cm^{-1}), assuming that each fluorescein molecule binds to one accessible cation. The charge density was measured in triplicate and the result is reported as the mean ± standard deviation.

6.2.8 Measurement of Mass Swelling Ratio in Water

The **MLP⁺** UV-cured film from the cure percentage analysis were used to measure the mass swelling ratio in water by immersing the film in 10 mL deionized water for 24 h. Afterward, the film was removed from the water, the excess water on the film was removed with Kimwipe, and the film was weighed. The value of ($\frac{final\ mass - initial\ mass}{initial\ mass} \times 100\%$) was calculated and reported as the mass swelling %. Mass swelling ratio in water was determined in triplicate and the value was reported as the mean ± standard deviation.

6.1 Results and Discussion

Tertiary alkylated lignophine (**MLP^Hex**, 0.60 g) was synthesized and isolated (See chapter 5), swelled in CH_3CN (100 mL), and heated with excess 4-vinylbenzyl chloride at 45 °C for 18 h (Figure 6-2a). The mixture was filtered, the precipitate was washed and dried *in vacuo* to give a light brown powder (109 wt% recovered mass yield). The $^{31}P\{^1H\}$ NMR spectrum of the swelled, isolated material showed one signal at $\delta_P = 32$, consistent with the preparation of a phosphonium cation (Figure 6-2b) and the product was assigned as the "lignophonium" (**MLP⁺**; lignin-based phosphonium salt). A mixture of **MLP⁺** (15 wt.%), EB-1360 (crosslinker, 80 wt.%), 2-hydroxy-2-methylpropiophenone (HDMAP, photoinitiator, 5 wt.%) was diluted 2-fold with *N,N*-dimethylformamide (DMF), cast on a glass slide, and cured using a UV-curing conveyor, producing **MLP⁺**-incorporated cured networks as free-standing films (**MLP⁺N**) that were ca. 150 µm thick, with a surface area of 0.28 cm² (Figure 6-2c).
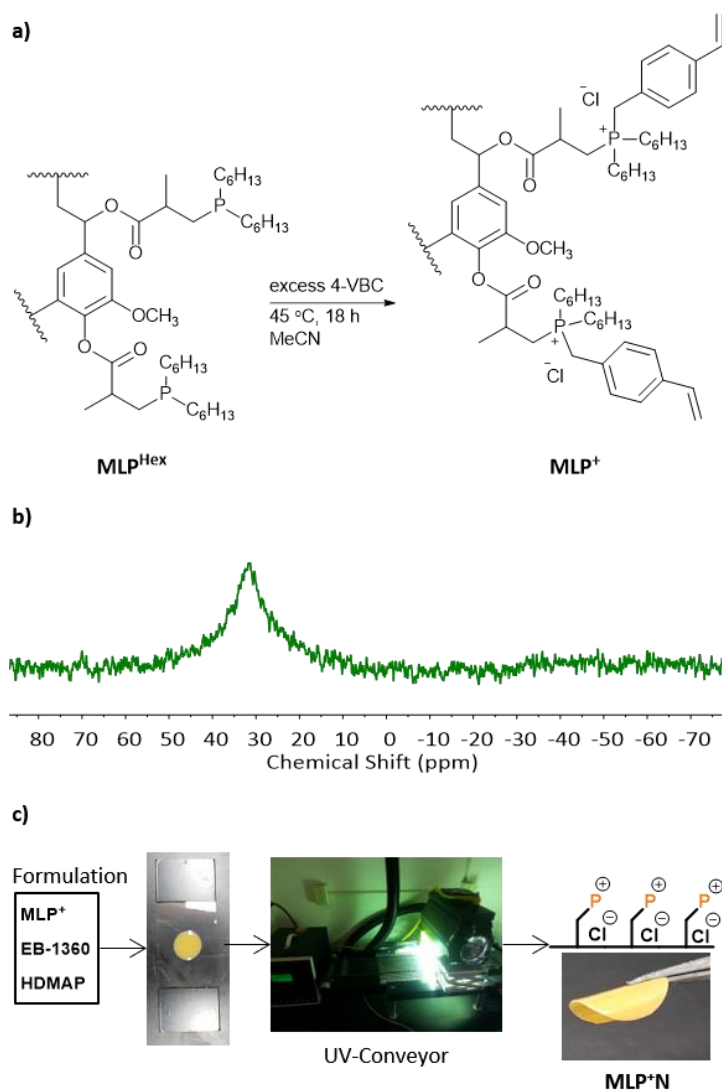
Figure 6-2 a) Reaction scheme for the synthesis of **MLP⁺** from **MLP^Hex** and **b)** ^{31}P{^{1}H} NMR spectrum of **MLP⁺**, and **c)** process scheme for the preparation of **MLP⁺N** UV-cured films.

Surface-accessible charge density was calculated using a procedure reported by Murata *et al.*[55] through immersing the dried **MLP⁺N** film in a 1% w/v aqueous fluorescein sodium solution (Fl.; 5 mL) to allow for the replacement of the chloride anions with fluorescein via anion exchange. The film was then washed with water to remove any unbound fluorescein, then placed in a 0.1% v/v aqueous cetyl trimethyl ammonium chloride (CTAC, 5 mL) solution to release the surface-bound fluorescein into the solution. Phosphate buffer (10 mM; pH = 8) was then added to the CTAC solution and the absorbance at 501 nm was

measured (Figure 6-3a), which corresponds to the absorption of the conjugated π system in fluorescein. The concentration of accessible charges on the surface was then determined according to the extinction coefficient of fluorescein (ε = 54,760 $M^{-1} \cdot cm^{-1}$), with the assumption that each fluorescein molecule binds to one accessible cation and it was determined that the **MLP⁺N** film has $5.33 \pm 0.38 \times 10^{18}$ cations per cm^2 (Figure 6-3b), a value well above the suggested minimum surface accessible charges required for antimicrobial activity.[56]

a)
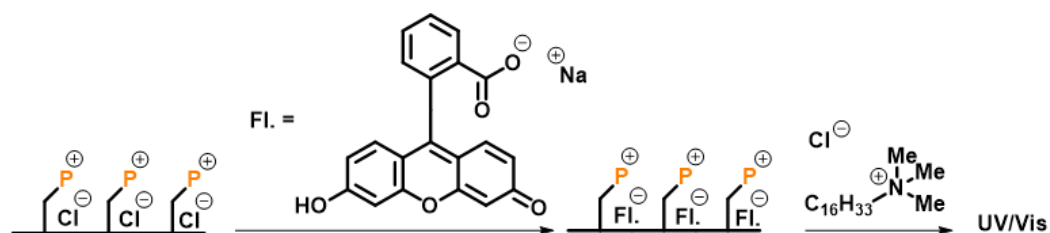
b)
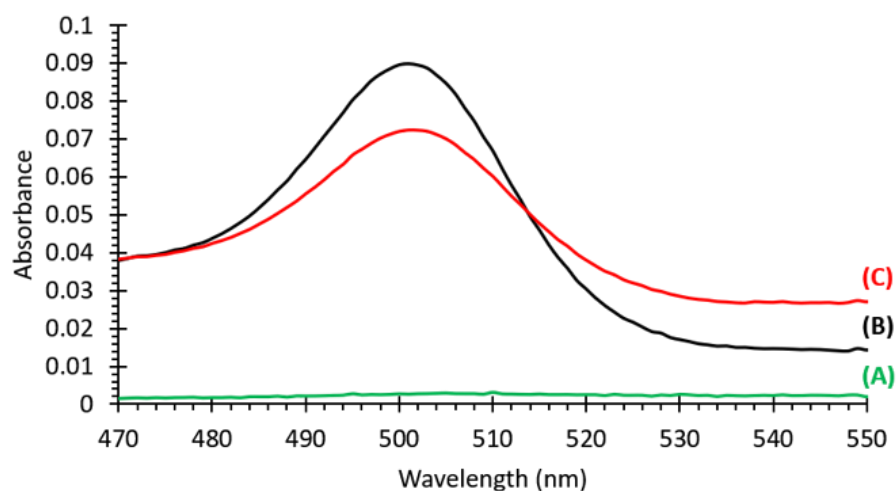
Figure 6-3 a) Process scheme for the measurement of surface charge density and **b)** UV-Vis of the CTAC solution containing the **MLP⁺N** at12 h (A), 60 h (B), and 180 h (C).

Drop shape analysis was used to measure the water contact angle (WCA) and it was determined that the **MLP⁺N** film had a WCA value of $88 \pm 1.2°$, which was more than twice the same value for standard siloxane-based UV-cured films prepared without **MLP⁺** in the formulation (Figure 6-4a). ATR-FTIR was used to determine the cure percentage for the **MLP⁺N** film, which was calculated at $84.7 \pm 0.3\%$. The same value for the standard film was calculated at $36.1 \pm 0.2\%$, showing improved crosslinking within the network because of the **MLP⁺**-incorporation (Figure 6-4b). Moreover, it was determined that the **MLP⁺N** film swelled to $55.5 \pm 3.8\%$ its original weight after immersion in water for 24 h. The hydrophobicity of the film, along the degree of swelling make the films potential candidates for slow, controlled release of ionic molecules in aqueous media.
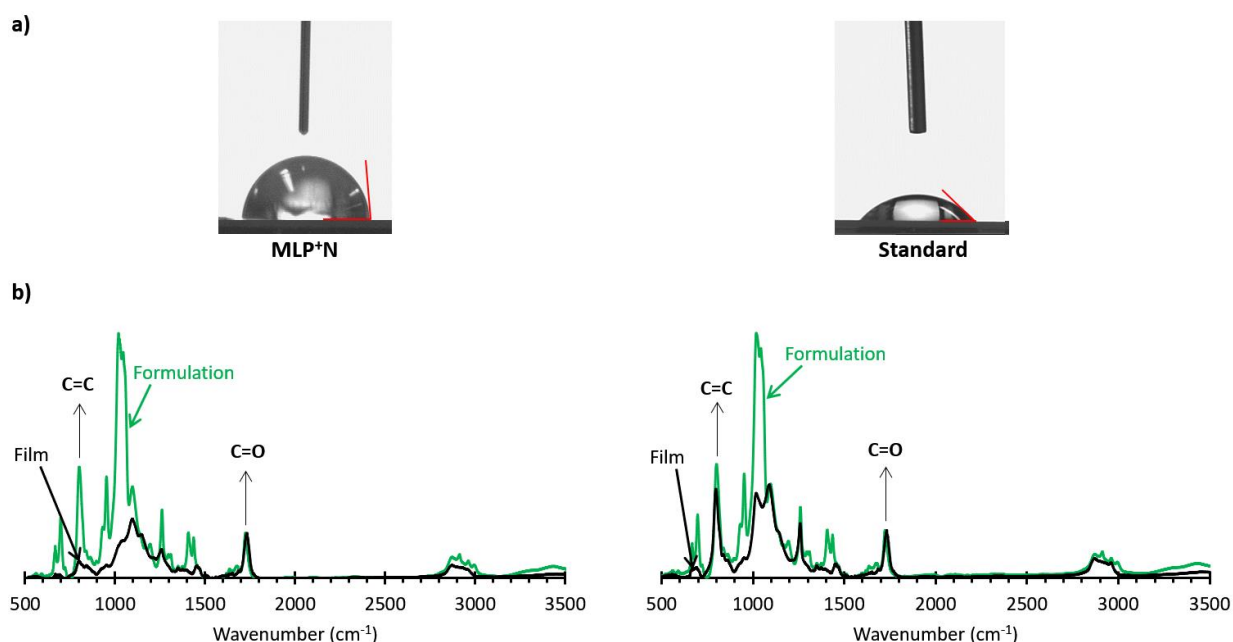
Figure 6-4 a) Drop shape images for standard siloxane-based films and the **MLP⁺N** film and **b)** ATR-FTIR spectra for both the liquid formulations and cured films of standard siloxane-based films and the **MLP⁺N film** showing the intensity reduction for the C=C signal.

The controlled drug release ability of the **MLP⁺N** films was probed by incubating the film in a solution containing 1 wt% diclofenac sodium salt (10 mL) for 24 h, followed by washing with deionized water to remove any unbound molecules and submerging into a PBS solution (10 mL) to release diclofenac. The concentration of released diclofenac into

the PBS solution from the film was then determined according to the extinction coefficient of diclofenac in PBS ($\varepsilon = 4245.8$ M$^{-1} \cdot$cm^{-1}), assuming that each diclofenac molecule binds to one accessible cation and it was determined that the **MLP$^+$N** film released $6.23 \pm 0.19 \times 10^{18}$ diclofenac molecules per cm^2 over the timespan of 173 h, while complete release was observed at 157 h timepoint (Figure 6-5), which was in close agreement with the surface charge density as measured earlier.
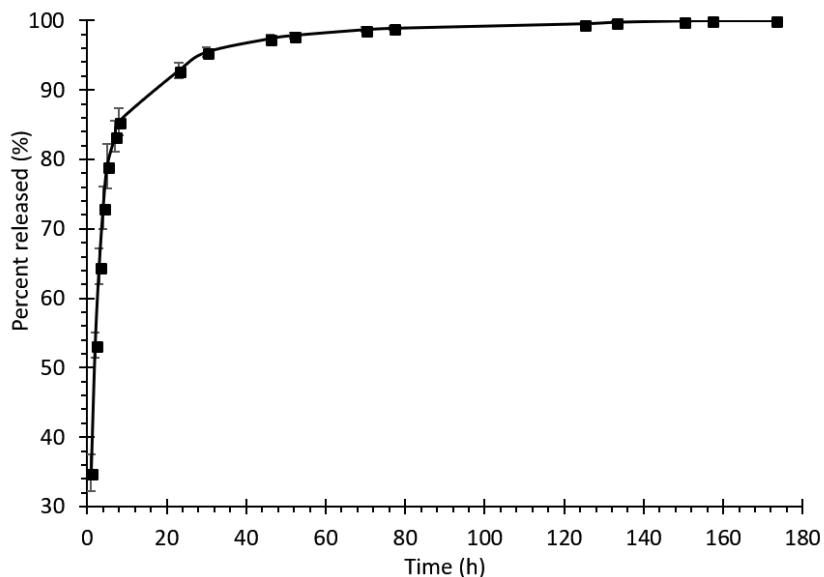
Figure 6-5 Release profile of the **MLP$^+$N** film.

6.2   Conclusion

Lignin-based polyphosphonium salt (Lignophonium; **MLP$^+$**) was successfully synthesized through the reaction of lignin-based tertiary alkylated polyphosphine (tertiary alkylated lignophine; **MLP^{Hex}**) with 4-vinylbenzyl chloride and characterized by ^{31}P{^{1}H} NMR spectroscopy. The lignophonium was then incorporated into a UV-crosslinked free-standing film (**MLP$^+$N**) using a siloxane-based crosslinker. The obtained films showed high cure percentages and water contact angles, along with a surface charge density value well over the necessary threshold for antimicrobial films and swelling degrees suitable for controlled drug release. The films were probed for their controlled drug release ability

using diclofenac as the loaded drug and examining the release in PBS and showed a promising release profile.

6.3   References

(1)   Chabannes, M.; Ruel, K.; Yoshinaga, A.; Chabbert, B.; Jauneau, A.; Joseleau, J.-P.; Boudet, A.-M. In Situ Analysis of Lignins in Transgenic Tobacco Reveals a Differential Impact of Individual Transformations on the Spatial Patterns of Lignin Deposition at the Cellular and Subcellular Levels. *Plant J.* **2001**, *28* (3), 271–282.

(2)   Jones, L.; Ennos, A. R.; Turner, S. R. Cloning and Characterization of Irregular xylem4 (irx4): A Severely Lignin-Deficient Mutant of Arabidopsis. *Plant J.* **2017**, *26* (2), 205–216.

(3)   Patil, S. V.; Argyropoulos, D. S. Stable Organic Radicals in Lignin: A Review. *ChemSusChem* **2017**, *10* (17), 3284–3303.

(4)   Laurichesse, S.; Avérous, L. Chemical Modification of Lignins: Towards Biobased Polymers. *Prog. Polym. Sci.* **2014**, *39* (7), 1266–1290.

(5)   Boerjan, W.; Ralph, J.; Baucher, M. Lignin Biosynthesis. *Annu. Rev. Plant Biol.* **2003**, *54* (1), 519–546.

(6)   Sakakibara, A. A Structural Model of Softwood Lignin. *Wood SciTechnol* **1980**, *14* (2), 89–100.

(7)   Upton, B. M.; Kasko, A. M. Strategies for the Conversion of Lignin to High-Value Polymeric Materials: Review and Perspective. *Chem Rev* **2016**, *116* (4), 2275–2306.

(8)   Silva, E. A. B. da; Zabkova, M.; Araújo, J. D.; Cateto, C. A.; Barreiro, M. F.; Belgacem, M. N.; Rodrigues, A. E. An Integrated Process to Produce Vanillin and Lignin-Based Polyurethanes from Kraft Lignin. *Chem. Eng. Res. Des.* **2009**, *87* (9), 1276–1292.

(9)   Bruijnincx, P.; Weckhuysen, B.; Gruter, G.-J.; Engelen-Smeets, E. *Lignin Valorisation: The Importance of a Full Value Chain Approach*; **2016**.

(10)   Ferdosian, F.; Yuan, Z.; Anderson, M.; Xu, C. (Charles). Synthesis of Lignin-Based Epoxy Resins: Optimization of Reaction Parameters Using Response Surface Methodology. *RSC Adv.* **2014**, *4* (60), 31745–31753.

(11)   Ferdosian, F.; Yuan, Z.; Anderson, M.; Xu, C. (Charles). Sustainable Lignin-Based Epoxy Resins Cured with Aromatic and Aliphatic Amine Curing Agents: Curing Kinetics and Thermal Properties. *Thermochim. Acta* **2015**, *618* (Supplement C), 48–55.

(12)   Ismail, T. N. M. T.; Hassan, H. A.; Hirose, S.; Taguchi, Y.; Hatakeyama, T.; Hatakeyama, H. Synthesis and Thermal Properties of Ester-Type Crosslinked Epoxy Resins Derived from Lignosulfonate and Glycerol. *Polym. Int.* **2010**, *59* (2), 181–186.

(13)   Sun, G.; Sun, H.; Liu, Y.; Zhao, B.; Zhu, N.; Hu, K. Comparative Study on the Curing Kinetics and Mechanism of a Lignin-Based-Epoxy/Anhydride Resin System. *Polymer* **2007**, *48* (1), 330–337.

(14)   Gordobil, O.; Herrera, R.; Llano-Ponte, R.; Labidi, J. Esterified Organosolv Lignin as Hydrophobic Agent for Use on Wood Products. *Prog. Org. Coat.* **2017**, *103*, 143–151.

(15)   Hambardzumyan, A.; Foulon, L.; Chabbert, B.; Aguié-Béghin, V. Natural Organic UV-Absorbent Coatings Based on Cellulose and Lignin: Designed Effects on Spectroscopic Properties. *Biomacromolecules* **2012**, *13* (12), 4081–4088.

(16)   Yan, R.; Yang, D.; Zhang, N.; Zhao, Q.; Liu, B.; Xiang, W.; Sun, Z.; Xu, R.; Zhang, M.; Hu, W. Performance of UV Curable Lignin Based Epoxy Acrylate Coatings. *Prog. Org. Coat.* **2018**, *116*, 83–89.

(17)   Bonini, C.; D'Auria, M.; Emanuele, L.; Ferri, R.; Pucciariello, R.; Sabia, A. R. Polyurethanes and Polyesters from Lignin. *J. Appl. Polym. Sci.* **2005**, *98* (3), 1451–1456.

(18)   Cateto, C. A.; Barreiro, M. F.; Rodrigues, A. E.; Brochier-Salon, M. C.; Thielemans, W.; Belgacem, M. N. Lignins as Macromonomers for Polyurethane Synthesis: A Comparative Study on Hydroxyl Group Determination. *J Appl Polym Sci* **2008**, *109* (5), 3008–3017.

(19)   Cateto, C. A.; Barreiro, M. F.; Ottati, C.; Lopretti, M.; Rodrigues, A. E.; Belgacem, M. N. Lignin-Based Rigid Polyurethane Foams with Improved Biodegradation. *J. Cell. Plast.* **2014**, *50* (1), 81–95.

(20)   Hatakeyama, H.; Hirogaki, A.; Matsumura, H.; Hatakeyama, T. Glass Transition Temperature of Polyurethane Foams Derived from Lignin by Controlled Reaction Rate. *J Therm Anal Calorim* **2013**, *114* (3), 1075–1082.

(21)   Liu, Y.; Li, K. Preparation and Characterization of Demethylated Lignin-Polyethylenimine Adhesives. *J. Adhes.* **2006**, *82* (6), 593–605.

(22)   Pizzi, A. Recent Developments in Eco-Efficient Bio-Based Adhesives for Wood Bonding: Opportunities and Issues. *J. Adhes. Sci. Technol.* **2006**, *20* (8), 829–846.

(23)   Mansouri, N. E.; Pizzi, A.; Salvadó, J. Lignin-Based Wood Panel Adhesives without Formaldehyde. *Holz Als Roh- Werkst.* **2007**, *65* (1), 65.

(24)   Mansouri, N.-E. E.; Pizzi, A.; Salvado, J. Lignin-Based Polycondensation Resins for Wood Adhesives. *J. Appl. Polym. Sci.* **2007**, *103* (3), 1690–1699.

(25)   Wang, C.; Venditti, R. A. UV Cross-Linkable Lignin Thermoplastic Graft Copolymers. *ACS Sustain. Chem Eng* **2015**, *3* (8), 1839–1845.

(26)   Wang, J.; Yao, K.; Korich, A. L.; Li, S.; Ma, S.; Ploehn, H. J.; Iovine, P. M.; Wang, C.; Chu, F.; Tang, C. Combining Renewable Gum Rosin and Lignin: Towards Hydrophobic Polymer Composites by Controlled Polymerization. *J. Polym. Sci. Part Polym. Chem.* **2011**, *49* (17), 3728–3738.

(27)   Kai, D.; Jiang, S.; Low, Z. W.; Loh, X. J. Engineering Highly Stretchable Lignin-Based Electrospun Nanofibers for Potential Biomedical Applications. *J. Mater. Chem. B* **2015**, *3* (30), 6194–6204.

(28)   Liu, X.; Yin, H.; Zhang, Z.; Diao, B.; Li, J. Functionalization of Lignin through ATRP Grafting of poly(2-Dimethylaminoethyl Methacrylate) for Gene Delivery. *Colloids Surf. B Biointerfaces* **2015**, *125*, 230–237.

(29)   Shah, T.; Gupta, C.; Ferebee, R. L.; Bockstaller, M. R.; Washburn, N. R. Extraordinary Toughening and Strengthening Effect in Polymer Nanocomposites Using Lignin-Based Fillers Synthesized by ATRP. *Polymer* **2015**, *72*, 406–412.

(30)   Sadeghifar, H.; Sen, S.; Patil, S. V.; Argyropoulos, D. S. Toward Carbon Fibers from Single Component Kraft Lignin Systems: Optimization of Chain Extension Chemistry. *ACS Sustain. Chem. Eng.* **2016**, *4* (10), 5230–5237.

(31)   Steudle, L. M.; Frank, E.; Ota, A.; Hageroth, U.; Henzler, S.; Schuler, W.; Neupert, R.; Buchmeiser, M. R. Carbon Fibers Prepared from Melt Spun Peracylated Softwood Lignin: An Integrated Approach. *Macromol. Mater. Eng.* **2017**, *302* (4), 1600441.

(32)   Zhang, M.; Ogale, A. A. Carbon Fibers from Dry-Spinning of Acetylated Softwood Kraft Lignin. *Carbon* **2014**, *69*, 626–629.

(33)   Park, C.-W.; Youe, W.-J.; Han, S.-Y.; Kim, Y. S.; Lee, S.-H. Characteristics of Carbon Nanofibers Produced from Lignin/Polyacrylonitrile (PAN)/Kraft Lignin-G-PAN Copolymer Blends Electrospun Nanofibers. *Holzforschung* **2017**, *71* (9), 743–750.

(34)   Figueiredo, P.; Lintinen, K.; Kiriazis, A.; Hynninen, V.; Liu, Z.; Bauleth-Ramos, T.; Rahikkala, A.; Correia, A.; Kohout, T.; Sarmento, B.; et al. In Vitro Evaluation of Biodegradable Lignin-Based Nanoparticles for Drug Delivery and Enhanced Antiproliferation Effect in Cancer Cells. *Biomaterials* **2017**, *121*, 97–108.

(35)   Yiamsawas, D.; Beckers, S. J.; Lu, H.; Landfester, K.; Wurm, F. R. Morphology-Controlled Synthesis of Lignin Nanocarriers for Drug Delivery and Carbon Materials. *ACS Biomater. Sci. Eng.* **2017**, *3* (10), 2375–2383.

(36)   Lievonen, M.; Valle-Delgado, J. J.; Mattinen, M.-L.; Hult, E.-L.; Lintinen, K.; Kostiainen, M. A.; Paananen, A.; Szilvay, G. R.; Setälä, H.; Österberg, M. A Simple Process for Lignin Nanoparticle Preparation. *Green Chem.* **2016**, *18* (5), 1416–1422.

(37)   Chen, N.; Dempere, L. A.; Tong, Z. Synthesis of pH-Responsive Lignin-Based Nanocapsules for Controlled Release of Hydrophobic Molecules. *ACS Sustain. Chem. Eng.* **2016**, *4* (10), 5204–5211.

(38)   Farhat, W.; Venditti, R.; Mignard, N.; Taha, M.; Becquart, F.; Ayoub, A. Polysaccharides and Lignin Based Hydrogels with Potential Pharmaceutical Use as a Drug Delivery System Produced by a Reactive Extrusion Process. *Int. J. Biol. Macromol.* **2017**, *104*, 564–575.

(39)   Feng, Q.; Li, J.; Cheng, H.; Chen, F.; Xie, Y. Synthesis and Characterization of Porous Hydrogel Based on Lignin and Polyacrylamide. *BioResources* **2014**, *9* (3), 4369–4381.

(40)   Argyropoulos, D. S. 31P NMR in Wood Chemistry: A Review of Recent Progress. *Res. Chem. Intermed.* **1995**, *21* (3–5), 373–395.

(41)   Argyropoulos, D. S. Quantitative Phosphorus-31 NMR Analysis of Lignins, a New Tool for the Lignin Chemist. *J. Wood Chem. Technol.* **1994**, *14* (1), 45–63.

(42)   Argyropoulos, D. S. 31P NMR in Wood Chemistry: A Review of Recent Progress. *Res Chem Intermed* **1995**, *21* (3–5), 373–395.

(43)   Ferry, L.; Dorez, G.; Taguet, A.; Otazaghine, B.; Lopez-Cuesta, J. M. Chemical Modification of Lignin by Phosphorus Molecules to Improve the Fire Behavior of Polybutylene Succinate. *Polym. Degrad. Stab.* **2015**, *113*, 135–143.

(44)   De Chirico, A.; Armanini, M.; Chini, P.; Cioccolo, G.; Provasoli, F.; Audisio, G. Flame Retardants for Polypropylene Based on Lignin. *Polym. Degrad. Stab.* **2003**, *79* (1), 139–145.

(45)   Mansur, H. S.; Mansur, A. A. P.; Bicallho, S. M. C. M. Lignin-Hydroxyapatite/Tricalcium Phosphate Biocomposites: SEM/EDX and FTIR Characterization https://www.scientific.net/KEM.284-286.745 (accessed Jun 17, 2018).

(46)   Xiong, W.; Yang, D.; Zhong, R.; Li, Y.; Zhou, H.; Qiu, X. Preparation of Lignin-Based Silica Composite Submicron Particles from Alkali Lignin and Sodium Silicate in Aqueous Solution Using a Direct Precipitation Method. *Ind. Crops Prod.* **2015**, *74*, 285–292.

(47)   Guterman, R.; Gillies, E. R.; Ragogna, P. J. Phosphane–ene Chemistry: The Reactivity of Air-Stable Primary Phosphines and Their Compatibility with the Thiol–ene Reaction. *Dalton Trans.* **2015**, *44* (35), 15664–15670.

(48)   Guterman, R.; Rabiee Kenaree, A.; Gilroy, J. B.; Gillies, E. R.; Ragogna, P. J. Polymer Network Formation Using the Phosphane–ene Reaction: A Thiol–ene Analogue with Diverse Postpolymerization Chemistry. *Chem. Mater.* **2015**, *27* (4), 1412–1419.

(49)   Cuthbert, T. J.; Jadischke, J. J.; de Bruyn, J. R.; Ragogna, P. J.; Gillies, E. R. Self-Healing Polyphosphonium Ionic Networks. *Macromolecules* **2017**, *50* (14), 5253–5260.

(50)   Cuthbert, T. J.; Harrison, T. D.; Ragogna, P. J.; Gillies, E. R. Synthesis, Properties, and Antibacterial Activity of Polyphosphonium Semi-Interpenetrating Networks. *J. Mater. Chem. B* **2016**, *4* (28), 4872–4883.

(51)   Cuthbert, T. J.; Guterman, R.; Ragogna, P. J.; Gillies, E. R. Contact Active Antibacterial Phosphonium Coatings Cured with UV Light. *J. Mater. Chem. B* **2015**, *3* (8), 1474–1478.

(52)   Hisey, B.; Ragogna, P. J.; Gillies, E. R. Phosphonium-Functionalized Polymer Micelles with Intrinsic Antibacterial Activity. *Biomacromolecules* **2017**, *18* (3), 914–923.

(53)   Béland, V. A.; Ross, M. A. S.; Coady, M. J.; Guterman, R.; Ragogna, P. J. Patterned Phosphonium-Functionalized Photopolymer Networks as Ceramic Precursors. *Chem. Mater.* **2017**, *29* (20), 8884–8891.

(54)   Dulbecco, R. Production of Plaques in Monolayer Tissue Cultures by Single Particles of an Animal Virus. *Proc. Natl. Acad. Sci.* **1952**, *38* (8), 747–752.

(55)   Murata, H.; Koepsel, R. R.; Matyjaszewski, K.; Russell, A. J. Permanent, Non-Leaching Antibacterial surfaces—2: How High-Density Cationic Surfaces Kill Bacterial Cells. *Biomaterials* **2007**, *28* (32), 4870–4879.

(56)   Kügler, R.; Bouloussa, O.; Rondelez, F. Evidence of a Charge-Density Threshold for Optimum Efficiency of Biocidal Cationic Surfaces. *Microbiology* **2005**, *151* (5), 1341–1348.

Chapter 7

7 Conclusions and Recommendations for Future Work

7.1 General Conclusions

The goal of this thesis was to conduct novel research on lignin valorization using the chemical modification of the hydroxyl functionalities of lignin. These groups are the most reactive sites within the macromolecule, and the most practical in terms of susceptibility to chemical modification. The chemical modification of these groups provides several possibilities regarding post modification processes. To graft onto the macromolecule, vinyl groups were chosen, primarily because of their crucial role in materials science, particularly in free radical polymerization. This thesis aimed at finding a chemical modification capable of grafting kraft lignin with vinyl-containing functionalities in the most facile fashion, using mild reaction conditions contrary to the other processes typically used for modifying lignin modification. The grafted macromolecule was probed with regards to its ability to be used in applications such as UV-curable coatings, and advanced materials with more complex and higher-value applications such as metal-scavengers and drug release vehicles.

7.2 Detailed Conclusions

Despite the inherently UV-absorbing nature of lignin, grafting of methacrylate groups in place of its hydroxyl functionalities successfully modified lignin into a UV-curable material. The modified lignin was quantitatively analyzed using a more readily available quantification reagent than the ones reported in literature. The modified lignin was crosslinkable in UV-cured coating samples at percentages up to 31 wt.%. The effect of crosslinking the modified lignin in the coating systems was evaluated regarding different characteristics of the UV-cured samples, particularly crosslinking percentage, hydrophobicity, surface adhesion, thermal stability, and retained weight at high temperatures. The chemical modification process developed for lignin (methacrylation) was then optimized using response surface methodology and central composite design. The developed mathematical model for the methacrylation process optimized reaction parameters to obtain the highest possible yield of modified lignin, while minimizing the

reaction temperature, time, and lignin/catalyst ratio. The optimized modified lignin was then examined at 30 wt.% in a siloxane-based UV-cured coating system as a proof of concept to determine the practicality of the developed optimization process.

The methacrylated lignin was utilized in a hydrophosphination reaction to report the first ever grafting of -C-P functionalities onto lignin, yielding lignin-based primary polyphosphines, referred to in this thesis as "primary lignophines", which were then converted into lignin-based tertiary polyphosphines, referred to in this thesis as "tertiary lignophines," before examining them in metal-scavenging settings. It was determined that the tertiary lignophine can coordinate to transition metals (e.g. silver). The tertiary lignophine was also probed as an effective transition-metal scavenger in lab-scale settings. It was determined that the tertiary lignophine had the ability to effectively sequester a catalyst (Grubbs I) in a ring closing metathesis reaction of diethyl diallylmalonates. This is the first report of lignin being used as a catalyst scavenger under normal catalytic conditions and an interesting potential new application for lignin.

Once the lignophines were synthesized and fully characterized, they were utilized in a quarternization process to yield lignin-based polyphosphonium salts, referred to in this thesis as "lignophoniums," which were then crosslinked with a siloxane-based crosslinker to give free-standing lignophonium films. Moreover, the films were examined with regards to their surface accessible charge density, hydrophobicity, swelling degree, and cure percentage, showing excellent surface charge density values, well over the threshold required to create antimicrobial films. The films were also probed as effective controlled drug release materials by examining the release profile of diclofenac-loaded films in PBS.

7.3   Contributions and Novelty

The main novelties and contributions of the research reported in this thesis can be summarized as follows:

- First report of crosslinked UV-cured networks made from modified lignin (31 wt.%).

- First report on the optimization of lignin's methacrylation process, capable of being utilized in scale-up production.

- First report of hdyrophosphination of a lignin derivative and subsequent utilization in phosphane-ene chemistry.

- First report of developing a lignin-based metal/catalyst scavenger.

- First report of synthesis and preparation of polyphosphonium salts and subsequent networks (free-standing films) from lignin, with potential applications as antimicrobial films and effective controlled drug delivery vehicles.

7.4 Recommendations for Future Work

7.4.1 Tunable Lignin-based UV-cured Coatings and Up-scale Production

Although the effect of incorporating chemically modified lignin into UV-curable lignin-based coatings was determined in this thesis, the effect of different crosslinkers in such systems remains unexamined. Utilizing different crosslinkers can give the ability to tune the coatings' properties and their behavior on different substrates according to the end-use in mind and be an important step towards possible commercialization of the lignin-based UV-curable coatings. Moreover, while scaled up methacrylation processes were performed by our research group in a scale up to 1L (reactor size), larger scale production of methacrylated lignin can be an important step in further proving the practicality of the optimized methacrylation process and make methacrylated lignin an interesting starting material for different target biomaterials. Preparing a mixed package comprised of up-scale production of methacrylated lignin can be an interesting package, capable of being proposed to coating industries.

7.4.2 Design of Experiments for Up-scale Production of Primary Lignophines

Design of experiment, like the central composite design used in chapter 4 of this thesis can be utilized to optimize the hydrophosphination of lignin as reported in chapter 5 of this thesis. Optimizing this process will give the ability to produce primary lignophines in much larger amounts, which can be greatly impactful on potential industrial applications of these materials. Moreover, the same approach can be utilized for the synthesis of tertiary

lignophines to prepare a complete synthetic package, capable of synthesizing each material in desired yields using optimized reaction settings.
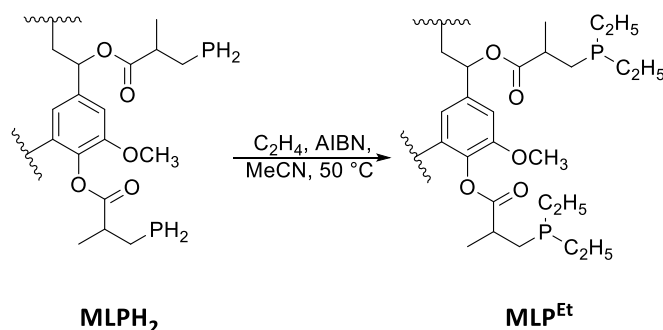
7.4.3 Tunable Lignin-based Tertiary Polyphosphines

Changing the capping reagents in the synthesis of tertiary lignophines can give the ability to tune some properties of the obtained material such as swellability. As the lignophine materials are not solvent-soluble and both their characterization and utilization in metal scavenging settings relied on their swellability in common organic solvents, making more swellable materials by changing the capping reagent might enhance such properties in the final products. Capping reagents such as 4-penten-1-ol can be reacted with the primary lignophine (**MLPH₂**) to give corresponding tertiary lignophine (**MLP^OH**). This can increase the swellability of the tertiary lignophine in common organic solvents considerably and affect the metal-scavenging ability of the material (Scheme 7-1).
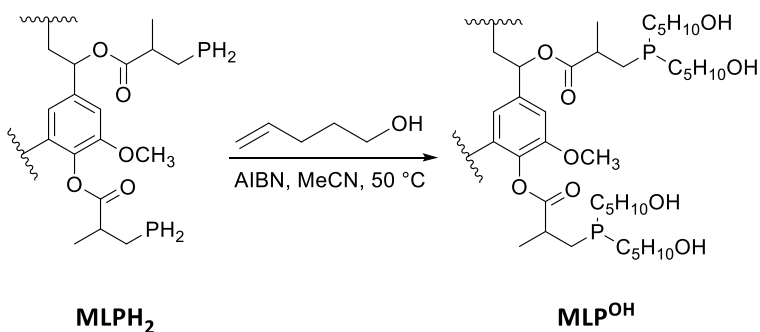
Scheme 7-1 Proposed reaction scheme for the synthesis of **MLP^OH**.

Moreover, less hindered capping reagents such as ethylene gas can also be utilized in the synthesis of tertiary lignophines (Scheme 7-2). The synthesized ethylated lignophine (**MLP^Et**) will consequently have hindrance around the phosphorus atoms. Such alteration can in turn induce the ability to scavenge oxygen, which can be of great interest as a highly novel packaging material.

Scheme 7-2 Proposed reaction scheme for the synthesis of **MLP^{Et}**.

7.4.4 Synthesis of Metal-Phosphides from Lignin-based Tertiary Polyphosphines

Tertiary lignophines were probed for their ability to coordinate to transition metals in this thesis. The next step in this research area can focus on coordinating the tertiary lignophines to different metal carbonyls such as $Mo(CO)_6$, $W(CO)_6$, and $Cr(CO)_6$. The resulting metal-coordinated networks can then be pyrolyzed to yield corresponding metal-phosphides of MoP, PW, and CrP (Scheme 7-3). These are promising candidates for lignophines to act as ceramic precursors, which have applications in several industries such as batteries and energy storage.
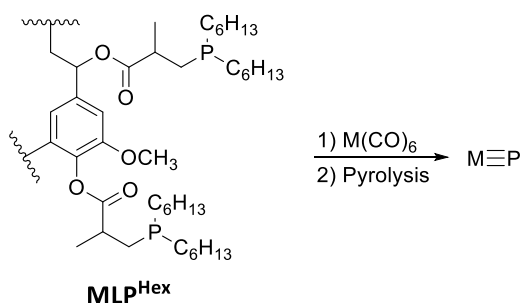
Scheme 7-3 Proposed scheme for the synthesis of metal-phosphides from **MLP^{Hex}** through coordination to different metal carbonyls (M = Mo, W, and Cr) and subsequent pyrolysis.

7.4.5 Studying the Tunability and Further Utilization of Lignin-based Polyphosphonium Salts

Using different halides as the quarternization reagents for the synthesis of the lignin-based polyphosphonium salts ("lignophoniums"), as well as different crosslinkers for the

preparation of the free-standing films can enhance the tunability of the material with regards to its wettability, cure percentage, and swelling degrees, which can enhance its usefulness in controlled drug delivery systems.

Moreover, antimicrobial studies need to be performed on the lignophonium networks to further demonstrate their antimicrobial performance in real-world or lab settings. Like the catalyst sequestration studies for the lignophines, collaborating with research groups active in the field of biology and microbial studies would lead to promising results for the lignophoniums.

Appendices

Appendix 1. Supporting Information for Chapter 3

UV-Vis spectra

UV-Vis spectra were obtained of the KL, ML, and DMPA (photoinitiator) samples to evaluate the effect of the methacrylation reaction on the UV-curability of lignin (Figure S3-1). It was determined that while the KL sample had a complete overlap in absorbance with the photoinitiator (hence the non-UV-curable nature of lignin), the absorbance is significantly reduced in the ML sample, proving the detrimental effect of the chemical modification on converting lignin into a UV-curable material.
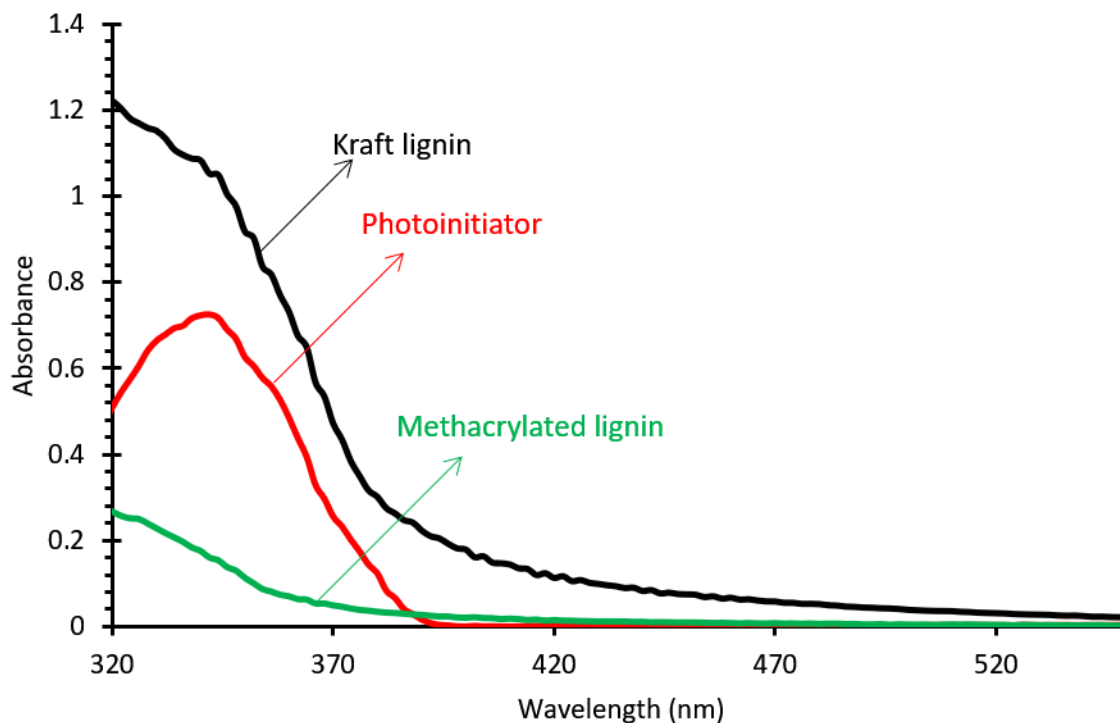
Figure S3-1 UV-Vis spectra of kraft lignin, methacrylated lignin, and the photoinitiator (DMPA) used for the preparation of the lignin-based UV-cured coatings.

Reaction of Lignin with Chlorodi(isopropyl)phosphine
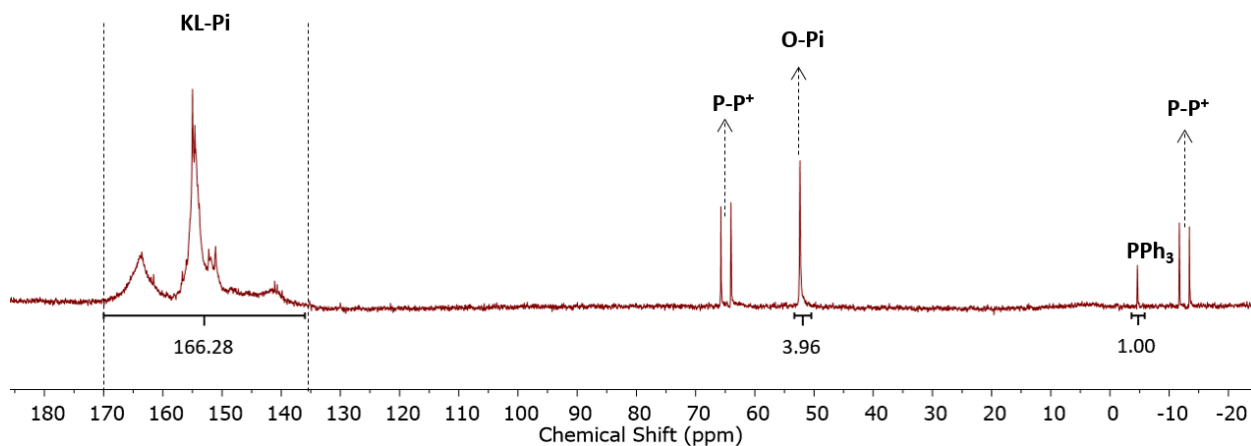
KL was reacted with chlorodi(isopropyl)phosphine ($[CH(CH_3)_2]_2PCl$) to determine the types and amounts of hydroxyl functionalities within the native sample (Scheme S1).
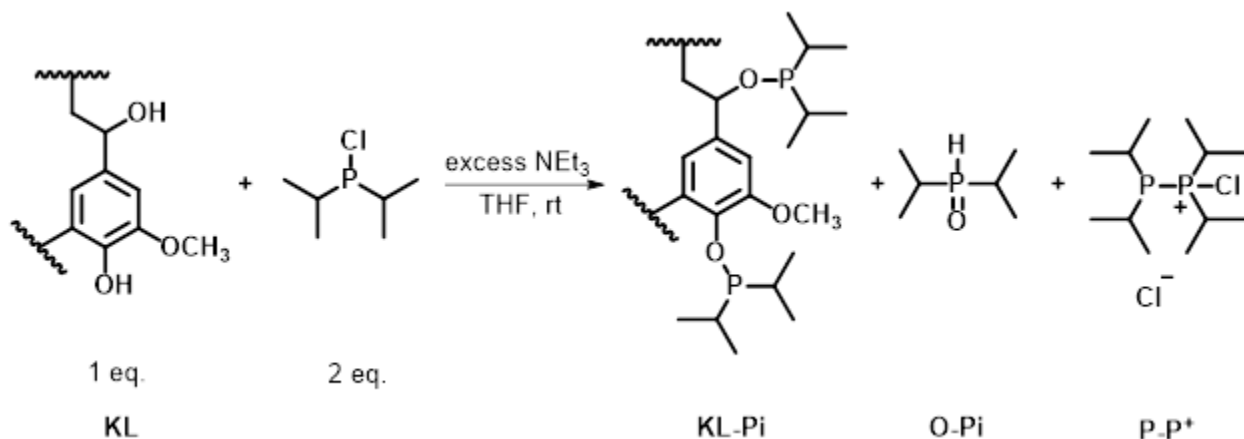
Scheme S3-1 Reaction of KL with chlorodi(isopropyl)phosphine ($[CH(CH_3)_2]_2PCl$).

Upon examining the $^{31}P\{^1H\}$ NMR spectrum of the obtained product, signals corresponding to the main product (**KL-Pi**, $\delta_P = 136.0\text{-}170.0$) and two bi-products, chlorodi(isopropyl)phosphine oxide (**O-Pi**, $\delta_P = 52.0$) and di(isopropyl)phosphino chlorodi(isopropyl)phosphonium chloride[1] (**P-P⁺**; $\delta_P = 65.0, 64.0$, d, $^1J_{P\text{-}P}=275.3$ Hz, $[_2[(CH_3)_2(CH)]P^+(Cl)\text{-}P[CH(CH_3)_2]_2]^-Cl$; $\delta_P = -11.3, -13.0$, d, $^1J_{P\text{-}P}=275.3$ Hz, $[_2[(CH_3)_2(CH)]P^+(Cl)\text{-}\mathbf{P}[CH(CH_3)_2]_2]^-Cl$) were observed (Figure S2).

Figure 0-2 ^{31}P{^{1}H} NMR spectrum of the product of the reaction of KL with chlorodi(isopropyl)phosphine.

O-Pi was determined to be the product of the reaction of chlorodi(isopropyl)phosphine with residual water present in the native **KL** sample and the formation of **P-P$^+$** was attributed to the reaction of two molecules of chlorodi(isopropyl)phosphine.

Appendix 2. Permission to Use Copyrighted Materials

Permission for Figure 1-1

Order License Id: 4385941359048

Requestor type	Academic institution
Format	Print, Electronic
Portion	chart/graph/table/figure
Number of charts/graphs/tables/figures	1
The requesting person/organization	Soheil Hajirahimkhan
Title or numeric reference of the portion(s)	Figure 3
Title of the article or chapter the portion is from	Hemicelluloses
Editor of portion(s)	N/A
Author of portion(s)	Henrik Vibe Scheller, Peter Ulvskov
Volume of serial or monograph	N/A
Page range of portion	265
Publication date of portion	2010
Rights for	Main product
Duration of use	Life of current and all future editions
Creation of copies for the disabled	no
With minor editing privileges	no
For distribution to	Worldwide
In the following language(s)	Original language of publication
With incidental promotional use	no
Lifetime unit quantity of new product	Up to 499
Title	Lignin Valorization through Chemical Modification
Instructor name	n/a
Institution name	n/a
Expected presentation date	Aug 2018

Permission for Figure 2-3

This Agreement between Mr. Soheil Hajirahimkhan ("You") and Elsevier ("Elsevier") consists of your license details and the terms and conditions provided by Elsevier and Copyright Clearance Center.

License Number	4373050442788
License date	Jun 20, 2018
Licensed Content Publisher	Elsevier
Licensed Content Publication	Elsevier Books
Licensed Content Title	Polymer Science: A Comprehensive Reference
Licensed Content Author	E. Windeisen,G. Wegener
Licensed Content Date	Jan 1, 2012
Licensed Content Pages	11
Start Page	255
End Page	265
Type of Use	reuse in a thesis/dissertation
Portion	figures/tables/illustrations
Number of figures/tables/illustrations	1
Format	both print and electronic
Are you the author of this Elsevier chapter?	No
Will you be translating?	No
Original figure numbers	Table 3
Title of your thesis/dissertation	Lignin Valorization through Chemical Modification
Expected completion date	Aug 2018
Estimated size (number of pages)	200
Requestor Location	Mr. Soheil Hajirahimkhan
Publisher Tax ID	GB 494 6272 12
Billing Type	Invoice
Billing Address	Mr. Soheil Hajirahimkhan
Total	0.00 CAD

Permission for Scheme 2-1

This Agreement between Mr. Soheil Hajirahimkhan ("You") and Elsevier ("Elsevier") consists of your license details and the terms and conditions provided by Elsevier and Copyright Clearance Center.

License Number	4372691313514
License date	Jun 19, 2018
Licensed Content Publisher	Elsevier
Licensed Content Publication	Progress in Polymer Science
Licensed Content Title	Chemical modification of lignins: Towards biobased polymers
Licensed Content Author	Stéphanie Laurichesse,Luc Avérous
Licensed Content Date	Jul 1, 2014
Licensed Content Volume	39
Licensed Content Issue	7
Licensed Content Pages	25
Start Page	1266
End Page	1290
Type of Use	reuse in a thesis/dissertation
Portion	figures/tables/illustrations
Number of figures/tables/illustrations	1
Format	both print and electronic
Are you the author of this Elsevier article?	No
Will you be translating?	No
Original figure numbers	Figure 5
Title of your thesis/dissertation	Lignin Valorization through Chemical Modification
Expected completion date	Aug 2018
Estimated size (number of pages)	200

Requestor Location	Mr. Soheil Hajirahimkhan
Publisher Tax ID	GB 494 6272 12
Total	0.00 CAD

Permission for Scheme 2-2

JOHN WILEY AND SONS LICENSE
TERMS AND CONDITIONS

Jul 19, 2018

This Agreement between Mr. Soheil Hajirahimkhan ("You") and John Wiley and Sons ("John Wiley and Sons") consists of your license details and the terms and conditions provided by John Wiley and Sons and Copyright Clearance Center.

License Number	4385950124804
License date	Jul 11, 2018
Licensed Content Publisher	John Wiley and Sons
Licensed Content Publication	ChemSusChem
Licensed Content Title	Lignin as Renewable Raw Material
Licensed Content Author	Francisco García Calvo-Flores, José A. Dobado
Licensed Content Date	Sep 13, 2010
Licensed Content Volume	3
Licensed Content Issue	11
Licensed Content Pages	9
Type of use	Dissertation/Thesis
Requestor type	University/Academic
Format	Print and electronic
Portion	Figure/table
Number of figures/tables	1
Original Wiley figure/table number(s)	scheme 8
Will you be translating?	No
Title of your thesis / dissertation	Lignin Valorization through Chemical Modification

Expected completion date	Aug 2018
Expected size (number of pages)	200
Requestor Location	Mr. Soheil Hajirahimkhan
Publisher Tax ID	EU826007151
Total	0.00 CAD

Permission for Scheme 2-11

JOHN WILEY AND SONS LICENSE
TERMS AND CONDITIONS

Jul 19, 2018

This Agreement between Mr. Soheil Hajirahimkhan ("You") and John Wiley and Sons ("John Wiley and Sons") consists of your license details and the terms and conditions provided by John Wiley and Sons and Copyright Clearance Center.

License Number	4385931478829
License date	Jul 11, 2018
Licensed Content Publisher	John Wiley and Sons
Licensed Content Publication	Journal of Polymer Science Part A: Polymer Chemistry
Licensed Content Title	Combining renewable gum rosin and lignin: Towards hydrophobic polymer composites by controlled polymerization
Licensed Content Author	Jifu Wang, Kejian Yao, Andrew L. Korich, et al
Licensed Content Date	Jun 20, 2011
Licensed Content Volume	49
Licensed Content Issue	17
Licensed Content Pages	11
Type of use	Dissertation/Thesis
Requestor type	University/Academic
Format	Print and electronic
Portion	Figure/table
Number of figures/tables	2

Original Wiley figure/table number(s)	Scheme 3 and scheme 2
Will you be translating?	No
Title of your thesis / dissertation	Lignin Valorization through Chemical Modification
Expected completion date	Aug 2018
Expected size (number of pages)	200
Requestor Location	Attn: Mr. Soheil Hajirahimkhan
Publisher Tax ID	EU826007151
Total	0.00 CAD

Permission for Scheme 2-13

JOHN WILEY AND SONS LICENSE
TERMS AND CONDITIONS

Jul 19, 2018

This Agreement between Mr. Soheil Hajirahimkhan ("You") and John Wiley and Sons ("John Wiley and Sons") consists of your license details and the terms and conditions provided by John Wiley and Sons and Copyright Clearance Center.

License Number	4385940152797
License date	Jul 11, 2018
Licensed Content Publisher	John Wiley and Sons
Licensed Content Publication	Polymer International
Licensed Content Title	Synthesis and thermal properties of ester-type crosslinked epoxy resins derived from lignosulfonate and glycerol
Licensed Content Author	Tuan Noor Maznee Tuan Ismail, Hazimah Abu Hassan, Shigeo Hirose, et al

Licensed Content Date	Dec 1, 2009
Licensed Content Volume	59
Licensed Content Issue	2
Licensed Content Pages	6
Type of use	Dissertation/Thesis
Requestor type	University/Academic
Format	Print and electronic
Portion	Figure/table
Number of figures/tables	1
Original Wiley figure/table number(s)	scheme 2
Will you be translating?	No
Title of your thesis / dissertation	Lignin Valorization through Chemical Modification
Expected completion date	Aug 2018
Expected size (number of pages)	200
Publisher Tax ID	EU826007151
Total	0.00 CAD

Curriculum Vitae

Name:	Soheil Hajirahimkhan
Post-secondary Education and Degrees:	K.N. Toosi University of Technology Tehran, Iran 2005-2011 B.Sc. I.K. International Univresity Qazvin, Iran 2011-2013 M.Sc. The University of Western Ontario London, Ontario, Canada 2014-2018 Ph.D.
Related Work Experience	Research Assistant the University of Western Ontario 2014-2018 Teaching Assistant The University of Western Ontario 2014-2018